MASSACHUSETTS INSTITUTE OF TECHNOLOGY

AEROELASTIC AND STRUCTURES RESEARCH LABORATORY

Technical Report 107-2

August 1964

THEORETICAL DETERMINATION
OF
ROTOR BLADE HARMONIC AIRLOADS

by

R. H. Miller

MASSACHUSETTS INSTITUTE OF TECHNOLOGY

AEROELASTIC AND STRUCTURES RESEARCH LABORATORY

Technical Report 107-2

August, 1964

THEORECTICAL DETERMINATION

OF

ROTOR BLADE HARMONIC AIRLOADS

by

R. H. Miller

FOR THE

TABLE OF CONTENTS

LIST OF FIGURES

I. SUMMARY

A helicopter rotor in forward flight is subjected to a complex system of loads, both aerodynamic and inertial in origin. Of particular interest are the oscillatory airloads occurring at harmonics of the rotor speed. These loads are the primary source of the blade stresses which establish the fatigue life of the structure and of the oscillatory hub loads which determine the fuselage vibration level. Unlike a wing, the trailing- and shed-vortex system of the blade generates a spiral wake which returns close to the blade under most normal flight conditions. This returning wake critically influences the downwash distribution over the rotor disc and is the primary source of the higher harmonic airloading. The higher harmonic components of the airloading arise primarily from the downwash perpendicular to the plane of the rotor disc generated by this wake. Their analytical determination, therefore, requires some means of computing the downwash, which takes into account the spiral wake geometry, and of determining the unsteady aerodynamic effects associated with the blade passage through this variable velocity field. A better definition of the aerodynamics of a rotor in forward flight will also help in the design of hub and blades for minimum drag at the higher speeds envisaged for the next generation of helicopters.

It is the purpose of this report to present a solution to the problem of determining rotor-blade harmonic loading which includes both the unsteady aerodynamic effects and the actual three-dimensional wake geometry. The basic aerodynamic theory is first discussed and then related to the more familiar finite-wing theory. A general discussion of the results of the investigation to date follows, including an outline of the suggested approach based on certain simplifying assumptions which are substantiated in later sections of the report.

The problem is formulated for the complete case of the three-dimensional rotor with a finite number of blades in forward flight. Methods of solution are discussed starting with a relatively exact approach in which the airloads on the blade

generated by the near wake are treated using lifting-surface theories, while the far wake is treated using the lifting-line approximation. This suggested treatment is then evaluated by applying it to the simpler two-dimensional case and comparing the results with the exact two-dimensional solution available in the literature.

Analytical solutions are then obtained for the three-dimensional rotor in vertical flight. This results in a simple solution for the lift-deficiency function and provides a useful check on the numerical solutions obtained using the complete theory.

The relationships required for the solution of the complete problem of the airloads on a three-dimensional rotor in forward flight are then developed. The concept of a "nonrigid" wake is introduced. It is shown that a more careful definition of the wake geometry than the assumption of a rigid spiral of constant spacing becomes important at the lower advance ratios.

Finally, approximate solutions are discussed and compared with the more exact theory. It is shown that for many engineering applications, reasonably accurate airloads may be calculated using fairly simple techniques of analysis.

During the course of the research outlined in this report, some fifty different computer programs were developed and approximately 100 hours of 7090 computer time were used. Many of these programs were developed primarily for research and testing of various techniques of analysis and are not of permanent interest. The final versions of the programs for the computation of downwash and airloads, both exact and approximate, are given in Reference 36.

II. INTRODUCTION

Probably one of the most difficult problems facing the designer of rotary wing aircraft at the present time is that of determining the blade aerodynamic loading, and, in particular, the oscillatory content of this loading. The magnitude of the problem may be appreciated if it is realized that an equivalent ignorance on the part of the fixed wing designer would mean that no method existed for predicting the spanwise-load distribution on a conventional wing. Consequently, no rational design of the wing structure could be effected until the aircraft had flown and extensive test data obtained which would permit substantiation of the structure for all anticipated flight conditions. Until the advent of swept-back wings, conventional aircraft were sufficiently stiff or the speed sufficiently low so that aeroelastic effects could be neglected in computing airload distributions, at least to first order, and the simple elliptical load distributions obtained from uniform downwash theory were known to give reasonable approximations for most flight conditions. No such simplifications were ever permissible for rotor blades, aeroelastic effects always being predominant. The nature of the airload distributions furthermore can certainly not be generalized by elliptical, triangular or any other simplified function, since even an approximate theory for the airload distribution is lacking and no exact analysis has been attempted.

In the absence of a working theory, design of rotor blades has proceeded on an empirical basis with rotor-blade life substantiated by flight-test experimentation. Although costly, such procedure is, of course, adequate. Provided no major design changes are attempted with each new model and advances made in small steps, even the costs are not excessive since extrapolation from previous experience is not too difficult. However, rotary wing aircraft at present are on the threshold of a major advance in both speed and design technology which will result in a considerable reduction in maintenance cost and increase in utility for the short haul market. Empirical design techniques are certainly no longer admissible if real advances are to be achieved with reasonable cost and effort. Some knowledge of the nature of the aerodynamic loading on rotor blades and,

1

in particular, of the higher harmonic loading which determines the fatigue lift must, therefore, be acquired if the design of helicopter and VTOL rotors is to be placed on a rational basis and new structural design concepts introduced safely and rapidly as required.

In addition to the all-important problem of rotor-blade-structural integrity, the control of vibration levels is another important problem facing the helicopter designer. Through the years much careful work has been done to determine the dynamic response characteristics of rotor blades and of fuselage to vibratory inputs and this has resulted in a major reduction in helicopter vibration levels on most existing helicopters. However, the process has been a costly and time-consuming one and has been greatly handicapped by a lack of information on the nature of the inputs which cause the vibratory response of the aircraft. These inputs are, of course, directly associated with the higher harmonic airloads acting on the rotor blades.

Finally, as helicopter speeds advance above 200 knots, it is necessary to define as carefully as possible the angle-of-attack distribution over the rotor so as to reduce the drag represented by the in-board shanks of the rotor blade and the hub fairings. This problem is closely related to the two described above and is a further reason for a more careful definition of rotor-blade aerodynamics in forward flight.

III. DISCUSSION AND REVIEW OF BACKGROUND LITERATURE

A rotor blade in forward flight is subjected to a time-varying flow field in which the forward velocity adds to the rotational velocity on the advancing side and substracts on the retreating side. The resulting first harmonic velocity change will generated first- and second-harmonic-lift changes, lift being proportional to the square of velocity. A flexible blade or a blade with mechanical hinges at the root will flap in the presence of this flow variation in such a way as to maintain almost constant lift around the azimuth. Because a considerable amount of inter-harmonic coupling exists, this flapping in response to the first- and second-harmonics of lift change will generate higher harmonic lift changes ad infinitum. The simple theory of rotor blade loading in forward flight in which a uniform or triangular inflow distribution is assumed, indicates that these loadings will decrease as μ^n where μ is the advance ratio and n indicates the nth harmonic of loading. This does not fit the observed facts since harmonics as high as the fifth or sixth are known to produce appreciable blade stresses and vibratory shaft loads at advance ratios of the order of 0.1 or 0.2 where the simplified theory would indicate such loadings to be negligible. See, for example, Reference 1.

One of the earliest attempts to compute the induced velocity field at the rotor disc was that presented in the 1948/49 Cierva Memorial Prize Essay by Drees in which, by an ingenious approximation, values for the average and first harmonic inflow variation were obtained, primarily for the purposes of performance estimation (Reference 2).

In Reference 3 a solution was obtained for the harmonic loading on a disc with a prescribed loading distribution along the span and constant around the azimuth with the further assumption that the forward velocity is high compared to the disturbance velocities. This solution indicates the presence of appreciable higher harmonic inflows with a strong concentration towards the tips of the blades.

In Reference 4 it was shown that the lift-deficiency function of classical nonstationary-flow theory could approach very small values at integers of rotor speed when the effects of the returning wake were taken into consideration. This implies a reduction in damping, but also a reduction in lift generated by the higher harmonic inflow variations. However, the blade will respond elastically in distributed modes to a higher harmonic loading concentrated at the tip and, if the harmonic approaches one of the natural frequencies of the blade, the mechanism evidently exists for the excitation of appreciable blade stresses and hub shears.

In Reference 5 the theory of Reference 4 was applied to the calculation of blade stability. Figure 1 taken from Reference 5 shows that, as might be expected, neglect the effects of the returning wake in such calculations is conservative. Experimental verification of these effects was obtained in the tests reported in Reference 6. When an attempt was made to excite the blade aerodynamically by harmonic pitch variation, no appreciable effects of the returning wake were noticed; however, with mechanical excitation of the rotor hub, a pronounced reduction in damping was evidenced by the large increase in blade response. This is shown in Figure 2.

It is, therefore, clear that any attempt to predict the blade harmonic loading and response to this loading must treat the effects of the returning wake with some care. Furthermore, since interharmonic coupling in the presence of first- and second-harmonic-lift variations and a uniform wake cannot predict the observed order of magnitude of these loads, the mechanism of their generation must come from the harmonic content of the interference velocities generated at the rotor disc by the rotor wake. A three-dimensional model is required if the harmonic content of this downwash is to be predicted with any degree of accuracy.

Wake-interference effects have been considered in great detail in the literature for the case of airfoils operating at sufficiently high forward speeds so

4

that the wake may be assumed to remain in the plane of the airfoil. A clear inter-
pretation of the physics of this problem is given in Reference 7. The concept of
vortex pairs used therein is particularly adoptable to the problem considered in this
paper. An extension of the theory to a helicopter rotor was made in References 8
and 9, but these analyses were limited to the relatively secondary effects of the
harmonically varying forward velocity. The distortion of the wake due to this
variation was considered in Reference 8, for a somewhat simplified input; a more
exact blade motion was considered in Reference 9, but the effects of wake dis-
tortion were eliminated from the analysis. In either case, the results were found
to be negligible, most probably because of the low reduced frequency represented
by first harmonic velocity variations. A useful extension of the theory to the
calculation of rotor-blade bending moments is contained in Reference 10.

The first analysis of the important effects of the returning wake was contained
in Reference 4. Similar analyses are contained in References 11 and 12. All these
analyses are limited to two-dimensional models. An extension to the three-dimen-
sional case of a hovering rotor is contained in Reference 13. The results of this
analysis confirm experience with similar high-aspect-ratio fixed-wing solutions in
which the two-dimensional model is found to be generally adequate for the prediction
of rotor-blade stability boundaries in the presence of pitch-flap coupling. A valuable
contribution of Reference 13 lies in its development of the concept of the rotor as
operating in a straight "sheared" flow representing the velocity variations along the
blade, a concept which is particularly useful in the development of the theory of
this paper.

The three-dimensional solution of the time-averaged wake-interference
effects was first given in Reference 14, which extended the concepts of classical
propeller vortex theory, in which the wake is represented by an infinite vortex
cylinder to the case of a skewed cylinder. Reference 15, which contains a useful
table of induced velocities generated by displaced vortex rings, computes the veloci-
ties induced by an infinite vortex cylinder at several points in the vicinity of a

rotor. Both these references assumed constant blade circulation both with azimuth (timewise) and radially along the blade. The latter limitation was removed in Reference 16 although the less important assumption of constant circulation with time was retained. In Reference 17 the induced velocities generated by an infinite vortex cylinder with time-varying circulation and containing an infinite number of inner sheets representing the shed vorticity in the presence of time variations in circulation were considered. The induced velocities were presented for several points in the lateral plane of the rotor, but at only one azimuth and, consequently, the harmonic content of the wake could not be directly determined. However, it is probable that this model will give a close approximation to the wake-induced velocities, although the assumption of an infinitely small wake displacement and, hence, an infinite number of blades precludes any prediction of one of the important effects of nonstationary-flow theory arising from the nonuniform downwash induced by the wake along the blade chord. Unless this effect is introduced, the phase shift in lift generation represented by the imaginary part of the lift deficiency function, $C(k,m,h)$ of Reference 4, disappears. At the present time the importance of this limitation is not clear, but the approximation is certainly valid for the purpose for which the theory of Reference 17 was originally developed.

In Reference 18 the infinite vortex cylinder is replaced by segments of straight wakes oriented below the rotor. Since this permits integration to infinity in both directions, a combined analytical and digital approach is possible, utilizing the techniques developed in the lifting-line theory for fixed wings. Although the solution has been limited to the quasi-static case, extension to that of variable wake strength would appear to present no major problems.

The effect of a finite wake spacing of spiral form was analyzed in Reference 19 where it is shown that a highly time-dependent-interference velocity is generated as the blade passes over the immediately adjacent returning wake. An interesting suggestion for further analyses is contained in Reference 20 in which the first spiral is retained and the remaining wake replaced by an infinite vortex cylinder.

Experimental verification of the nonuniformity of rotor inflow was obtained in flight and is presented in Reference 21. Wind tunnel tests reported in Reference 22 gave quantitative information on the first harmonic downwash variations deduced from measured blade aerodynamic loading. In Reference 23 measurements of higher harmonic airloads were presented for a teetering blade and in Reference 1 valuable flight test information was obtained for blades of varying stiffness. Correlation with existing theory of all these tests was disappointing and it was quite evident that a considerable amount of further analytical effort is required if a reasonable method of predicting airloads is to be established.

In order to obtain some quantitative information on the harmonic airloads and some understanding of the mechanism by which they are produced, and in order to determine the importance of the unsteady aerodynamic effects throughout the flight regime, a solution using a finite number of blades and applicable nonstationary flow theory was, therefore, attempted. Some of the results of this study were presented in References 24, 25, 26, 27, and 28. The program is a continuing one and this report is based on the interpretation of the results obtained to date. Agreement between theory and experiment is, in general, good at advance ratios corresponding to cruise conditions, but poorer at lower advance ratios where the effects at the nonuniform wake probably dominate in establishing the wake geometry.

Furthermore, it should be noted that a rotor blade is a highly complex aeroelastic system subjected to powerful coupling effects, due to the high centrifugal force field not encountered on fixed wings as discussed in Reference 5. Consequently, any experimental verification of theory should include consideration of these effects. It is probable that, for this reason, model tests under controlled conditions may be most useful for the purpose of establishing such correlation. A promising test technique, which may prove particularly useful for determining the importance of certain assumptions, for example, that of a rigid wake, is reported in Reference 20. In these tests flow visualization was achieved by smoke generation at the blade tips. Continuation of these tests and extension of such tests to include the generation of smoke at intermediate blade stations would appear most desirable.

7

IV. BASIC CONCEPTS

1) The Separate Elements of Helicopter Vibration

The dynamics of helicopter vibration may be conveniently discussed by considering the three basic factors which contribute to this vibration as separable, although heavily interacting, elements. These three elements are:

1) Rotor Aerodynamic Loading
2) Blade and Rotor Dynamics
3) Fuselage Dynamics

The combination of a highly flexible blade attached to a flexible fuselage and subjected to periodic aerodynamic loads, which, in turn, are proportional to the blade motion, presents a dynamic problem of some magnitude. However, methods for handling the last two items, fuselage and rotor dynamics, in a routine fashion are now available using the well-established techniques of aeroelasticity. It is with the first item, blade loads, that we are mainly concerned. Once it becomes possible to predict the magnitude and time history of the aerodynamic loads, the resultant phasing and magnitude of the hub loads can be predicted, as well as the degree to which these loads are amplified by rotor dynamics. Knowing the nature of these loads, the fuselage response, which determines the vibration levels to which the passengers and structure will be subjected, can be determined. Unless each element in the chain of vibration buildup can be separately defined, mitigation and control of the vibration level, except on a hit and miss basis, is impossible. Obviously, the first element in the chain on which all others depend is the harmonic airloading.

In emphasizing the need for quantitative information on this primary forcing function, it is not intended to imply that the remaining steps in vibration control are simple and straightforward, but rather that they then become subjected to

8

systematic analysis. As mentioned before, of considerable concern is the nature of the blade torsion-bending coupling and its effect on the airloads. Accepting that higher harmonic aerodynamic loads of appreciable magnitude do exist, then it is evident that the blade will bend periodically in the presence of these loads out of the plane of rotation and out of the plane of its twist axis. The potential significance of this phenomenon may be demonstrated by a simple illustration. In Figure 3 a blade is shown with its normal elastic deflection. Torsional flexibility is assumed, for simplicity, to occur primarily at the feathering hinge located near the blade root. As the blade twists about, the feathering hinge components of centrifugal force act to increase the twist. That is, a rotor blade bent out of its plane of rotation is not in static equilibrium. Since the centrifugal force is several times the gross weight of the ship, clearly powerful blade twisting moments can be produced by this mechanism unless relieved by motion about the lag hinge. In Reference 5 it was shown that in certain cases, such as a teetering rigid blade, these moments could be equivalent to those produced by a 6 per cent chord shift in CG of the rotor blades.

Since rotor blades must bend elastically in the presence of aerodynamic lift, this centrifugal force component, and also the steady state drag, will cause periodic twisting moments due to the periodic changes in blade bending deflection caused by the higher harmonic airloads. In addition, periodic changes in induced drag due to the higher harmonic content of the downwash will combine with the steady state bending deflection of the blade to produce another source of periodic twisting moments. Twisting moments from these sources will cause harmonic change in angle of attack. Consequently, coupling between elastic flapping and torsion is potentially of considerable importance in establishing blade loads.

Pitch flap coupling may also be used to reduce the oscillatory loads acting on the rotor. In Reference 5 it was shown that by tuning the torsional frequency of the blade to the frequency of the harmonic, which it was desired to attenuate, and by offsetting the aerodynamic center and center of gravity of the blade about 3 per cent of the chord, reductions in the harmonic hub loads of the order of 50 per cent could be achieved. This was later demonstrated in flight using a

9

blade whose AC-CG offset was obtained by means of an aerodynamic surface (servo flap). The desired reduction in vertical vibratory force was achieved; however, the inplane forces were not appreciably attenuated and, in this particular synchropter configuration, these forces were the primary source of fuselage vibration.

The importance of establishing the magnitude and phasing of all components of rotor hub loads is particularly important for the tandem helicopter. A cancellation of vibratory input, due to the phasing of the forces from the two hubs, is conceivable for this configuration and probably for most other configurations, were it possible to evaluate and control, by design modification, both the phasing and magnitude of forces entering the hubs and the hub loads themselves.

Pursuing the analogy of helicopter dynamics as consisting of separable elements, it is possible to show these elements and their interaction schematically as in Figure 4. The interaction between the elements determines the degree of complexity required for numerical solutions. To date our studies have indicated that the interactions shown by broken lines are not of primary importance. Consequently, blade flapping and the dissymmetry of flow over the rotor disc have little direct influence on the higher harmonic airloading. Also, the unsteady aerodynamic effects can be treated independently of blade motions as a lift-deficiency function and phase shift for the higher harmonic airloads, much as in the fixed wing case.

The effect of these conclusions is to largely uncouple the elements in our schematic of the dynamics and, hence, to simplify the analysis, since each element can now be separately investigated. Unfortunately, a further conclusion is that the harmonic loading is critically dependent on wake geometry and this considerably complicates the analysis, since wake geometry is not subject to exact definition and is certainly far different from any of the rigid wake concepts used in propeller analysis. Reasonable agreement has, however, been obtained between theory and test for the normal cruising and high speed flight regimes. At the lower speeds, we are at least beginning to understand some of the factors which contribute to transition roughness.

2) Analogy with Fixed-Wing Aerodynamics

The underlying aerodynamic theory required will be better understood if the equivalent fixed-wing problem is first examined. Consider a wing advancing at constant angle of attack in a uniform airstream. By virtue of its geometrical angle of attack, the airfoil will generate circulation and, consequently, lift. Assuming for simplicity that this circulation is constant along the span, it must leave the wing at the tips and trail downstream since, by one of the fundamental laws of hydrodynamics, circulation cannot end abruptly but must continue back in a closed circuit to the starting vortex generated at the beginning of the motion (Figure 5). After the motion has continued for a sufficient length of time, this starting vortex may be assumed to be at an infinite distance from the airfoil, and its effects may be neglected. The trailing vortex will induce velocities, w, at the wing which will, in effect, reduce the angle of attack to something less than the geometric angle. This results in the well-known aspect-ratio correction to the slope of the lift curve of a finite airfoil. In practice, of course, the circulation is not constant along the span and, therefore, the trailing vortices are distributed in a sheet all along the span. The mathematical treatment of this problem is well known and is covered in any text on wing theory. In its most useful applications, the wing is replaced by a single vortex line whose strength is equal to the bound circulation on the airfoil, resulting in the so-called lifting-line theory of classical aerodynamics. Simple solutions are then obtained by assuming that the wake remains in the plane of the airfoil and extends rearwards to infinity.

Retaining the analogy of a fixed wing in forward flight, consider now the case where the geometrical angle of attack changes as the wing advances. Under such conditions it is evident that the circulation will change, but since, in the case of ideal fluid, total circulation must remain constant, there must be a counter vortex in the wake corresponding to the change in circulation on the airfoil. This wake vorticity is generally referred to as the shed vorticity to differentiate it from the trailing vorticity which occurs both in the steady-state condition and when the blade is changing angle of attack. Since, as was seen above, the spiral vortex

system, even with constant strength, will generate harmonic downwash at the rotor disc, it is evident that the rotor blade in forward flight will have associated with it a shed as well as a trailing vortex system. For the simple analogy of a wing with constant circulation, the shed vorticity will be constant and parallel to the span resulting in the picture shown in Figure 5. It is evident that the shed vortex bears the same relationship to the trailing vortex as the starting vortex in the case cited above of an airfoil at constant angle of attack. However, since these vortices are continuously being shed, they cannot be assumed to be at infinity but must be correctly placed in the wake relative to the airfoil at a point in space determined by the airfoil position at the instant of shedding. In the simple picture shown in Figure 5 corresponding to an abrupt change of angle of attack at time $t - \Delta t$ with the airfoil moving at constant velocity V, the distance ξ^* of the airfoil from the shed vortex at any time t, is simply

$$\xi^* = V \Delta t$$

where the star indicates that ξ^* is dimensional. In forward flight, the velocity V at the blade section is not constant but varies with azimuth position. Consequently, this effect must be taken into account in positioning the vortices in the wake. Also, discrete line vortices are not shed if the blade is changing angle of attack harmonically, but instead a continuous sheet of vorticity whose strength varies harmonically is created.

Evidently, this shed vorticity will also induce downwash at the airfoil and will, in effect, result in a further reduction in angle of attack in addition to that generated by the trailing vortex system. This change in angle of attack can be evaluated for the simple two-dimensional case in terms of Bessel functions, and since it results in a reduction in lift, it is frequently referred to as a lift-deficiency function similar to the aspect-ratio effect of finite wing theory.

Because of the time varying nature of the loading, it is, therefore, necessary, in the case of a rotor, to consider not only the case of a trailing tip vortex and distributed trailing vortices, but also that of a spiral represented by the shed vorticity.

V. GENERAL DISCUSSION OF ROTOR LOADING

1) The Nature of the Aerodynamic Loading

In light of the discussions presented in the previous section, it becomes possible to discuss the physics of rotor aerodynamic loading in fairly simple terms. The primary element is the steady rotor lift generated by the bound circulation on the rotor blades. This bound circulation, as it leaves the blades, generates a spiral vortex system in the wake of constant strength dependent only on mean rotor thrust. The vertical component of induced velocity generated by this vortex system at a point on the blade, when combined with the horizontal velocity at the blade due to the blade rotation and forward speed, determines the induced angle. In the case of hovering flight, and for constant blade circulation along the span, it is well known that the induced velocity is constant over the rotor disc. However, in forward flight the wake spiral is not symmetrically located below the rotor but it is distorted by the forward velocity as shown in Figure 6. The induced velocity due to this distorted wake may be computed in terms of the wake geometry by the expressions given in Section VII. As might be expected, it is far from uniform over the disc. Consequently, the blade is subjected to a constantly varying induced angle as it rotates, and this is the primary source of the higher harmonic-blade loading.

Since the blade is subjected to time-varying airloads caused by the wake generated by the steady-state lift. In particular, for example, the airload varying as the nth harmonic of rotor speed must generate a trailing-wake system of variable strength which, in turn, will induce all harmonics of downwash at the rotor disc. Since the blade circulation is changing, there must also be a vortex system shed from the trailing edge of the blade at any instant equal and opposite in magnitude to the change in bound circulation, and this shed wake will also induce all harmonics of downwash at the rotor disc. Consequently, interharmonic coupling is potentially important. For example, if the nth harmonic airload induced large steady-state components of downwash to the mth harmonic, then the mth harmonic lift

13

would be appreciably changed by the harmonic airload and no direct solution to the problem could be obtained. It would be necessary to use an iterative procedure which would involve many hours of computer time in order to arrive at one numerical solution, and the question of convergence would always arise.

The numerical solutions for the forward flight case reported in Reference 24 were undertaken in order to explore the importance of this interharmonic coupling. It was found that the results of the analysis could be more easily interpreted by considering the wake in two parts; the "near" wake representing that portion in the immediate vicinity of the blade in question, and the "far" wake consisting of that portion from a quarter of a quadrant away from the blade and extending to infinity down the spiral. The exact boundaries of the near and far wakes are not of primary importance.

The near wake is relatively undistorted since it induces only a small portion of the spiral and, indeed, could be represented by a straight wake extending aft of the blade to infinity. It must, therefore, induce primarily the frequency of the bound circulation by which it was generated. The far wake induces all harmonics at the rotor disc due to its distorted spiral form; however, it is swept further downstream and, hence, becomes of decreasing importance as the advance ratio increases. Consequently, the contribution of a particular harmonic of circulation, say the nth, to another harmonic, say the mth, of downwash is usually of an order of magnitude less than its contribution to the nth harmonic of downwash. Also, the steady-state or 0th harmonic of circulation, which determines the rotor thrust, is an order of magnitude greater than any other harmonic of airload and so is the downwash which its wake induces at the rotor disc. Consequently, to first order, the nth harmonic of downwash at the blade consists primarily of two components:

a) The nth harmonic of downwash induced by the vorticity in the wake generated by the steady-state blade lift, and

b) The nth harmonic of downwash induced by the vorticity in the wake generated by the nth harmonic variation in circulation.

14

The lift changes due to (α) alone may be considered as a quasi-static lift change arising from a harmonic variation in angle of attack due to the nonuniform wake. This harmonic variation may be computed once the rotor and wake geometry are known, and is unaffected by any other blade motions or harmonic lift variations. The downwash components (b) result in a reduction and a phase shift of the quasi-static lift by an amount which again depends only on the rotor and wake geometry. This effect can, therefore, be tabulated as a generalized lift-deficiency function, C(k), as has been done for the fixed wing case in, for example, Reference 29. In Theodorsen's nomenclature

$$C(k) \ = \ F + i \, G$$

where F represents the reduction in lift and $\text{Tan}^{-1} \, G/F$ represents the phase shift.

Typical results are presented in Figure 7 for a shed wake of constant radial strength. The computation of these functions is a lengthy process involving extensive machine time and much manipulation because of the classical singularities of nonstationary flow theory as discussed in Section XI-3, but once having been computed, they are universally applicable.

In Figure 8, the contribution of all components of the wake to the lift deficiency is plotted as a function advance ratio. The increasing importance of the near wake, as the advance ratio increases, is evident as well as the relative unimportance of the trailing wake. In fact, at an advance ratio of 0.2, the reduction in lift, F, is substantially that which would be predicted by the two-dimensional theory. Since the hovering flight case, $\mu = 0$, is subject to a simple closed form solution, as will be discussed later, it is possible that for many engineering applications a reasonable approximation to this very complex analysis for F and G could be obtained by fairing a simple curve through the two known points at $\mu = 0.2$ and $\mu = 0$.

The convergence of C (k) for all harmonics towards the classical two-dimensional

15

solution for the higher advance ratios is shown in Figure 8, together with the insensitivity of this function to frequency at hovering, which is a conclusion of the closed form solution for this case.

Before leaving this general discussion of the aerodynamic loading, it is of interest to examine the components of downwash (a) and the general nature of the trailing-wake system generated by the steady rotor lift.

Minimum induced drag and, hence, the minimum energy and preferred condition can be shown for the case of hovering flight to correspond to the case of uniform bound circulation along the blade. Our computations indicate that this condition appears to persist in forward flight so that, regardless of twist, the circulation remains substantially constant over at least the outer 50 per cent of the blade span. The drop-off in circulation at the tip is quite rapid, depending on the blade chord to span ratio. The trailing-wake system due to steady rotor lift may, therefore, for purposes of discussion, and indeed for most analyses, be assumed to consist of a single tip vortex of known strength, since the rotor thrust is known, and another of equal strength located somewhat inboard of the 50 per cent span point. These vortices are swept back relative to the rotor by the forward speed and, consequently, a blade, as it advances toward the leading edge of the rotor, must pass over a series of vortices generated by itself and the other blades (Figure 6). Similarly, in returning towards the trailing edge, it must repass over this system of vortices. Consequently, any point on the blade will experience a fairly abrupt change in downwash on the advancing and retreating sides of the rotor, and this is a primary source of rotor vibration.

Figure 9 taken from Reference 24 shows the abrupt change in computed downwash as a function of azimuth induced by the tip vortex at the 95 per cent span location for a three-bladed rotor. The experimental data used for comparison was taken from some early tests conducted at M. I. T. in 1949 (Reference 22) in which the higher harmonics were attenuated. The rapid fluctuation in downwash predicted by theory was, therefore, not clearly defined by the tests. More recent experimental

16

data has, however, supported the prediction of these abrupt changes in downwash near the 90° and 270° azimuth positions. In particular, flight test data obtained on a four-bladed rotor by NASA (Reference 30) is compared in Figure 10 with loads computed in the manner described above. The abrupt change in load near the 90° azimuth is almost impulsive in nature and will have a high harmonic content. The number of blades used in a rotor will, therefore, have relatively little effect on the vibratory loads induced at the hub.

The computations of Reference 24 indicated that this abrupt load change is largely dominated by the vortex generated by the immediately-preceding blade, in the case of the four-bladed rotor, that located 90° anead of the blade in question. As the number of blades is increased, the vortex strength generated by each blade is reduced; however, the blade spacings will pass closer to the following blade. Computation for two-, three-, or four-bladed rotors thus shows little effect on the nature of this impulsive change in downwash.

The impulsive load, however, is highly localized along the blade and, as evident from Figure 10, travels down the blade as it advances from 90° to 180°. The localized nature of the downwash, due to the proximity of the vortex to the blade and also the rapid fluctuations in downwash associated with both the intensity of the vortex and this proximity, requires that all aspects of unsteady aerodynamics be carefully examined in predicting the resultant blade loads.

2) Unsteady Aerodynamic Effects

The effects which are of main concern in the classical treatment of wings in non stationary flow are those due to

a) The existence of the shed wake in addition to the usual trailing wake

b) The addition of an oscillatory component to the trailing wake, and

c) the existence of an additional pressure change on the airfoil due to its passage through a time-varying flow field.

If the nonstationary flow is defined as being oscillatory in nature, exact solutions are possible in terms of tabulated functions for the two-dimensional airfoil (Reference 29). Solutions have also been obtained for a two-dimensional approximation to the rotor in which the rotor wake is replaced by infinite vortex sheets at corresponding locations below the blade (References 4, 11, and 12). These investigations have shown that, for oscillations at harmonics of the rotor speed, the unsteady aerodynamic effects become of paramount importance and, for certain flight conditions, could result in values of the lift-deficiency function, F, close to zero. More usual values for the case of conventionally loaded rotors are of the order of 0.5 which, in effect, means that the slope of the lift curve of the blade for oscillatory loads is reduced by 50 per cent; evidently not a negligible effect.

Once the change in blade circulation has been defined as being oscillatory in nature, the strength of the shed vortex and its position, at any instant relative to the blade, can be defined for any three-dimensional system such as a rotor in forward flight. Consequently, the instantaneous velocity which the shed wake induces at any point on a blade can be computed. Similarly, the strength of the trailing vortex at any point in the wake is defined and its induced velocity field established.

Computation of the airloads is complicated by the existence of singularities in the solution. These occur as the shed wake approaches the trailing edge of the rotor and whenever the blade passes through a trailing vortex line generated by itself or another blade. The treatment of the singularities and of the nonuniform flow field presents no basic problem providing lifting-surface theory is used. However, this requires the numerical evaluation of the downwash at several chordwise as well as spanwise stations and, hence, may involve a prohibitive amount of machine computation time. Approximate methods have, therefore, been used to evaluate the unsteady aerodynamic effects and these will be discussed in Section V-3 below.

Before considering these treatments, it is interesting to review the case of vertical flight for which closed form solutions to the integrals presented in Section VII have been obtained. If it is assumed that the rotor has an infinite number of blades, the vortex spiral may be replaced by a column of vorticity and the vortex strength at any point in the column defined by the nature of the assumed circulation change along the blade. This circulation change could, for example, come from periodic change in pitch of the blade. By integrating Eqs. 15 and 16 in Section VII for the hovering case, $\mu = 0$, from the rotor plane to infinity, around the azimuth, $\mu = 0$ to 2π, and along the blade from root to tip, it was shown in Reference 24 in Section IX the lift deficiency function $C(k) = F + i G$ has the value

$$F = \frac{1}{1 + \dfrac{\sigma}{4} \dfrac{\pi}{\lambda_o}} \quad , \quad G = 0$$

where σ is the blade solidity and λ_o the mean inflow through the rotor. This result agrees almost exactly with the digital solution using a finite number of blades, except that G, for the case shown in Figure 7, does have a small value.

The interesting conclusion from this analysis is the fact that the lift-deficiency function is independent of frequency and can be given by a simple expression depending only on blade solidity and downwash. For the particular case of hovering flight and an ideally twisted blade an alternative form is

$$F = \frac{1}{1 + \dfrac{\lambda_o}{\alpha_T}}$$

where α_T is the blade angle of attack at the tip.

The reduction in lift curve slope at a given steady angle of attack will, therefore, become greater as the rotor loading and, hence, λ_o increases. Evidently the effect of increasing the spacing of the vortex spirals is offset by the increased intensity of the wake vorticity.

The singularities normally encountered in the solution of the downwash integrals have been cancelled for the hovering case by the assumption of an infinite number of blades which permits the solution in closed form given above. However, in the forward flight case, the existence of a finite number of blades has been shown in the previous section to be the dominant factor in determing rotor loads and it is, therefore, necessary to devise techniques capable of handling these singularities.

3) Lifting-Line Approximations to the Unsteady Aerodynamic Effects

One of the most troublesome of the singularities is that associated with a shed vortex approaching the blade. In the simplest solution for the blade airloads, it is convenient to replace the blade by a single vortex line. Normally, the high-aspect ratio of conventional rotors would suggest that this is a reasonable approach. However, the following brief analysis illustrates the nature of the errors associated with the lifting-line approximation.

Consider, for simplicity, the classical two-dimensional case in which the wake is assumed to extend in the plane of the airfoil to infinity. The airfoil will now be replaced by a point vortex and the geometric incidence, α, varied harmonically with frequency ω so that at any time t

$$\alpha(t) = \alpha_s \sin \omega t + \alpha_c \cos \omega t$$

The bound circulation Γ will, therefore, also vary harmonically or

$$\Gamma(t) = \Gamma_s \sin \omega t + \Gamma_c \cos \omega t$$

At a point in the wake a distance ξ from the blade, an element of vorticity $\gamma(\xi) \, d\xi$ will have been shed at time $t - \Delta t$ of strength equal and opposite

20

to the change in circulation on the airfoil when it passes this point. Therefore,

$$\gamma'(\xi)\,d\xi = - \frac{d\,\Gamma\,(t-\Delta t)}{dt}\,dt$$

$$= -\omega\left[\,\Gamma_s\cos\omega(t-\Delta t) - \Gamma_c\sin\omega(t-\Delta t)\,\right]\,dt$$

If the airfoil is moving with constant velocity V then

$$V = \frac{d\xi}{dt} \quad,\text{ hence }\quad \Delta t = \frac{\xi}{V}\quad\text{ and}$$

$$\gamma(\xi) = -\frac{\omega}{V}\left[\,\Gamma_s\cos\omega(t-\frac{\xi}{V}) - \Gamma_c\sin\omega(t-\frac{\xi}{V})\,\right]$$

The velocity induced at the airfoil by the infinite wake in the plane of the airfoil is

$$w = \int_\epsilon^\infty \frac{\gamma(\xi)\,d\xi}{2\pi\,\xi}$$

where ϵ is a lower limit yet to be defined. The induced velocity w in turn induces an angle w/V at the airfoil. The corresponding circulation, Γ_w induced by the wake is, therefore, for the simple lifting line case, $\Gamma_w = 2\pi bw$ where b is the half chord.

After substitution and expansion of the trigonometric functions, the wake-induced circulation becomes

$$\Gamma_w = -\,k\,I_c\left[\,\Gamma_s\cos\omega t - \Gamma_c\sin\omega t\right]$$

$$-k\,I_s\left[\Gamma_s\sin\omega t + \Gamma_c\cos\omega t\right]$$

where k is the reduced frequency, $\omega b/V$, and

$$I_c = \int_{\epsilon_c^*}^\infty \frac{\cos k\,\xi^*}{\xi^*}\,d\xi^* \quad,\quad I_s = \int_{\epsilon_s^*}^\infty \frac{\sin k\,\xi^*}{\xi^*}\,d\xi^*$$

21

$$F = \frac{1}{1 + k \, I_s}$$

If the lower limit $\mathcal{E}_s$ is replaced by zero, that is, if the wake is integrated up to the vortex representing the airfoil, I_s has the value $\pi/2$ and

$$F = \frac{1}{1 + \frac{\pi}{2} \cdot k}$$

This value agrees closely with the exact value up to k of about 0.5.

However, if I_c is not to be an improper integral, $\mathcal{E}_c$ must have some value other than zero. Several methods of establishing the limit $\mathcal{E}_c$ for the purpose of evaluating the rotor airloads in forward flight will now be discussed.

The simplest method is to eliminate I_c by choosing a sufficiently large value of $\mathcal{E}_c$, for example, equal to the interval size used in numerical integration. The interval size is usually of the order of five degrees of azimuth or greater, and the nature of I_c is such that this interval size is sufficient to make i_c insignificant, since the numerical value of the cosine integral is highly sensitive to the lower limit. On the other hand, the numerical value of the sine integral I_s is not sensitive to the lower limit, at least for values of k less than 0.5. The result of using this computation technique is, therefore, to estimate the value of F with reasonable accuracy at the lower reduced frequencies but to lose most of the phase shift due to the shed wake. Such a solution, however, is certainly a first approximation to the unsteady aerodynamic effects.

Another method is that suggested in Reference 24 in which combined lifting-line and lifting-surface theory was used. A limit $\mathcal{E}$ was chosen well away from the blade, and this defines the limit of the far wake as previously discussed. The far

22

wake was treated using lifting-line theory and the remainder of the wake, from $\mathcal{E}$ to the blade, was treated using lifting-surface theory. Since the near wake is relatively undistorted, the curved wake was replaced by a straight wake extending aft to infinity. Also, since the work of Reference 13 indicated that a two-dimensional solution closely approximates the three-dimensional solution for such a case, the near wake was treated using techniques similar to the classical two-dimensional theory. However, the computational sequences for such a combined analytical and digital solution are clumsy and not well suited to machine computational techniques. Consequently, a simpler method was developed in Reference 25 in which $\mathcal{E}$ was chosen so that the lift deficiency and phase shift predicted by the simple lifting-line theory developed above would be the same as that predicted by the equivalent lifting-surface theory, for example, by F and G of Reference 29. The identities to be satisfied are

$$1 + k \, I_s = \frac{F}{F^2 + G^2} \qquad \text{and} \qquad k \, I_c = \frac{G}{F^2 + G^2}$$

from which, for any value of k, the lower limits to the sine and cosine integrals may be obtained from tabulated results. These limits are shown in Figure 11 and, for $\mathcal{E}_c$, are close to the rear neutral point of the blade. By assuming that the limits will be unchanged by the small curvature of the near wake, they may be used directly in the numerical integration of the expressions for rotor-wake induced flow given in Section VII. The equivalent limit in azimuth position at blade station ηR is $\Delta \phi = \mathcal{E}^* b / \eta R$ and is of the order of one to two degrees for normal rotor blades.

4) Lifting-Surface Theory for Unsteady Aerodynamics

The airloads acting on a blade of finite chord due to an induced flow field with rapid fluctuations may be conveniently obtained using thin airfoil theory. This method is readily adaptable to the machine computational techniques used for obtaining the induced flow.

The method used here consists of representing the airfoil by a sheet of

distributed chordwise vorticity. It will be assumed that the spanwise components of vorticity on the airfoil may be neglected, although this assumption is certainly open to question in view of the rapid spanwise variations in load associated with passage over the intense tip vortex. However, the assumption is believed to represent a reasonable compromise between computational complexity and accuracy.

The chordwise vorticity may be represented by the series

$$\gamma(x) = A_o \tan \frac{\theta}{2} + \sum_1^\infty A_n \sin n\theta$$

where the distance from the center of the airfoil to any point on the airfoil is given by

$$x = b \cos \theta$$

Then the induced flow at any point x on the blade due to the bound vorticity is (Reference 31)

$$v(x) = \frac{A_o}{2} + \sum_1^\infty \frac{A_n}{2} \cos n\theta$$

if the vorticity w(x) induced at any point on the airfoil by the wake vorticity is expressed as a similar series

$$w(x) = \frac{B_o}{2} + \sum_1^\infty \frac{B_n}{2} \cos n\theta$$

it follows that, in the linearized solution, $A_n = B_n$ since the boundary conditions on the airfoil require that $w(x) + v(x) + u(x) = 0$, where $u(x)$ is the velocity normal to the airfoil due to the geometric angle of incidence and the blade motions. If the downwash is computed at a sufficient number of stations along the chord, the coefficients B_n can be determined by harmonic analysis for any wake-induced velocity distribution which it is desired to examine.

24

Analytical solution of the problem would require the evaluation of integrals obtained from the expressions for the velocities w, u, and v derived in Sections VI and VII in order to obtain the Fourier coefficients of chordwise vorticity distribution along the blade chord. It is evident, from the expressions derived in the next section for the velocity $w(x)$, that direct solution for this type is not possible because of the obvious difficulty of solving the resulting integral equations in closed form. However, several approximate solutions have been obtained for the case of finite wings, and exact solutions are available for the two-dimensional airfoil. A brief derivation, using the approach developed in this report for the rotor, is presented in the following section, since it has been found convenient to modify slightly the familiar treatments when considering the three-dimensional rotor.

Following this derivation the downwash is defined for the case of a three-dimensional rotor and a method of solution suggested using the concept of a near and far wake. This is the most accurate solution of the several developed in this report and was developed in order to establish a reference for later approximations. The adequacy of this solution is established by comparison with an equivalent two-dimensional approximation.

Closed-form solutions are then obtained for the case of hovering rotor, giving the results briefly referred to in Section V-2 above.

Techniques are then developed, using lifting-line theory, which result in considerable simplifications in the analysis. The effects of a finite chord are then separately evaluated. Finally, the possibility of developing generalized lift-deficiency functions are evaluated and some typical values are presented.

nts

25

VI. TWO-DIMENSIONAL SOLUTION FOR OSCILLATING AIRFOIL

The following very brief analysis is included in order to relate the treatment of the nonstationary flow effects contained in this paper to the classical analyses in the literature. Chapters 5 and 7 of Reference 32 contain a complete development and review of both the two- and three-dimensional cases.

If the chordwise vorticity is represented by the series

$$\gamma(x) = A_o \tan \frac{\theta}{2} + \sum_{n=1}^{\infty} A_n \sin n\theta \tag{1}$$

and the distance from the center of the airfoil to a point aft on the airfoil is given by

$$x^* = b \cos \theta$$

then the induced flow at x^*, due to an element of vorticity on the airfoil at η, is

$$d v(x) = \frac{\gamma(\eta)\, d\eta}{2\pi(x^* - \eta)}, \text{ positive down} \tag{2}$$

which, when integrated from $-b$ to $+b$ gives (Reference 31 - Chapter VII)

$$v(x) = \frac{A_o}{2} + \sum_{i}^{\infty} \frac{A_n}{2} \cos n\theta \tag{3}$$

Assume now that the airfoil is moving with velocity, V, and has a velocity perpendicular to its surface, $u(x)$ (positive down), at station x resulting from the angle of attack, α, positive down and the vertical velocity at the center of twist, $\dot{Z}$, positive down. If the center of twist is located a distance ab aft from the center of the airfoil, then

$$u(x) = \alpha V - \dot{Z} + (x^* - ab) \dot{\alpha}$$

26

Every change in circulation associated with these motions results in an element of vorticity, $\gamma d\xi^*$, being shed at the trailing edge whose strength is equal and opposite to the change in bound circulation. Thus,

$$\gamma d\xi^* = -d\Gamma_b \tag{3a}$$

ξ^* is the distance of the element of vorticity from the center of the airfoil, dimensional when starred. The velocity at the airfoil perpendicular to its surface induced by $\gamma d\xi^*$ is, for the sign convention of Figure 3,

$$w(X) = \frac{-\gamma \, d\xi^*}{2\pi(\xi^* - x^*)} \tag{4}$$

In the linearized solution, the boundary conditions on the airfoil require that, for each element of vorticity in the wake,

$$v(x) + u(x) + w(x) = 0 \tag{5}$$

or

$$\frac{A_o}{2} + \sum_{1}^{\infty} \frac{A_n}{2} \cos n\theta + [\alpha V - \dot{z} + (x^* - ab)\dot{\alpha}] - \frac{\gamma \, d\xi^*}{2\pi(\xi^* - x^*)} \tag{6}$$

The Fourier coefficients A_n may be readily determined with the aid of Reference 3, Page 99, from which is obtained

$$\int_0^\pi \frac{\cos n\theta}{\xi - \cos\theta} \, d\theta = \frac{\pi[\xi - \sqrt{\xi^2 - 1}]^n}{\sqrt{\xi^2 - 1}} \tag{7}$$

whence

$$A_o = \frac{\gamma \, d\xi}{\pi} \frac{1}{\sqrt{\xi^2 - 1}} + 2(\dot{z} - \alpha V + ab\dot{\alpha})$$

$$\frac{A_1}{2} = \frac{\gamma d\xi}{\pi} \left[\frac{\xi}{\sqrt{\xi^2 - 1}} - 1 \right] - b\dot{\alpha}$$

$$\frac{A_n}{2} = \frac{\gamma d\xi}{\pi} \left[\xi - \sqrt{\xi^2 - 1} \right]^n \frac{1}{\sqrt{\xi^2 - 1}} \tag{8}$$

The incremental lift and moment on the airfoil, due to the instantaneous displacements and in the presence of the flow field generated by $\gamma d\xi^*$, may now be computed for the vortex pair consisting of $\gamma d\xi^*$ and $d\Gamma_b$ on the airfoil, postulating that these are the only two elements of vorticity existing in the system. Bernoulli's equation, extended to unsteady flow, gives the pressure difference on the upper and lower surfaces as

$$(P_U - P_\ell) = -2\rho \left[\frac{\partial \phi}{\partial t}(x) + V \frac{\partial \phi}{\partial x^*}(x) \right] \tag{9}$$

The second term includes the quasi-static effects arising from the instantaneous airfoil geometry; the first term accounts for the time rate of change of velocity perpendicular to the airfoil, including apparent mass effects and those arising from the nonuniform velocity, $w(x)$, at the airfoil due to $\gamma d\xi$. Therefore, when replacing the blade by a lifting line, terms in $\partial\phi/\partial t$ due to $\partial\xi/\partial t$ should be dropped. When $z \neq 0$, as in the far wake, $\partial\phi/\partial t$ will contain terms due to $\dot{z}$. However, in general, $\dot{z} \ll \dot{\xi}$ and its effects have, therefore, been neglected, except as they determine the instantaneous vertical position of $\gamma d\xi$ in the "semi-rigid" wake solutions.

The velocity potential, in terms of the distributed vorticity, is

$$\phi(x) = \frac{1}{2} \int_{-b}^{x^*} \gamma \, dx^*$$

whence

$$\frac{\partial \phi}{\partial x^*}(x) = \frac{1}{2} \gamma(x)$$

and

$$\frac{\partial \phi}{\partial t}(x) = \frac{1}{2} \frac{\partial}{\partial t} \int_{-b}^{x^*} \gamma(x) \, dx^*$$

28

The lift on the airfoil is

$$L = - \int_{-b}^{+b} (P_u - P_\ell) \, dx^*$$

and after substituting $\gamma(x)$ in the form given by Eq. (1), the lift is obtained in terms of the coefficients A_n, as

$$dL = \rho \pi b \left\{ \frac{1}{2} \frac{\partial}{\partial t} (A_o - \frac{1}{2} A_2) b + \frac{\partial}{\partial t} (A_o + \frac{1}{2} A_1) b + V (A_o + \frac{1}{2} A_1) \right\} (10)$$

The circulation on the airfoil is

$$d\Gamma = \int_{-b}^{+b} \gamma \, dx^* = \pi (A_o + \frac{1}{2} A_1) b \tag{11}$$

This is the lift and circulation on the airfoil at any instant due to the element of vorticity, $\gamma \, d\xi$, in the wake and its counter vortex on the airfoil, $d\Gamma_b$. Since the rigid wake of constant strength is assumed, this element of vorticity in the wake has constant strength with time or

$$\frac{\partial}{\partial t} (\gamma \, d\xi) = 0$$

If the element of vorticity and the blade circulation, $d\Gamma_b$, are to constitute a vortex pair, then

$$d\Gamma_b = - \gamma d\xi^*$$

and

$$\frac{\partial}{\partial t} d\Gamma = \frac{\partial}{\partial t} (A_o + \frac{1}{2} A_1) = 0$$

which also defines the time history of airfoil motion required so that in moving a distance ξ^* after shedding the element of vorticity, $\gamma \, d\xi^*$, no additional circulation has been generated by the airfoil. Then

$$dL = \rho \pi b \left\{ \frac{1}{2} \frac{\partial}{\partial t} (A_o - \frac{1}{2} A_2) b + V (A_o + \frac{1}{2} A_1) \right\}$$

Differentiating the first term with respect to t and noting that $\partial / \partial t = (V/b) \, \partial / \partial \xi$ results in

29

$$dL = \frac{\rho V \gamma \, d\xi}{\sqrt{\xi^2 - 1}} - 2\pi\rho V b \, [\alpha V - \dot{z} + \dot{\alpha}(.5b - a^*)] + \rho\pi(\ddot{z} - \dot{\alpha}V + a^*\ddot{\alpha})b^2$$

The first two terms represent the lift due to the vortex pair of which the second term is the "quasi-static" lift, L_q. The third term represents the apparent mass and damping effects due to the noncirculatory flow. Integrating the first term for the effects of all elements of vorticity, which have been shed from the start of the motion, and leading to the present instantaneous airfoil position,

$$L = \rho V \int_1^\infty \frac{\gamma \, d\xi}{\sqrt{\xi^2 - 1}} + L_q - \rho\pi(\dot{\alpha}V - \ddot{z} - a^*\ddot{\alpha})b^2 \qquad (12)$$

Similarly, the total circulation acting on the airfoil is, from Eq. (11)

$$\Gamma_b = \int_1^\infty \left[\frac{\xi + 1}{\sqrt{\xi^2 - 1}} - 1\right]\gamma \, d\xi - 2\pi b \, [\alpha V - \dot{z} - \dot{\alpha}(.5b - a^*)]$$

and this must be equal and opposite to the total circulation in the wake or

$$\Gamma_b = -\int_1^\infty \gamma \, d\xi$$

Whence

$$\int_1^\infty \frac{\xi + 1}{\sqrt{\xi^2 - 1}} \gamma \, d\xi = 2\pi b \, [\alpha V - \dot{z} - \dot{\alpha}(.5b - a^*)] = \frac{-L_q}{\rho V} \qquad (13)$$

Combining Eqs. (12) and (13)

$$L = L_q \frac{\int_1^\infty \frac{\xi\gamma \, d\xi}{\sqrt{\xi^2 - 1}}}{\int_1^\infty \frac{\xi\gamma \, d\xi}{\sqrt{\xi^2 - 1}} + \int_1^\infty \frac{\gamma \, d\xi}{\sqrt{\xi^2 - 1}}} - \rho\pi b^2(\dot{\alpha}V - \ddot{z} - a^*\ddot{\alpha})$$

If the displacements z and α vary harmonically with time, then L will also be of the form $L = L_o e^{i\omega t}$ and, as in Section VIII, the first term, may be readily identified as the classical lift-deficiency function $C(k)$.

30

The incremental moment about the center of twist acting on the airfoil is

$$dM = \int_{-b}^{+b} (P_u - P_\ell)(x^* - ba)\, dx^*$$

$$= a\, b\, dL - \frac{\pi \rho}{4} b^2 \left\{ b\frac{\partial A_o}{\partial t} + \frac{3}{4} b \frac{\partial A_1}{\partial t} - \frac{1}{4} b \frac{\partial A_3}{\partial t} - V(2A_0 - A_2) \right\}$$

After substituting for the coefficients A_n and their time derivatives,

$$dM = a\, b\, dL + \frac{\rho V b^2 \gamma\, d\xi}{2\sqrt{\xi^2 - 1}} + \frac{\pi \rho \ddot{\alpha} b^4}{8} - \rho \pi V(\alpha V - \dot{z} - ab\dot{\alpha})b^2$$

Adding dL from the previous analysis and summing up over the entire wake gives

$$M = -\rho V b^2 \int_{1}^{\infty} \frac{\xi a - .5}{\sqrt{\xi^2 - 1}} \gamma\, d\xi - \rho\pi [\dot{\alpha} V - \ddot{z} - ab\ddot{\alpha}]ab^3 + \frac{\rho\pi \ddot{\alpha} b^4}{8} - \rho\pi V(\alpha V - \dot{z} - ab\dot{\alpha})b^2$$

Substituting Eq. (13) results in

$$M = L_q (a + .5) \frac{\int_{1}^{\infty} \frac{\xi\gamma\, d\xi}{\sqrt{\xi^2 - 1}}}{\int_{1}^{\infty} \frac{\xi\gamma\, d\xi}{\sqrt{\xi^2 - 1}} + \int_{1}^{\infty} \frac{\gamma\, d\xi}{\sqrt{\xi^2 - 1}}}$$
$$+ \rho\pi a(\ddot{z} + ab\ddot{\alpha})b^3 + \rho\pi V\dot{\alpha}(.5 - a)b^3 + \frac{\rho\pi \ddot{\alpha} b^4}{8} \tag{14}$$

Examination of Eq. (14) and the expression for L_q,

$$L_q = -2\pi \rho V b [\alpha V - \dot{z} + \dot{\alpha} b(.5 - a)],$$

indicates that the forces and moments acting on the oscillating airfoil may be resolved into the following components:

a) a force acting at the 25 per cent chord due to the angle of attack at the 75 per cent chord (rear neutral point) and multiplied by $C(k)$,

b) a force due to the angular velocity $\dot{\alpha}$ of the airfoil acting at the 75 per cent chord point and given by $\rho\pi V \dot{\alpha} b^2$,

31

c) a force due to the apparent mass term, $\pi \rho b^2 \ddot{z}$, acting at the center of the airfoil, and a moment $\pi \rho b^4 \ddot{\alpha} / 8$.

Identification of the forces and moments in this manner frequently permits a considerable amount of simplification in handling the aerodynamic coupling terms when

$$\dot{\alpha} \, b \, (\, .5 - a) \ll \dot{z}$$

as is generally the case for helicopter rotor blades. This point is discussed further in Reference 5.

VII. THREE-DIMENSIONAL ROTOR-DOWNWASH RELATIONSHIPS

The basic relationship required to compute the downwash at the rotor disc for a three-dimensional rotor operating in forward flight at an advance ratio, μ, will now be developed. Certain statements must first be made as to the nature of the wake vorticity.

First, the concept of a "semirigid" wake will be introduced; i.e., every element of vorticity will be assumed to retain the instantaneous vertical velocity imparted to it at the moment it was shed or trailed. This establishes a spiral wake descending at every spanwise station with a constant velocity in time, but permits different vertical velocities azimuthwise. The spiral sheet representing the wake thus continuously changes shape as it descends. Other than establishing the in-stantaneous wake location, the effects of this wake velocity will be neglected (see Section VI). The effect of the wake on its own velocity will also be neglected. Changes in the mean velocity, which establish the spiral spacing as the wake descends, are thus ignored as well as the tendency for vortex-vortex interaction of the individual spirals. Since the induced velocity at the rotor plane is determined primarily by the first few spirals, this assumption is believed to be valid. Furthermore, it is most probable that the vortex sheets will roll up and form two individual vortex lines in the fully developed wake as in the case of fixed wing aircraft; particularly since a variable downward velocity, decreasing towards the center of the rotor, implies an eventual crossing and almost certain intermingling of the vortex sheets in the wake. Further refinement of the mathematical model does not, therefore, appear to be warranted at the present time.

Second, the assumption, inherent in all fixed wing analyses, of a vortex strength constant in time will be made; that is, viscous effects will be ignored. Although this assumption is less satisfying for the case of the returning spiral wake of the relatively lightly-loaded rotor than in the case of a wing in which the wake extends rearward to infinity or for a highly-loaded propeller, it is consistent with the previous assumption and is justifiable on the same basis.

Finally, the effect of the wake-induced velocities in the plane of the blade will be ignored.

The basic relationship required to compute the downwash at the rotor disc for a three-dimensional rotor, operating at an advance ratio, μ, will now be developed (Figure 12). The downwash generated by an element $d\bar{s}$ of a trailing vortex line with strength Γ at a distance $\bar{A}$ from the element is, in vector notation,

$$d\bar{q} = \frac{\Gamma \, d\bar{s} \times \bar{A}}{4 \pi a^3}$$

It will be assumed that the element of vorticity has been generated from the trailing edge of the blade at a spanwise station ℓ from the center of rotation when the blade was at azimuth angle ϕ. The vertical component of downwash, dw_1, which this element induces at another spanwise station η and chordwise station x of the blade when the blade has rotated to an azimuth angle ψ, is

$$dw_1 = \frac{\Gamma}{4\pi R} \cdot \frac{ds_2 \, A_1 - ds_1 \, A_2}{(A_1^2 + A_2^2 + A_3^2)^{3/2}} \qquad (15)$$

$$= f(\phi) \, d\phi$$

where

$$ds_1 = \mu \, d\phi \cos\phi \qquad ds_2 = \mu \, d\phi \sin\phi + \ell \, d\phi.$$

and

$$A_1 = \ell + d \cos\phi - \eta \cos(\psi - \phi) - x \sin(\psi - \phi)$$

$$A_2 = x + d \sin\phi + \eta \sin(\psi - \phi) - x \cos(\psi - \phi)$$

$$A_3 = -z$$

All distances are nondimensional in terms of blade radius, R.   x is a chordwise distance measured from a reference point on the blade; for example, the quarter chord point and χ is the distance from this point to the origin of the trailing vortex line. d is the distance travelled by the rotor hub during the time $t = \frac{\psi - \phi}{\Omega}$ and z is the vertical distance of the element of vorticity below the blade.   If m is the number of wake spirals to be used, then

$$d = [(2\pi m + \psi) - \phi + \xi] \mu$$
$$z = [(2\pi m + \psi) - \phi + \xi] \lambda + z_{\ell}(\eta) - z_0(\ell)$$

where z_0 is the steady-state displacement of the blade out of the tip path plane, and ξ is the spacing between the blade generating the vorticity and the blade at which the downwash is to be computed.   For a rigid blade $z_{\ell}(\eta) - z_{\ell}(\ell) = a_{\ell}(\eta - \ell)$.

If the rigid wake is assumed, λ is the mean inflow through the rotor determined from the known thrust and rotor attitude.   If nonrigid wake concepts are to be used, then λ is represented by the series:

$$\lambda = \lambda_0 + \sum_{n=1}^{\infty} \lambda_{nc} \cos n\phi + \lambda_{ns} \sin n\phi$$

The coefficients λ_n may be approximated, at advance ratios below $\mu = 0.1$, by the various harmonics of inflow at the rotor disc obtained from a first iteration using initially uniform inflow.   This is equivalent to assuming that each element of vorticity retains the velocity imparted to it at the rotor disc at the instant it left the blade. More accurately, the coefficients λ_n may be established by using a mean value of inflow experienced by each element in one revolution as it travels rearward under the rotor.

The total downwash due to a single trailing vortex is obtained by integrating Eq. (15) up the wake for each blade.

This determines the downwash in terms of the strength Γ of a trailing-vortex filament in the wake generated by the change in bound circulation along the blade. In the quasi-static solution, this change may be assumed to occur in n (usually five)

35

increments along the blade and a vortex filament trailed between each increment of strength, equal to the change in bound circulation between two adjacent increments. The downwash at the midpoint of each increment can be then expressed in terms of the wake vortex strengths. The bound vortex strength is, in turn, expressed in terms of the downwash and the blade pitch angle. The n resulting simultaneous equations may then be solved for the downwash and loading.

The downwash due to the shed vortex system is

$$dw_2 = - \frac{1}{4\pi R} \times \frac{d\Gamma}{d\phi} d\phi \frac{A_2 \, d\ell}{(A_1^2 + A_2^2 + A_3^2)^{3/2}}$$

$$= F(\phi) \, d\phi \tag{16}$$

This expression should be integrated with respect to ℓ over each finite interval of the blade before integrating with respect to ϕ (see Eq. (21), page 57).

VIII. SUGGESTED THREE-DIMENSIONAL SOLUTION AND COMPARISON WITH EQUIVALENT TWO-DIMENSIONAL SOLUTION

1) Method of Solution

In this section a combined analytical and numerical procedure will be considered to obtain the desired solutions. The rotor wake will be divided into a "near" wake and a "far" wake, the near wake including that portion attached to the blade and extending approximately one-quarter quadrant from the blade trailing edge.

The chordwise variations in the velocity w induced at the airfoil by the far wake will be neglected. This is equivalent to using lifting-line theory when computing the effects of the far wake on the airfoil bound circulation and lift. If $f(\phi)$ and $F(\phi)$ of Eqs. (15) and (16) are independent of x, then the Fourier coefficients of blade chordwise vorticity are zero except for A_o whose value, for a uniform wake induced downwash, w, along the blade chord is, from Eq. (5) and Eq. (3), $A_o = -2w$. The bound circulation induced on the blade by w is, therefore, from Eq. (11),

$$\Gamma_b = -2\pi bw \tag{17}$$

and the corresponding lift is, from Eq. (10)

$$L = -2\pi\rho b w V = \rho \Gamma_b V \tag{18}$$

The lifting-line approximation will also be used for the near trailing wake, an approximation which is clearly justified for the high "aspect ratios" of rotors and rotor/propellers.

The near shed wake will be treated using analytical techniques and lifting surface theory. In order to examine the validity of this approach, the two-dimensional

37

treatment of the rotor of Reference 6 will be rederived using a similar treatment of the near and far wake.

2) Evaluation of Far Wake Lifting-Line Approach for Two-Dimensional Case

In Reference 4, the effect of the returning wake is determined using a two-dimensional model for the three-dimensional rotor. The far wake is replaced by rows of distributed shed vorticity extending to $\xi = \pm\infty$ below the rotor (Figure 12) at distances $z = nh$ from the rotor plane in which the near wake is contained. The near wake extends from the trailing edge, $\xi = 1$, to infinity. All distances are nondimensionalized in terms of the blade semichord, b.

The velocity induced by an element of vorticity, $\gamma' d\xi$, in the far wake will now be averaged over the blade chord (Eq. (17)), using the results derived in Section VI for the element of vorticity, $\gamma d\xi$, in the near wake, and the integrations performed over both portions of the wake separately. This results in an expression for blade circulation

$$
\Gamma_b = \int_1^\infty b \left[\frac{\xi + 1}{\sqrt{\xi^2 - 1}} - 1 \right] \gamma \, d\xi
$$
$$
+ \sum_{n=1}^\infty b \int_{-\infty}^\infty \frac{\xi}{n^2 h^2 + \xi^2} \gamma' \, d\xi + \frac{L_q}{\rho V}
$$

where L_q is the quasi-static lift; that is, the lift generated in the absence of wake effects. It is shown in Section VI that the lift may be written in terms of the coefficients of Eq. (1) as

$$
dL = b\rho\pi \left\{ \frac{1}{2} \frac{\partial}{\partial t} (A_o - \frac{1}{2} A_2) b + V (A_o + \frac{1}{2} A_1) \right\} ,
$$

38

and again, if the velocity induced over the blade by the far wake is constant over the chord and $\partial\phi/\partial t = 0$, as discussed in Section VI for the lifting-line approximation, then, after substitution for the coefficients and integration over near and far wake,

$$L = \rho V b \int_{1}^{\infty} \frac{\gamma \, d\xi}{\sqrt{\xi^2 - 1}} + \rho V b \sum_{n=1}^{\infty} \int_{-\infty}^{\infty} \frac{\xi}{n^2 h^2 + \xi^2} \gamma' \, d\xi$$

$$+ L_q - \rho \pi \ddot{z} b^2$$

The last term represents the apparent mass or impulsive force. Identifying the shed vorticity with the position of the blade at the time of its shedding, $t - \Delta t$, and assuming a harmonic variation, $\gamma(t) = \gamma_o e^{i\omega t}$,

$$\gamma(t - \Delta t) = \gamma_o e^{i\omega[t - \frac{b}{\Omega R}(\xi - 1)]}$$

$$\gamma'(t - \Delta t) = \gamma_o e^{i\omega[t - \frac{b}{\Omega R}(\xi - 1) - \frac{2\pi n}{\Omega}]}$$

and with $\gamma \, d\xi^* = -\frac{d\Gamma}{dt} \, dt$ (from Eq. (3a)), the lift-deficiency function is obtained after manipulations identical to those outlined in Section VI, as

$$C(k, m, h) = \frac{L}{L_q} = \frac{\int_{1}^{\infty} \frac{\xi}{\sqrt{\xi^2 - 1}} e^{-ik\xi} \, d\xi}{\int_{1}^{\infty} \frac{\xi + 1}{\sqrt{\xi^2 - 1}} e^{-ik\xi} + \sum_{n=1}^{\infty} e^{-2\pi i m} \int_{-\infty}^{\infty} \frac{\xi}{n^2 h^2 + \xi^2} e^{ik\xi} \, d\xi}$$

where $m = \frac{\omega}{\Omega}$ and $k = \frac{\omega b}{\Omega R}$. The integrals may be evaluated as in References 4 and 29, whence,

$$C(k, m, h) = \frac{J_1 - iY_1}{J_1 - iY_1 + Y_0 + iJ_0 + \frac{2i}{e^{ik}e^{2\pi i m} - 1}}$$

Since the intermediate steps in the above derivation follow the methods of Reference 4, only the essential derivations have been included in the above very brief outline. The nomenclature is the same as that of Reference 4, consequently, care should be taken to avoid confusion of the n and m used here (in Reference 4, n defines the nth wake below the rotor and $m = \frac{\omega}{\Omega}$) with the n and m used elsewhere in this paper, which define the harmonic of rotational speed and the mth wake spiral. For the conditions

39

of harmonic loading, to which the analyses of this paper are confined, $m = \frac{\omega}{\Omega}$, is always an integer; therefore, $e^{2\pi i m} = 1$.

In Figure 13, a comparison of the exact solution of Reference 4 with the approximate solution given above is made for the range of reduced frequencies of interest in the present analysis. The real portion of $F(k)$, which establishes the reduction in slope of the lift curve, is closely approximated. At the lower values of h, the error in phase shift, represented by $G(k)$, becomes appreciable. Since the h of interest in rotors is usually above 1, this difference does not introduce serious error.

The relative unimportance of the phase shift in determining the magnitude of harmonic loading suggests a further simplification in which the rows of distributed vorticity are replaced by a continuous vortex sheet, an assumption which has a close parallel in the classical vortex theory of the propeller. When the frequency of oscillation ω is now restricted to harmonics of the rotational speed, the vortex strength of any horizontal distance ξ from the airfoil will be the same at all values of z, where z is the vertical distance below the rotor and now replaces nh. The induced velocity at the airfoil, due to an element of vorticity in the wake, is

$$d w = - \frac{1}{2 \pi b} \left[\frac{\xi - x}{Z^2 + (\xi - x)^2} \right] \gamma (\xi, Z) \, d\xi^*$$

An infinite spiral sheet implies an infinite number of blades in which case $x \longrightarrow 0$ in the above expression. For harmonic loadings, the blade circulation, Γ_b, will be of the form

$$\Gamma_b = \Gamma_n e^{in\Omega t} \qquad\qquad \gamma = \gamma_n e^{in\Omega t}$$

and the element of vorticity in the wake, $\gamma (\xi, z)$, may be identified with the circulation at the time of shedding at time $t - \Delta t$. For any spiral at distance z below the rotor and using Eq. (3a)

$$\gamma(\xi, \overline{z}) \, d\xi^* = \gamma(\xi) \, d\xi^* = -\frac{d}{dt} \frac{d\Gamma}{dz} \, dz \, dt$$

Also,

$$\frac{d\xi^*}{dt} = \Omega R \qquad \text{and} \qquad \Delta t = \frac{\xi^*}{\Omega R}$$

whence

$$\gamma_n(\xi) = -\frac{in}{R} \frac{d\Gamma_n}{dz} \times e^{\frac{-in\xi^*}{R}} \, dz$$

For the "rigid" wake, the spacing between vortex rows, h, is given by

$$\frac{Q h b}{2 \pi R} = \lambda_o \qquad \text{or} \qquad h = \frac{2 \pi R \lambda_o}{Q b}$$

where Q is the number of blades. Therefore, in the limit

$$\frac{d \Gamma}{d z} = \frac{Q b}{2 \pi R \lambda_o} \Gamma_n \, e^{in\Omega t}$$

Integrating the effect of the entire wake results in an expression for the mean velocity at the airfoil

$$w = \frac{in \Gamma_n \, e^{in\Omega t} \, Q}{4 \pi^2 R \lambda_o} \cdot b \int_0^\infty \int_{-\infty}^\infty \frac{e^{inb \, \xi/R}}{z^2 + \xi^2} \, d\xi \cdot dz$$

The integrals may be evaluated with the help of Reference 32, Table 103, giving the result

$$w = \frac{Q}{4 \pi \lambda_o R} \Gamma_n \, e^{in\Omega t}$$

This is the instantaneous downwash at the blade. Since the airfoil dimension in the x plane has not been considered, the instantaneous lift will be determined by the quasi-static lift and this induced velocity. Assuming a blade pitch variation of the form

$$\theta = \theta_n e^{in\Omega t}$$

the instantaneous circulation is

$$\Gamma_n = 2\pi \Omega R b \left[\theta_n - \frac{w}{\Omega R} \right] = \frac{2\pi \Omega R b \theta_n}{1 + \frac{\varphi b}{2\lambda_o R}}$$

Following the usual definition, the blade solidity, σ, is given by $\sigma = \frac{2 Q b}{\pi R}$. Since the quasi-static circulation is $\Gamma_q = 2\pi \Omega R b \theta_n$, and the lift, when average downwash velocities over the blade are used, is

$$L = \rho V \Gamma_b$$

it follows that the lift-deficiency function now takes the form

$$C = \frac{1}{1 + \frac{\sigma \pi}{4 \lambda_o}}$$

and is independent of the frequency.

At the lower reduced frequencies, it gives an excellent approximation to the more exact solution although, by the nature of the analysis, the phase shift cannot be predicted by this method.

An alternate form of the expression C, in terms of the wake spacing, h, is

$$C = \frac{1}{1 + \frac{\pi}{h}}$$

42

and this form has been used to obtain Figure 14 which shows a comparison with the exact values, replotted from Figure 13. In view of the excellent agreement, between the exact and approximate two-dimensional solutions, it is of interest to attempt a similar analytical solution for the three-dimensional case in vertical flight.

IX. THREE-DIMENSIONAL SOLUTIONS FOR VERTICAL FLIGHT

1) Uniform Downwash

Rotor-vortex theory is generally developed on the basis of uniform downwash. This condition is satisfied if the blade has constant circulation along the span, and this, in turn, is satisfied only for the case of ideal twist or taper; that is, varying inversely as the radius. In practice, such a condition is closely approximated by the usual linear twist distribution, since the contributions of the blade sections in the region close to the blade root, where the ideal twist is clearly not satisfied, are small.

Constant circulation implies a tip and center vortex only, with the tip vortex alone contributing to downwash. For this specialized condition, Eq. (15) becomes, for hovering or vertical flight,

$$
dw_1 = \frac{\Gamma}{4 \pi R} \frac{[1 - \eta \cos(\psi - \phi)] \, d\phi}{[1 + \eta^2 + z^2 - 2\eta \cos(\psi - \phi)]^{3/2}}
$$

The next step involves replacing the spiral of trailing vorticity, Γ, by a vortex cylinder, which implies an infinite number of blades. The distribution of vorticity along the z axis, as developed in the previous section, is then

$$
\frac{d\Gamma}{dz} = \frac{\Gamma Q}{2 \pi \lambda_o}
$$

All distances are nondimensionalized in terms of the blade radius, R.

The downwash velocity may now be obtained by integration over the complete wake as

$$
w_1 = \frac{Q}{8 \pi^2 \lambda_o R} \int_0^\infty \int_0^{2\pi} \frac{\Gamma [1 - \eta \cos(\psi - \phi)]}{[1 + \eta^2 + z^2 - 2\eta \cos(\psi - \phi)]^{3/2}} \, d\phi \, dz
$$

$$
= \frac{Q}{8 \pi^2 \lambda_o R} \int_0^{2\pi} \frac{\Gamma [1 - \eta \cos(\psi - \phi)]}{[1 + \eta^2 - 2\eta \cos(\psi - \phi)]} \, d\phi
$$

44

$$= \frac{Q}{8\Gamma^2 \lambda_o R} \int_0^{2\pi} \Gamma \left[1 + \eta \cos(\psi - \phi) + \eta^2 \cos 2(\psi - \phi) + \cdots \right] d\phi \qquad \eta < 1$$

Considering first the simple case of constant thrust and, hence, Γ constant. This results in

$$w = \frac{\Gamma_o \, Q}{4\pi \, \lambda_o \, R}$$

independent of η. Since $\lambda_o = \frac{w}{\Omega R}$ in hovering flight

$$\Gamma = \frac{4\pi \, \lambda^2 \, \Omega R^2}{Q}$$

The total rotor thrust is

$$T = QR^2 \int_o^1 \rho \, \Omega \eta \Gamma_b \, d\eta \;=\; 2\rho \, \pi R^2 \cdot \Omega^2 R^2 \cdot \lambda^2$$

or, with the definition $C_T = T / \rho \, \pi R^2 \Omega^2 R^2$

$$\lambda = \sqrt{\frac{C_T}{2}}$$

as in actuator disc theory.

Consider next the case when Γ_n varies harmonically with azimuth such that

$$\Gamma = \Gamma_{ns} \sin n\phi + \Gamma_{nc} \cos n\phi$$

Then

$$w = \frac{\Gamma_{ns} Q}{8 \pi^2 \lambda_o R} \pi \eta^n \sin n\psi + \frac{\Gamma_{nc} Q}{8\pi^2 \lambda_o R} \pi \eta^n \cos n\psi$$

The downwash, thus, has the same periodicity as the circulation change. The spanwise distribution is increasingly concentrated at the tip as the order of the harmonic increases, a result somewhat similar to that obtained in Reference 3. However, a complete solution requires the introduction of the contributions of the shed

45

vorticity. From Eq. (16), specialized for hovering, the total downwash due to the shed vorticity is

$$w_2 = \int_0^{2\pi} \int_0 \int_0' \frac{d}{dz} \frac{d\Gamma}{d\phi} d\phi \frac{1}{4\pi R} \frac{\eta \sin(\psi - \phi)}{[\eta^2 + \ell^2 + z^2 - 2\eta\ell \cos(\psi - \phi)]^{3/2}} d\ell \, dz$$

The order of integration may be interchanged since the singularities are retained in either process. After integrating with respect to z and expanding in a sine series

$$w_2 = \frac{Q}{8\pi^2 \lambda_o R} \int_0^{2\Gamma} \int_0^{\eta} \frac{d\Gamma}{d\phi} d\phi \left[\frac{1}{\eta} \sin(\psi - \phi) + \frac{\ell}{\eta^2} \sin 2(\psi - \phi) + \cdots \right] d\ell$$

$$+ \frac{Q}{8\Gamma^2 \lambda_o R} \int_0^{2\Gamma} \int_\eta' \frac{d\Gamma}{d\phi} d\phi \left[\frac{\eta}{\ell^2} \sin(\psi - \phi) + \frac{\eta^2}{\ell^3} \sin 2(\psi - \phi) + \cdots \right] d\ell$$

which reduces, after substituting $\Gamma = \Gamma_{ns} \sin n\phi + \Gamma_{nc} \cos n\phi$ and integrating over ϕ and η to

$$w_2 = \frac{Q}{8\pi^2 \lambda_o R} \left[\Gamma_{ns}(2 - \eta^n) \pi \sin n\psi + \Gamma_{nc}(2 - \eta^n) \pi \cos n\psi \right]$$

Summing the downwash due to the trailing and shed vorticity results in the interesting result

$$w = \frac{Q}{4\pi \lambda_o R} \left[\Gamma_{ns} \sin n\psi + \Gamma_{nc} \cos n\psi \right]$$

This is the same result as was obtained in the previous section for the two-dimensional case, and, in a similar manner results in a lift-deficiency function

$$C = \frac{1}{1 + \frac{\sigma \pi}{4 \lambda_o}}$$

2) Nonuniform Downwash

A more general solution may be obtained for the case where the circulation

46

on the blade is expressed as a power series

$$\Gamma'_b(\ell) = 2\pi \, b \, \Omega R \sum_{\gamma=0}^{\infty} \gamma_\gamma \ell^\gamma$$

dz

Solutions to this case may be more readily obtained if the periodicity of the circulation is expressed in complex form

$$\Gamma = \Gamma_n e^{in\phi}$$

Furthermore, it will be assumed that the mean downwash through the rotor is initially uniform over the disc.

The trailing vortex system will now consist of the tip vortex, whose value is

$$\Gamma'(1) = 2\pi \, b \, \Omega R \sum_{\gamma=0}^{\infty} \gamma_\gamma$$

and a sheet of trailing vorticity due to the change in circulation, $-d\Gamma_\bullet/d\ell$, along the span. The downwash due to this sheet of vorticity is given by Eq. (16) specialized for the hovering case. The total downwash is obtained by integration over the complete wake:

$$w_i(\psi, \eta) = -\frac{1}{4\pi R} \int_0^\infty \int_0^1 \int_0^{2\pi} \frac{d}{d\ell} \frac{d\Gamma'}{dz} \frac{[\ell - \eta \cos(\psi-\phi)]\ell}{[\ell^2 + \eta^2 + z^2 - 2\eta\ell\cos(\psi-\phi)]^{3/2}} \, d\phi \, d\ell \, dz$$

which, after integration with respect to z, results in

$$w_i(\psi, \eta) = \frac{-1}{4\pi R} \int_0^\eta \int_0^{2\pi} \frac{d}{d\ell} \frac{d\Gamma'}{dz} \frac{\ell}{\eta} \frac{\left[\ell/\eta - \cos(\psi-\phi) \right]}{\left[(\ell/\eta)^2 + 1 - 2\,\ell/\eta \cos(\psi-\phi) \right]} \, d\phi \, d\ell$$

$$-\frac{1}{4\pi R} \int_\eta^1 \int_0^{2\pi} \frac{d}{d\ell} \frac{d\Gamma'}{dz} \frac{[1 - \eta/\ell \cos(\psi-\phi)]}{[1 + (\eta/\ell)^2 - 2\,\eta/\ell \cos(\psi-\phi)]} \, d\phi \, d\ell$$

The first integral gives the downwash in the rotor plane outside a vortex cylinder extending to infinity from the rotor plane and is zero for Γ_o. This, however, is not the case when Γ varies with time or azimuth and the independence of blade

47

elements is not, therefore, as readily proved for this case.

Integration with respect to ϕ may be performed when Γ has the form $\Gamma_n e^{in\phi}$ by change of variable

$$y = e^{i(\psi - \phi)}$$

and application of the theorem of residues. The result is

$$w_1 = \frac{Q e^{in\psi}}{8\pi^2 \lambda_o R} \left[\pi \int_o^\eta \frac{d}{d\ell} \Gamma_n(\ell) \left(\frac{\ell}{\eta}\right)^n d\ell - \pi \int_\eta^1 \frac{d}{d\ell} \Gamma_n(\ell) \left(\frac{\eta}{\ell}\right)^n d\ell \right]$$

Similarly, the contribution of the shed wake may be obtained as

$$w_2 = \frac{Q e^{in\psi}}{8\pi^2 \lambda_o R} \left[n\pi \int_o^\eta \Gamma_n(\ell) \frac{\ell^{n-1}}{\eta} d\ell + n\pi \int_\eta^1 \Gamma_n(\ell) \frac{\eta^n}{\ell^{n-1}} d\ell \right]$$

To these must be added the contribution of the tip vortex

$$w_1 = \frac{Q e^{in\psi}}{8\pi^2 \lambda_o R} \pi \Gamma(1)$$

With $\Gamma_n = 2\pi b\Omega R \sum \gamma_r \ell^r$, the integrals may be evaluated by integrating term by term ($\ell < 1$). The result is, for the nth harmonic of downwash

$$\lambda_n = \frac{\sigma}{8\lambda_o} \left[2\pi \sum_o^\infty \gamma_r \eta^r \right] = \frac{\sigma\pi}{4\lambda_o} \sum_o^\infty \gamma_r \eta^r$$

The downwash at η thus depends only on the circulation at η , and the lift deficiency function is the same as that previously obtained. For example, if the variation in downwash $\gamma_r \eta^r$ is obtained by a pitch variation of the form $\theta = \theta_{nr} \eta^r$ then the instantaneous circulation is

$$\Gamma_n = 2\pi\Omega r b \left[\theta_{nr} \eta^r - \frac{\lambda_n}{\eta} \right]$$

or, since ℓ and η are interchangeable variables,

$$\sum_{r=0}^{\infty} \mathcal{T}_r \eta^r = \theta_{nr} \eta^{r+1} \qquad - \frac{\sigma \pi}{4 \lambda_o} \sum_0^{\infty} \mathcal{T}_r \eta^r$$

and
$$\frac{\mathcal{T}}{\theta_{nr}} = \frac{1}{1 + \frac{\sigma \pi}{4 \lambda_o}} \qquad \text{as before.}$$

This reduction in circulation, due to the wake, is of particular importance when it is desired to use a rigid or semirigid propeller as a control device by use of a first harmonic cyclic pitch variation. Since small stiff propellers suggest high disc loadings, C_T will be high, or alternatively downwash, λ_o, is high, and appreciable reductions in moment over those predicted by quasi-static aerodynamics will result.

For example, consider a rotor/propeller with a disc loading of 25 lb/ft^2, a tip speed of $\Omega R = 700$ ft/sec and operating at a mean angle of attack of $a_T = 0.1$ radians. Then $C_T = \dfrac{25}{\Omega^2 R^2} = 0.0214$ and $C = 0.49$, resulting in about half the moment predicted by simple blade element theory. Evidently, a similar result will occur following rapid increase of collective pitch of a control rotor, resulting in a lag in thrust which may become of importance if high-gain automatic-stabilization equipment is installed.

The above analysis has been developed with the usual assumption of a rigid wake. The effect of this assumption may be seen by deriving the same result from consideration of simple momentum and blade-element theory.

From momentum theory, for uniform steady inflow and a superimposed periodic thrust change, $T_n e^{in\Omega t} = 2 \times$ mass flow through rotor $\times w_n e^{in\Omega t}$ where w_n is the velocity change through the rotor disc due to T_n.

Considering mean velocity only, $w_o = \lambda_o \Omega R$ in determing the mass flow

$$T_n = 2 \times \rho \pi R^2 \times \lambda_o \Omega R \times \lambda_n \Omega R \qquad \text{or} \quad C_T = 2 \lambda_o \lambda_n$$

49

From the blade element theory for uniform flow through the rotor and periodic change in pitch, $\theta_n e^{in\Omega t}$

$$C_{T_n} e^{in\Omega t} = \frac{\sigma \pi}{2} (\theta_n - \lambda_n) e^{in\Omega t}$$

and with $C_{T_{qn}} = \frac{\sigma \pi}{2} \theta_n$, $\dfrac{C_{T_n}}{C_{T_{qn}}} = \dfrac{1}{1 + \dfrac{\sigma \pi}{4 \lambda_o}}$

as in the vortex theory.

If, on the other hand, the periodic thrust were to be computed using the nonrigid wake concept of vortex theory (Eq. (15)), then λ_n would have to be included in the computation of mass flow.

50

X. THREE-DIMENSIONAL SOLUTIONS IN FORWARD FLIGHT

i) Near Shed Wake - Γ_N^s

Having established the validity of the proposed approach and obtained an analytical solution for the limiting case of vertical flight, it is possible to proceed with some confidence to the solution for the three-dimensional rotor in forward flight. The treatment of the near wake will be considered first and, in particular, the near shed wake, since this wake introduces the important singularities of classical unsteady aerodynamic theory. The method of solution presented in the Appendix may be followed directly if the curvature of the wake is neglected as in Reference 13 and, furthermore, if the blade is treated as a two-dimensional airfoil in the presence of an element of vorticity $\gamma \, d\xi^*$ at ξ^* from the origin. The considerable simplification in the analysis, resulting from the latter assumption, appears justified on the basis of the results of Reference 14 in which the close agreement was obtained between the two-dimensional and three-dimensional solutions. This approximation is clearly inadmissible when treating the far wake.

The circulation due to the near wake may then be determined by assuming the straight near wake to extend aft of the blade to infinity. Following the treatment in Section VI and integrating over the near wake for all vortex elements, results in an expression for the bound circulation on the blade due to the near shed wake

$$\Gamma_N^s = \int_1^\infty b\,\gamma(\xi)\left[\frac{\xi+1}{\sqrt{\xi^2-1}} - 1\right] d\xi$$

To this must be added the circulation due to the far wake. Additional circulation arises from the velocity u of Eq. (5) which will be designated as the quasi-static circulation

$$\Gamma'_q = -2\pi b\, u$$

For a symmetrical blade spacing, when the frequency of oscillation is an

51

integer of rotational speed, the effects on one blade of the bound vortices from the remaining blades are zero for the case of Γ_o when n is equal to or a miltiple of the number of blades. This is not otherwise true. However, unless a very large number of wide chord blades are used, the effects of the bound vortices on each other are negligible and may be ignored. This may be readily verified from Eq. (16), as discussed in determining the choice of upper limit in the integral obtained from Eq. (21) below.

Since we are concerned here with harmonic blade loads and motions, the blade bound circulation Γ_b will be defined as

$$\Gamma_b(\psi) = \sum_{n=0}^{\infty} \Gamma_{ns_\ell} \sin n\,\Omega\,t + \Gamma_{nc_\ell} \cos n\,\Omega\,t \tag{19}$$

where the trigonometric rather than the complex form is employed in keeping with the more usual practice in rotary wing aerodynamics.

The distortion of the near shed-wake vorticity distribution, due to the first harmonic variations of forward velocity, will be neglected; hence, the relationship for velocity.

$$\frac{d\xi^*}{dt} = \Omega R$$

The shed vorticity in the wake may be related to the time rate of change of blade circulation (Eq. (3a)) as

$$\gamma(\xi)\,d\xi^* = -\frac{d}{dt}\,\Gamma_b\,dt$$

Whence, since Ω is constant,

$$\gamma(\xi) = -\frac{1}{\Omega\eta R} \cdot \frac{d}{dt}\,\Gamma_b = -\frac{n}{\eta R}\sum_o^{\infty}\Gamma_{ns}\cos n\,\Omega t - \Gamma_{s_{IN}} n\,\Omega t$$

52

An element of shed vorticity in the wake may then be identified with the position of the blade trailing edge, b, at the time of its shedding, $t - \Delta t$. Now $t = \frac{\psi}{\Omega}$ and $\Delta t = \frac{\xi^* - b}{\Omega \eta R}$. Therefore,

$$\gamma(\xi) = \sum_{n=0}^{\infty} - \frac{n}{\eta R} \left\{ \Gamma_{ns} \cos n[\psi - \frac{b}{\eta R}(\xi - 1)] - \Gamma_{nc} \sin n [\psi - \frac{b}{\eta R}(\xi - 1)] \right\}$$

Substituting in the integral for Γ_N^S above, results in

$$\Gamma_N^S(\psi) = \frac{-nb}{\eta R} \left\{ [\Gamma_{ns} \cos n\psi - \Gamma_{nc}\sin n\psi] I_c - [\Gamma_{ns} \sin n\psi + \Gamma_{nc} \cos n\psi] I_s \right\} \qquad (20)$$

where

$$I_c = \int_1^{\infty} \cos \frac{n b}{\eta R}(\xi - 1) \left[\frac{\xi + 1}{\sqrt{\xi^2 - 1}} - 1 \right] d\xi$$

$$I_s = \int_1^{\infty} \sin \frac{n b}{\eta R}(\xi - 1) \left[\frac{\xi + 1}{\sqrt{\xi^2 - 1}} - 1 \right] d\xi$$

The coefficient $nb/\eta R$ appearing in the solution is the well-known reduced frequency k specialized to the case of the nth harmonic of rotational speed at the blade station, η, in question. The integrals, first computed numerically in Reference 34, may be identified (Reference 29) as

$$I_c = -\frac{\pi}{2}(Y_0 + J_1) \cos k - \frac{\pi}{2}(Y_1 - J_0) \sin k$$

$$I_s = -\frac{\pi}{2}(Y_0 + J_1) \sin k - \frac{\pi}{2}(Y_1 - J_0) \cos k - \frac{1}{k}$$

53

2) Far Shed Wake - Γ_F^S

The far shed wake will be treated by neglecting the chordwise variation of velocity along the airfoil chord due to the wake. Since the primary effect of the wake appears as the blade passes over the shed or trailing vortex line generated by itself or by another blade, and since the distance of these vortex lines below the blade may be of the order of one chord length, the validity of the assumption may well be questioned. However, the analysis of the equivalent assumption for the two-dimensional case, given above for comparison with the exact solution obtained in Reference 4, indicates that the assumption is certainly valid, at least for the reduced frequencies of interest in rotor-blade loading analysis.

Setting x and χ equal to zero in line with the above assumption, it is possible to perform the integration of Eq. (16) with respect to $\mathcal{l}$ for the case where λ is constant and obtain the contribution of a vortex line extending from 0 to $\mathcal{l}$. This integration may be performed with the aid of Formula 167, Reference 35, giving the result

$$d w_2 (\psi, \phi) = -\frac{1}{4\pi R} \left\{ \frac{\eta \sin(\psi-\phi) + d\sin\phi}{z^2 + [\eta\sin(\psi-\phi) + d\sin\phi]^2} \times \right.$$

$$\left[\frac{\mathcal{l} + d\cos\phi - \eta\cos(\psi-\phi)}{[\mathcal{l}^2 + \eta^2 + z^2 + d^2 - 2\eta\mathcal{l}\cos(\psi-\phi) + 2d\mathcal{l}(\cos\phi - \eta\cos\psi]^{1/2}} \right.$$

$$\left. \left. - \frac{d\cos\phi - \eta\cos(\psi-\phi)}{[\eta^2 + z^2 + d^2 - 2\eta d\cos\psi]^{1/2}} \right] \right\} \frac{d\Gamma}{d\phi} d\phi = -\frac{1}{4\pi R} g(\phi) \frac{d\Gamma}{d\phi} d\phi \tag{21}$$

The total downwash at the blade at any station η and azimuth position ψ is obtained by integration over the far wake over m spirals

$$w_2 = -\int_{\psi + \zeta_k}^{2\pi m + \psi + \zeta_k - \frac{\pi}{2}} \frac{1}{4\pi R} g(\phi) \frac{d\Gamma}{d\phi} d\phi$$

54

The choice of the upper limit in the integration must be made with some care. Defining the end of the far wake at an azimuth angle $\pi/2$ from the blade appears to be reasonable, and little error is involved if this angle is varied from $\pi/2$ to $3\pi/2$ or decreased to $\pi/4$. Evidently, this choice must be made on the basis of blade and rotor geometry; however, a simple integration of Eq. (16) for the case $z = d = 0$ and $\psi - \phi$, varying from 0 to $\pi/2$ or greater, will generally clearly indicate the desirable choice of upper limit.

As in the case of the near wake, elements of vorticity in the far wake are identified with the position of the blade at the instant of their shedding and in terms of the time rate of change of bound circulation. Whence, from (19)

$$\frac{d\Gamma}{d\phi} = \sum_{n=0}^{\infty} -n \left[\Gamma_{ns} \cos n\phi - \Gamma_{nc} \sin n\phi \right]$$

When the bound circulation varies appreciably over the span, the actual circulation may be represented by a series of straight distributions extending from 0 to various spanwise locations, ℓ. Substituting in the integral for w_2,

$$w_2 = \sum_{\ell} \sum_{n=0}^{\infty} \frac{n}{4\pi R} \int_{\psi+\varsigma}^{2\pi m + \psi + \varsigma - \pi/2} [\Gamma_{ns} \cos n\phi - \Gamma_{nc} \sin n\phi] q(\phi) \, d\phi$$

which may be written in the form

$$w_2 = \sum_{\ell} \sum_{n=0}^{\infty} \frac{n}{4\pi R} \sum_{k=0}^{\infty} \left[\Gamma_{ns_\ell} (A^k_{nc_\ell} \cos k\psi + B^k_{nc_\ell} \sin k\psi) - \Gamma_{nc_\ell} (A^k_{ns_\ell} \cos k\psi + B^k_{ns_\ell} \sin k\psi) \right] \quad (22)$$

where the coefficients A and B are obtained from harmonic analysis with respect to ψ of the results of numerical evaluation of the integral over the wake for m spirals at values of ψ from 0 to 360 degrees.

A^k_{nc} identifies the cosine coefficient of the kth harmonic due to a cos n variation of bound circulation extending from 0 to ℓ and similarly with the remaining coefficients.

3) Trailing Wake - Γ^T

A treatment for the system of trailing vortices using Eq. (15) similar to that used for the far shed wake, results in

$$w_1 = \sum_{\ell}^{\infty} \sum_{n=0}^{\infty} \frac{1}{4\pi R} \int_{\psi + \xi}^{2\pi m + \psi + \xi} [\, \Gamma_{ns_\ell} \sin n\,\Omega t + \Gamma_{nc_\ell} \cos n\Omega t \,]\, f(\phi, \psi)$$

Whence

$$w_1 = \sum_{\ell} \sum_{n=0}^{\infty} \frac{1}{4\pi R} \sum_{k=0}^{\infty} [\, \Gamma_{ns}(P^k_{ns_\ell} \cos k\psi + Q^k_{ns_\ell} \sin k\psi\,)$$
$$+ \Gamma_{nc_\ell}(P^k_{nc} \cos k\psi + Q^k_{nc_\ell} \sin k\psi\,)\,] \tag{23}$$

where ℓ now identifies the spanwise blade station from which the trailing vortex is assumed to originate.

4) Determination of Blade Circulation and Lift

Substituting the expressions for w_1 and w_2 in (17) results in an expression for the bound circulation or the blade induced by a wake generated by changes in this bound circulation.

The total bound circulation on the blade may now be obtained as

$$\Gamma_b = \Gamma_N^S + \Gamma_F^S + \Gamma^T + \Gamma_q \tag{24}$$

where Γ_q is the quasi-static circulation, previously defined as that which would occur in the absence of any wake effects.

In order to obtain Γ_q, it is necessary to define the blade motion. This motion may consist of contributions from all the blade normal modes and, in cases where the blade is operating close to resonance, the dominant mode should be included. For the purpose of illustration, a rigid nontwisting blade flapping through the angle β will be used, operating a pitch setting θ (η), which includes the twist. Then u is uniform over the blade chord and is given by

$$u = -\Omega R [(\eta + \mu \sin \psi) \theta (\eta) - (\eta \dot{\beta} + \mu \beta \cos \psi)]$$

From (17) it follows that

$$\Gamma_q = 2 \pi b u$$

The contribution of the near shed wake is given by Eq. (20) which may be written in the form

$$\Gamma_N^S = - \sum_{n=1}^{\infty} (\Gamma_{ns} C_n + \Gamma_{nc} S_n) \cos n\psi + (\Gamma_{ns} S_n - \Gamma_{nc} C_n) \sin n\psi$$

where

$$C_n = I_c k \ , \quad S_n = I_s k \quad \text{and} \quad k = \frac{n b}{\eta R}$$

The contributions of the far shed wake and trailing wake may be expressed in terms of the total downwash normal to the tip path plane expressed nondimensionally as

$$\lambda = \frac{w_1 + w_2}{\Omega R} - \mu \tan i \tag{25}$$

57

where w_2 now contains only the far shed wake and i is the angle between the tip path plane and the relative wind, positive nose up. Then, from (17)

$$\Gamma^T + \Gamma^S_F = -2\pi b \Omega R \lambda$$

If the flapping angle β is expressed as

$$\beta = a_o - \sum_{n=1}^{\infty} \left[a_n \cos n\psi + b_n \sin n\psi \right]$$

and the bound circulation and inflow λ are defined in the series form given by Eq. (19), then equating coefficients in Eq. (24) results in an expression for Γ_n. At this point, a nondimensional form of the circulation will be introduced and defined as

$$\gamma_n = \frac{\Gamma_n}{2\pi b \Omega R}$$

Then in nondimensional form,

$$\gamma_o = [\eta\theta - \lambda_o - \frac{\mu}{2} a_1]$$

$$\gamma_{1s} = [\mu\theta - \lambda_{1s} - a_1\eta + \frac{\mu}{2} b_2] - (\gamma_{1s} s_1 - \gamma_{1c} c_1)$$

$$\gamma_{1c} = [-\lambda_{1s} + b_1\eta - a_o\mu + \frac{\mu}{2} a_2] - (\gamma_{1s} c_1 + \gamma_{1c} s_1)$$

and

$$\gamma_{ns} = [-\lambda_{ns} - n\eta a_n + \frac{\mu}{2} (b_{n+1} + b_{n-1})] - (\gamma_{ns} s_n - \gamma_{nc} c_n)$$

$$\gamma_{nc} = [-\gamma_{nc} + n\eta b_n + \frac{\mu}{2} (a_{n+1} + a_{n-1})] - (\gamma_{ns} c_n + \gamma_{nc} s_n)$$

(26)

The lift, after summing over the entire wake, may be obtained separately: for the near wake, from (12) in Section VI and, for the far wake, from (18) in the form

$$L(\eta) = \rho Vb \int \frac{\gamma\, d\xi}{\sqrt{\xi^2 - 1}} + \rho V(\Gamma^T + \Gamma^S_F + \Gamma_q) + \rho\pi \ddot{z} b^2$$

which, after the identification of $\gamma(\xi)$ with the blade position at the time of its shedding, as was done for the circulation, becomes

58

$$L(\eta) = -\frac{n\,b}{\eta R}\,\rho V \left[\, \Gamma_{ns} \cos n\psi \;-\; \Gamma_{nc} \sin n\psi \,\right] I'_c$$

$$-\; \frac{n\,b}{\eta R}\rho V \;\left[\, \Gamma_{ns} \sin n\psi + \Gamma_{nc} \cos n\psi \,\right] I'_s$$

$$+ \rho V \;\left[\, \Gamma^T + \Gamma^S_F \;+\; \Gamma_q \,\right] \;+\; \rho \,\pi \ddot{z}\, b^2$$

(27)

where, with $k = \dfrac{n\,b}{\eta R}$ as before,

$$I'_s = \int_1^{\infty} \sin \frac{n\,b}{\eta R}(\xi - 1)\,\frac{d\xi}{\sqrt{\xi^2 - 1}} = \frac{\pi}{2}\, J_o \cos k \;+\; \frac{\pi}{2}\, Y_o \sin k$$

and

$$I'_c = \int_1^{\infty} \cos \frac{n\,b}{\eta R}(\xi - 1)\,\frac{d\xi}{\sqrt{\xi^2 - 1}} = \frac{\pi}{2}\, J_o \sin k \;-\; \frac{\pi}{2}\, Y_o \cos k$$

That, Eq. (27) reduces to the classical case for a two-dimensional airfoil may be readily verified by letting

$$\Gamma^T = \Gamma^S_F = 0$$

and expressing the circulation in complex form

$$\Gamma = \Gamma_n \, e^{in\psi} \qquad\qquad \Gamma_q = \Gamma_{q_n} \cdot e^{in\psi}$$

Then with $\Gamma_{nc} = \Gamma_n$, $\Gamma_{ns} = i\,\Gamma_n$ we obtain from (20) and (24)

$$\Gamma_n = -ik\,\Gamma_n \left[\, I_c - i\,I_s \,\right] + \Gamma_{q_n}$$

$$= -ik\,\Gamma_n \left[\, \int_1^{\infty} e^{ik(1-\xi)}\,\frac{\xi+1}{\sqrt{\xi^2-1}}\,d\xi - e^{ik}\int_1^{\infty} e^{-ik\xi}\,d\xi \,\right] + \Gamma_{q_n}$$

or

$$\Gamma_n = \frac{\Gamma_{q_n}}{ik\,e^{ik}\displaystyle\int_1^{\infty} e^{-ik\xi}\,\dfrac{\xi+1}{\sqrt{\xi^2-1}}\,d\xi}$$

Similarly, with $L = L_n e^{in\Omega t}$ from

$$L_n = -i k \rho V \Gamma_n' \left[I_c' - i I_s' \right] + L_{q_n} + \rho \pi \ddot{z} b^2$$

$$= -i k \rho V \Gamma_n e^{ik} \int_1^\infty \frac{e^{ik\xi}}{\sqrt{\xi^2 - 1}} \, d\xi + L_{q_n} + \rho \pi \ddot{z} b^2$$

Since $L_{q_n} = \rho V \Gamma_{q_n}$, it follows that

$$L_n = L_{q_n} \frac{\displaystyle\int_1^\infty \frac{\xi\, e^{-ik\xi}}{\sqrt{\xi^2 - 1}} \, d\xi}{\displaystyle\int_1^\infty \frac{(\xi + 1) e^{-ik\xi}}{\sqrt{\xi^2 - 1}} \, d\xi} + \pi \rho \cdot \ddot{z} b^2$$

The coefficient of L_{q_n} may be readily identified as the lift-deficiency function C(k) of Reference 29.

5) Blade-Flapping Coefficients

The blade displacements are obtained from the blade-flapping equilibrium equation

$$I \Omega^2 \left(\frac{\ddot{\beta}}{\Omega^2} + \beta \right) = R^2 \int_0^' \eta L(\eta) d\eta$$

where the flapping hinge offset has been assumed substantially zero. The effect of the offset is not large unless the blade Lock number is low and the offset appreciable. The coefficients a_n, b_n decrease rapidly as n increases, consequently, the lift may be approximated for the purpose of determining a_n, b_n by its quasi-static value (Eq. (18)).

$$L(\eta) = \rho V \Gamma_b'(\eta)$$

or

$$I \Omega^2 \left(\frac{\ddot{\beta}}{\Omega^2} + \beta \right) = 2 \pi \rho b R^4 \Omega^2 \int_0^1 (\eta + \mu \sin \psi) \times$$
$$[\gamma_0 + \sum_{n=1}^{\infty} \gamma_{ns} \cdot \sin n\psi + \gamma_{nc} \cdot \cos n\psi] \eta \, d\eta$$

The mass constant of Lock number of the rotor blade is

$$LN = \frac{2 \rho \pi b R^4}{I}$$

where the designation LN is used in place of the more usual γ in order to avoid confusion with the circulation.

After solution of the differential equation for the particular integral representing steady-state flapping motion, the coefficients of the Fourier series for blade motion are obtained as

$$a_n = \frac{LN}{2 (n^2 - 1)} \int_0^1 \left\{ \eta^2 \gamma_{nc} + \frac{\mu}{2} \eta [\gamma_{(n+1)s} - \gamma_{(n-1)s}] \right\} d\eta \tag{28}$$

$$b_n = \frac{LN}{2 (n^2 - 1)} \int_0^1 \left\{ \eta^2 \gamma_{ns} + \frac{\mu}{2} \eta [\gamma_{(n-1)c} - \gamma_{(n+1)c}] \right\} d\eta$$

All relationships necessary for the determination of the blade loading have now been established.

As previously mentioned, solution of these equations for the blade loading presents no particular problem using the above equations and standard techniques of matrix inversion. However, the process is evidently a long and tedious one; in particular, when the circulation varies appreciably along the span so that a tip vortex, and a shed vortex extending from the root to the tip, cannot be used. For this reason the interharmonic coupling terms appearing in References 22 and 24 were examined in Reference 24 in some detail. As a result of these analyses, it is apparent

that a reasonably exact solution can be obtained by taking advantage of the predominant effect of the steady-state circulation in determining the harmonic content of the downwash, at least for the first iteration. A practical rotor blade, whether articulated at the root or restrained to flap elastically, will, by virtue of the blade motion, have small harmonic lift variations compared to the steady-state lift. Although these harmonic-lift variations are the primary source of the fatigue loading on the blade and the vibratory inputs to the rotor shafts, their magnitude is, nevertheless, small compared to the steady-state lift carried by the rotor. Evidently, if this were not so, the aircraft would be subjected to excessive vibration and would be otherwise unflyable. Consequently, the following approach suggests itself. First, assume a uniform inflow distribution through the rotor computed by the approximate momentum relations which are shown in Reference 24 to agree well with the exact values computed from vortex theory. Knowing the rotor-thrust coefficient and the blade-twist distribution, determine the downwash w_1 from (24) due to the steady circulation γ_o only. For constant circulation, $n = 0$, w_2 is evidently zero and Eq. (24) becomes

$$\frac{w_1}{\Omega R} = \sum_\ell \sum_n \frac{b}{2R} \, \gamma_{o\ell} \, P_o^n \tag{29}$$

and the steady-state inflow due to the constant circulation is from (25)

$$\lambda_o^o (\eta) = -\mu \tan i + \sum_\ell \frac{b}{2R} \, \gamma_{o\ell} \, P_{o\ell}^o \tag{30}$$

From Eq. (26), the bound circulation γ_o is given by

$$\gamma_o = [\eta \, \theta (\eta) - \lambda_o + \frac{\mu}{2} \cdot a_1] \tag{31}$$

In the first iteration a_1 may be computed from uniform inflow theory. The trailing vortex strength γ_{0_ℓ} at any station ℓ in the wake is related to the bound circulation on the blade by $\gamma_0(\ell) = (\gamma_\eta - \gamma_{\eta-\Delta\eta})$ and is obtained in the numerical solution by taking the change in bound circulation γ_0 over the desired increment of the blade. In the integration of Eq. (15) the ℓ stations are then located midway between the blade stations η. Substitution of the trailing vortex strength thus obtained in the system of Eq. (30) and simultaneous solution, results in the first iteration of the steady state downwash λ_0^0. Normally five to seven stations along the blade will adequately define the variation of downwash distribution.

New values of coefficient P_0^0 may now be obtained using the new values of λ_0^0 in Eq. (15). Physically, this has the effect of distorting the wake as shown in Figure 15 and discussed on Page 35. The iteration is rapid as indicated by Figure 16 which shows the downwash distribution for an untwisted blade computed by assuming constant λ_0 compared with the second iteration performed as described above. The effect of the first harmonic downwash λ_0^1 was small for the particular case investigated where the rotor is assumed to be inclined through a relatively large angle and the helicopter accelerated through transition. However, as shown in Reference 24, the effect of this first harmonic variation in λ may be of considerable importance for a helicopter in equilibrium flight at slow speeds.

Having established the harmonic variations in downwash on the rotor due to the steady-state lift of the blade, it is now possible to compute the harmonic airload corresponding to this downwash distribution from Eqs. (26) and (27). Simultaneous solution of this system of equations is evidently necessary. For the first iteration it may be noted that, at least for the harmonics higher than the second, Eq. (26) may be approximated by

$$\gamma_{ns} = -\lambda_{ns} \qquad \gamma_{nc} = -\lambda_{nc}$$

63

since, as is evident from Eq. (27), the flapping coefficients become small for values of n of three and above. Expressed in another way, the lift alleviation due to flapping becomes small for the higher harmonics. However, in the presence of resonance with one of the elastic modes or in the case where one harmonic of downwash predominates over the next highest or lowest, blade flapping becomes significant, and its effect should always be tested in the second iteration.

Treatment of the trailing-vortex system due to the higher harmonic airloading follows exactly the same procedure as has been outlined above for that due to the 0th harmonic or steady-state loading. The computation of the additional coefficients $P_{n\ell}^i$ represents the only major machine computation process required in the solution of the problem. These coefficients depend only on the wake spacing, the number of blades used, and the advance ratio μ. Of these parameters, the advanced ratio appears to be the more important.

As mentioned above, the computer time required to obtain a set of coefficients varies considerably with the interval size used and number of spirals represented. A considerable amount of time has been spent in an attempt to determine a reasonable compromise between computer time and accuracy. It has been concluded that a minimum spacing of 7 1/2° for ψ, and ϕ in the far wake appears desirable in order to obtain an accurate prediction of the harmonics up to the sixth, with errors not exceeding 20 per cent for harmonics up to the ninth. In the near wake minimum intervals in ϕ of 2 1/2° appear desirable except that, in the case of Eq. (21) and using the limits defined by Figure 11, a closer spacing of the last few stations may be required. The near wake is defined as that located approximately an eighth or a quarter of the disc away from the blade. The exact definition of the end of the near wake is not of major significance within the limits quoted.

Three spirals appear to define the harmonic content within a few per cent, although, if accuracies greater than 5 per cent are desired, six spirals should be included. It is not believed that the precision of the mathematical model used warrants this additional accuracy.

In particular, it should be noted that the mathematical model ignores wake interaction effects and, in particular, the tendency for vortex-vortex interaction, which will, in general, result in the rolling up of the vortex sheet after a few spirals. Since the major contribution to the airloads occurs from the first spiral, a more precise definition of the wake form is evidently not warranted and, as in the equivalent applications of fixed wing theory, the mathematical model used in developing Eqs. (15) and (16) is believed to be adequate.

Exact definition of the machine-computer time required for a particular problem depends on the program used. However, the computation of a set of coefficients P and Q for one value of η, ℓ and ζ requires approximately one-half minute on an IBM 7090 computer. The program is described in Reference 36.

The treatment of the shed vortex system follows a similar approach, providing the approximate treatment of the phase shift suggested above is used, and the integration stopped at the appropriate limit determined by the reduced frequency corresponding to the harmonic and spanwise station under consideration.

To summarize the approach suggested above, the following steps may be identified:

1. Assume a mean inflow through the rotor using approximate momentum relationships to determine the induced flow component. Integration of Eq. (15) for several values of ψ then defines the coefficients P and Q of Eq. (23).

2. Using Eq. (31), the trailing vortex stength at ℓ, corresponding to the blade spanwise pitch distribution and the assumed uniform downwash distribution, is obtained in terms of $\lambda_o (\eta)$. This value is then substituted into Eq. (29) and a simple matrix inversion gives the first iteration for λ_o^o along the span.

3. With this new value of λ_o^o, obtain revised values of the coefficients P and Q and repeat the process. Convergence is rapid and usually one repetition is

sufficient. All the desired harmonics of downwash λ_o^n due to γ_o may then be obtained directly from Eq. (29).

4. The airload corresponding to any higher harmonic downwash is obtained by computing the additional downwash from Eqs. (15) and (16), neglecting interharmonic coupling by setting $i = n$. γ_n is obtained from Eq. (26) where now $\lambda_n = \lambda_n^n + \lambda_o^n$ and the iterative procedure described above then followed.

The underlying assumption in the above-outlined approach is evidently the neglect of interharmonic coupling. This point has been discussed in some detail in Reference 24, and many examples of the magnitude of this coupling effect have been given. Evidently, the assumption must be used with some care in the presence of resonance with one of the higher harmonic blade loadings, since the interharmonic coupling effects may then induce appreciable airloads at the next lowest and highest harmonics. In general, however, neglect of these harmonics is generally valid because:

a) the primary contribution to the higher harmonic inflow distribution comes from the steady-state circulation on the blade, and the contribution of say, the nth harmonic to the ith harmonic is small in comparison.

b) the near wake induces primarily the harmonic of the bound circulation.

XI. EXAMPLES OF COMPUTATIONAL RESULTS

1) Computations of Downwash

In order to examine the nature of the induced flow through the rotor in forward flight, Eqs. (15) and (16) were programmed for numerical integration on high-speed digital computers to determine the number, m, of spirals and intervals in both ϕ and ψ required for an accurate prediction of the harmonic content of the wake up to at least the sixth harmonic. The number of spirals were varied from m = 3 to m = 12 and the interval sizes from $\Delta\phi = \Delta\psi = 2.5^\circ$ to 20°. A satisfactory compromise was found to be three spirals and intervals of 7.5° in the far wake and 2.5° in the near wake, giving a solution time on the 7090 computer of approximately one-half minute for the downwash at one spanwise location due to one blade wake and for one harmonic.

In Figures 17 and 18 are plotted the harmonic content, up to the sixth harmonic, of the downwash at the rotor generated by a tip vortex of constant strength for two values of μ corresponding to transition and to cruise flight regimes. Unlike the fixed wing, a rotor blade is highly loaded at the tip and much of the basic character-istics of the downwash may, therefore, be determined by examining the effects of the powerful system of trailing vortices shed over the outer few percent of the blade span, a system adequately represented by a single tip vortex of strength equal to the mean blade circulation.

Considering first the transition case $\mu = 0.1$, it is evident from Figure 17 that the steady-state value of downwash is substantially constant over the disc and the initial assumption of constant Γ_o is satisfied.

Of considerable interest is the pronounced first harmonic variation in downwash generated by the tip vortex which, at low advance ratios, will produce an upwash at the leading edge. The existence of this first harmonic variation in downwash was first predicted by the theory of Reference 14 and demonstrated by the flight-test observations in Reference 21 and the wind-tunnel tests of Reference 22. In forward

flight, the spiral formed by the tip vortex is displaced aft and, since the velocity field outside the spiral has a vertical component, all points ahead will experience an upwash. Evidently the assumption of uniform inflow is violated and a further cycle is necessary before the downwash can be defined with any accuracy. Before this can be done, it is necessary to relate the downwash characteristics to a particular flight condition and rotor configuration; in particular, to the total inflow through the rotor. This consists not only of the downwash; that is, the velocities induced at the rotor disc by the wake, but also contains components of the forward and climbing velocities. Although the curves of Figure 17 are specialized to a particular total inflow of $\lambda_o = 0.05$, to a three-bladed rotor and to a forward flight of $\mu = 0.10$, they are now otherwise generalized and will fit a wide variation of rotor attitudes, thrust coefficients and solidities.

Since the wake is generated by the blades, the inflows which have been computed are those relative to a particular blade. If the higher harmonic motions of the blade above the first are ignored, a valid assumption and certainly well within the limitations of the assumed wake geometry, then the inflows plotted are those perpendicular to the plane containing the blade tips, or the tip path plane. The steady-state values of λ and μ which appear in the solutions should, therefore, be computed on this basis. It should be noted that the bulk of published rotor information uses the control axis as reference; however, the conversion from one system to another involves minor corrections and is readily made. For a discussion of the different reference axes, see Reference 37.

The induced flow is directly proportional to the strength of the tip vortex. The steady-state component due to a steady-state tip vortex Γ_o is, from Eq. (23).

$$\frac{w_1}{\Omega R} = \lambda_{\theta i} = \frac{b}{2R} \gamma_o P_o^o$$

Hence, from Eq. (25), the total inflow is

$$\lambda_o = \frac{b}{2R} \gamma_o P_o^o - \mu \tan i$$

68

Now P^o_o is a function only of λ_o, and the number of blades used. Consequently, the numerical integrations from which P^o_o is obtained may be used to represent any desired combination of rotor solidity, represented by $\frac{b}{R}$, and the circulation γ_o, determined in turn by the collective pitch setting θ.

For example, consider a helicopter climbing out at an angle of incidence of $i \simeq -15^o$, or alternatively accelerating through transition with this tip path plane inclination. These would be typical operational flight regimes at advance ratios of the order of $\mu = 0.1$. The induced flow is then, for λ_o of 0.05,

$$\lambda_{o_i} = \lambda_o + \mu \tan i = 0.023$$

The corresponding rotor-thrust coefficient is, for constant bound circulation,

$$C_T = \frac{\sigma \pi}{2} \gamma_o$$

The rotor configuration must now be defined. Selecting a solidity of $\sigma = 0.07$ defines $\frac{b}{2R} = 0.0183$. From Figure 17, the mean steady downwash coefficient is $P^o_o \simeq 28$. Whence,

$$\gamma_o = \frac{\lambda_{o_i}}{P^o_o} \cdot \frac{2R}{b} = 0.045$$

and

$$C_T = 0.00495$$

Using the approximate momentum relations for forward flight suggested by Glauert would give

$$C_T = 2(\lambda_o + \mu \tan i) \sqrt{\lambda_o^2 + \mu^2} = 0.005$$

69

and evidently this approximate relationship is in good agreement with the vortex theory developed in this paper.

A correction will now be introduced in the numerical solutions for the first harmonic variation in downwash. The tip vortex will be assumed to descend with the steady and first harmonic inflows occurring at a representative tip station. z in Eq. (15) must then be multiplied by $\lambda_o + \lambda_1 \cos\phi$ or by

$$\lambda_o \left[1 + \frac{P_o^1}{P_o^o} \; (1 + \frac{\mu \tan i}{\lambda_o}) \cos\phi \right]$$

instead of simply λ_o. For the conditions selected, and using P_o^1 / P_o^o of 1.12 from Figure 17, results in

$$\frac{\lambda_1}{\lambda_o} = \frac{P_o^1}{P_o^o} \; (1 + \frac{\mu \tan i}{\lambda_o}) \simeq 0.5$$

The effect of introducing this correction is indicated in Figure 17.

If, instead of accelerating or climbing out through transition, a helicopter is required to maintain steady flight in this regime, then an interesting and highly significant phenomenon occurs which may be described as a tendency for the rotor to suck up its own wake into the leading edge of the tip path plane. Evidently if i is small or even positive as would occur in a flare, then the ratio λ_1 / λ_o may approach or exceed unity and the blades will pass through their own wake. When this occurs, large higher harmonic components in inflow can be computed, indicating large local variations in angle of attack. Such computations are, however, quantitatively meaningless since all the basic assumptions of the mathematical model employed are violated. For example, the concept of ideal fluids with lines of vorticity having infinite core velocities would have to be replaced by a core structure determined from viscous flow considerations. Single vortex lines should also be replaced by a more realistic drop off of circulation at the blade tip. Also, the blade itself can no longer be replaced by a lifting line since the far wake in

the vicinity of the leading edge has now very definitely become a near wake. The more exact treatment reserved for the near wake must, therefore, be used for the entire wake. However, even without the introduction of such refinements, it is possible to draw some important qualitative conclusions from the results of the simpler analysis.

Following a similar analysis to the one given above, consider a rotor operating at an incidence angle of -5°. Under these conditions, using as a first trial the values of $\lambda_1 / \lambda_o = 0.5$ obtained above, a new estimate for λ_1 / λ_o of

$$\frac{\lambda_1}{\lambda_o} \simeq 0.9$$

is obtained. A recomputation for the downwash using this value of λ_1 / λ_o results in a new value, at $\eta = 0.95$.

$$\frac{\lambda_1}{\lambda_o} = 1.28$$

Evidently, as the leading edge of the spiral approaches the leading edge of the disc, the upwash is intensified and a mildly unstable condition exists in which the wake is drawn up into the leading edge of the rotor disc. This phenomenon is believed to be of considerable qualitative significance, and to a large part accounts for the roughness in transition and flares experienced on most helicopters, and the characteristic noise generated by rotors under conditions of wake interference. Many methods of alleviating this condition may be envisaged; for example, ensuring as gradual a drop off of circulation at the blade tips as possible without unduly sacrificing performance in order to reduce the intensity of the tip vortex.

This may be done by moderating twist. Operationally, of course, the phenomenon may be greatly reduced by a climb-out or high acceleration through transition, a maneuver which will not always be possible. On tandem configurations, the possibility exists of providing relative tilt of the two tip path planes such that the front rotor provides most of the propulsive force, thereby operating at high inflows.

The rear rotor, operating in the downwash of the front rotors, presents a lesser problem. As shown in Reference 38, the transition characteristics of a tandem configuration may be widely varied by adjustment of stagger and overlap.

Finally, the experimental results in Reference 22 showed the marked reduction in the first harmonic inflow variations which occur when the rotor is allowed to carry a moment at the hub. This is because the blade no longer equalizes lift around the azimuth and Γ_1 becomes appreciable, thereby producing a first harmonic downwash reducing the first harmonic upwash arising from γ_o. In practice, carrying large rolling or pitching moments produces high cyclic loads in the rotor system with attendant weight penalties. Furthermore, large offset of the flapping hinge with low blade Lock numbers are required, since the blade cannot be stiffened structurally sufficiently to prevent elimination of most of the cyclic lift change by elastic flapping. A discussion of this phenomenon is given in Reference 39 together with estimates of the rolling moment as a function of the stall alleviation resulting from the cyclic lift variations.

2) Harmonic Content of the Downwash in Cruising Flight

In Figure 18 are plotted the harmonic contents of the wake at a μ of 0.3 due to the tip trailing vortex system for various harmonics. Of interest is the pronounced phase shift as evidenced by the relatively large sine components of downwash compared to the results of μ of 0.1.

Of particular interest is the persistence of the higher harmonic content at the higher advance ratio. At the lower advance ratio (Figure 17) the higher harmonic induced flows are of the order of 20 per cent of the steady-state induced flows. At the higher advance ratio (Figure 18) the mean value over the blade span of the steady-state component of the induced flow has been appreciably reduced, as indicated by a comparison of P_o^o from Figures 17 and 18. This is a might be expected since it is well known that, for a given lift, the induced flow decreases with forward speed. However, contrary to previous expectation, the higher harmonic

components of induced flow have not been appreciably reduced; hence, the vibration level and also the blade fatigue stresses, due to nonuniform downwash, are not alleviated with increasing forward speed.

In Figure 9 the downwash before harmonic analysis has been plotted against azimuth and compared with the experimentally-determined downwash of Reference 22. The two rotors are not strictly comparable; in particular, the rotor of Reference 22 operated at appreciably lower inflows, λ_o, than have been assumed here. However, at advance ratios of $\mu = 0.3$, the effect of z, and, hence, λ_o, may be expected to be small compared to the effect of d, and, hence, μ, and the two results should be comparable at least as regards distribution of inflow with respect to azimuth and span. Such a comparison can be made if both results are normalized at some azimuth position. $\psi = 0$, close to the point of a maximum downwash, has been selected for the common value. The agreement is excellent and it may, therefore, be concluded that, as far as the lower harmonics are concerned, the mathematical model chosen for this analysis is adequate. The higher harmonics were attenuated in tests of Reference 22 and, consequently, no direct comparison is possible between theory and experiment.

3) Lift-Deficiency Function in Forward Flight

It is of interest to examine the order to magnitude of C(k), the lift deficiency in forward flight for harmonic lift variations and to compare the phase shift resulting from the spiral form of the wake with that occurring in the two-dimensional case. As a model, a harmonic variation in blade bound circulation will be assumed invariant with span, a condition somewhat approximating the test techniques employed in Reference 6 in which the hub was displaced harmonically. All interharmonic coupling will be neglected.

For $\eta = 0.80$, $b/R = 0.05$, $n = 3$ the reduced frequency is $nb/\eta R = 0.187$ and

73

$$I_c = 2.95 \qquad I_s = 1.29$$

$$I_c = 2.05 \qquad I_s = 1.21$$

Considering only the shed near wake, from Eq. (26), the circulation deficiency (which is somewhat less than the lift deficiency) is

$$\frac{\gamma_{3c}}{\gamma_{3c_q}} = \frac{1 + S}{C^2 + (1 + S)^2} = 0.675$$

and

$$\frac{\gamma_{3s}}{\gamma_{3c_q}} = \frac{C}{1 + S} \frac{\gamma_{3c}}{\gamma_{3c_q}} = 0.298$$

where γ_{3c_q} is the "quasi-static" circulation and may be represented by terms in brackets in

Eq. (26). For example,

$$\gamma_{ns_q} \quad [-\lambda_{ns} - n\eta a_n + \frac{\mu}{2} (b_{n+1} + b_{n-1})]$$

The lift-deficiency function for this case is then, from Eq. (27),

$$\frac{L_{3c}}{\rho V \Gamma_{3cq}} = \left[-k I_c' \frac{\gamma_{3s}}{\gamma_{3cq}} - k I_s' \frac{\gamma_{3c}}{\gamma_{3cq}} + 1 \right] = 0.734$$

$$\frac{L_{3s}}{\rho V \Gamma_{3cq}} = \left[k I_c' \frac{\gamma_{3c}}{\gamma_{3cq}} - k I_s' \frac{\gamma_{3c}}{\gamma_{3cq}} \right] = 0.19$$

These values are readily verified as being the values for the conventional lift deficiency function of Reference 29 for $k = 0.187$.

To this lift deficiency will now be added that due to the shed far wake.

74

From numerical calculations of Eq. (21) and for $\mu = 0.10$

$$A_{3c}^3 = 0.57 \qquad B_{3c}^3 = 3.39$$

$$A_{3s}^3 = -2.73 \qquad B_{3s}^3 = 0.55$$

The coefficient $nb/2R$ is 0.075 for the parameters assumed above and Eq. (22) then gives, for the shed far wake only,

$$\lambda_{3c} = 0.043 \, \gamma_{3s} + 0.205 \, \gamma_{3c}$$

$$\lambda_{3s} = 0.254 \, \gamma_{3s} - 0.041 \, \gamma_{3c}$$

Since all interharmonic coupling has been neglected, a legitimate assumption when one harmonic predominates in the input, the circulation deficiency may now be computed directly from Eq. (26) with the above values of λ_{3c} and λ_{3s} substituted on the right-hand side.

The result is

$$\frac{\gamma_{3c}}{\gamma_{3c_q}} = 0.596 \quad , \quad \frac{\gamma_{3s}}{\gamma_{3c_q}} = 0.234$$

The corresponding lift-deficiency function is, from Eq. (27)

$$\frac{L_{3c}}{\rho V \Gamma_{3c_q}} = 0.734 - 0.043 \times -.234 - 0.205 \times -.596 = 0.602$$

$$\frac{L_{3s}}{\rho V \Gamma_{3c_q}} = 0.19 - 0.254 \times 0.234 + 0.041 \times 0.596 = 0.155$$

The effect of the trailing wake will now be considered. For the conditions chosen,

$$\dot{P}^3_{3c} = 6.07 \qquad\qquad Q^3_{3c} = 2.5\dot{1}$$

$$P^3_{3s} = 2.42 \qquad\qquad Q^3_{3s} = 6.78$$

Proceeding as before for the shed wake, Eq. (26) for the third harmonic components yields, for the complete wake

$$\frac{\gamma_{3c}}{\gamma_{3c_q}} = 0.570 \quad , \quad \frac{\gamma_{3s}}{\gamma_{3c_q}} = 0.186$$

The corresponding lift-deficiency function is, from Eq. (27)

$$\frac{L_{3c}}{\rho V \Gamma_{3c_q}} = 0.602 + 0.06 \times 0.186 - 0.152 \times 0.570 = 0.525$$

$$\frac{L_{3s}}{\rho V \Gamma_{3q}} = 0.155 - 0.170 \times 0.186 - 0.06 \times 0.570 = 0.090$$

It is apparent from the above, that the near and far wakes contribute about equally to the lift deficiency or reduction in slope of the lift curve, for the representative condition chosen.

It is of interest to compare the lift deficiency at $\mu = 0.1$ obtained above with that predicted from the simplified hovering solution in closed form. The numerical computations at a given μ required definition of λ, Q, and b/R only. The corresponding value of h is

$$h = \frac{2\pi R \lambda}{Qb} = \frac{2\pi \times 0.05}{3 \times 0.025} = \frac{2\pi}{3}$$

and the lift-deficiency function is then, from Eq. (24)

$$\frac{1}{1 + \frac{\pi}{h}} = 0.40$$

4) Examples of Load Computations

Applications of the theory to load computations and the degree of refinement required in the numerical solutions may best be discussed by considering certain typical cases.

The airloads of Figure 10 have been computed using lifting-line theory and the lift-deficiency functions obtained in the manner described above. Clearly, large and rapid changes in blade angle and lo al loading are indicated. It is, therefore, of interest to examine the effect of using lifting-surface theory as discussed in Sections VI and VII. In Figure 19, the lift due to downwash alone computed using lifting-surface theory (Eq. (10)), is compared with the lifting-line solution. These results have been obtained by computing the downwash at six chordwise stations on the blade and reducing the interval size to one degree for the case $\zeta = 90^{\circ}$ over the last 180° of the integration. Evidently, from Figure 10, the contribution of the time dependent terms is small except at the point of maximum change in downwash. It would, therefore, appear that reasonable approximations could frequently be obtained by using simply an average value of downwash along the blade chord and eliminating the time dependent terms in Eq. (10) such that $dL = \rho \pi b V A_o$. The lift deficiency functions of Figures 7 and 8 could then be applied directly to this lift.

Another problem encountered in the computation of loads is what may be termed the tip effect. The results in Figure 10 were obtained using five spanwise stations and six discrete trailing vortex lines. This is a satisfactory solution for

the rotor blade in question, which had a ratio of chord to radius of about 0.05. The outboard station was at 95 per cent of the span. This adequately defined the drop-off in lift at the tip of the blade. However, on a two-bladed rotor with a chord to radius ratio of 0.15, specifically that of Reference 23, ten spanwise stations were required before satisfactory agreement with the measured loads at the tip was obtained. This is shown in Figure 20. Also shown in Figure 20 is the effect of a two-station solution; that is, a tip vortex and one located at the 50 per cent radius point with constant circulation in between.

In Figure 21 has been plotted the theoretical and experimental harmonic airloads at the 85 per cent station in which the lower harmonics up to and including the second have been removed. Apart from emphasizing the effect of the higher harmonics, elimination of the lower harmonics avoids a major problem in computing airloads. The first harmonic airload is the small difference between two large quantities; the first harmonic variation in downwash which, as will be discussed in the next section, may be pronounced, and the blade first harmonic flapping, also a relatively large quantity. This harmonic flapping is difficult to measure experimentally because of the inevitable flexing of the rotor blade, which makes the root articulation a poor indication of the mean-blade flapping angle. However, harmonics above the second are relatively insensitive to blade-flapping motion and, providing the blade is not close to resonance with one of its elastic modes, the airloads above the second harmonic are substantially independent of all blade motion and are directly proportional to the higher harmonic downwash. Almost all the harmonic content of the airload, which is of interest for rotor vibration, is contained in the harmonics above the second. Consequently, the examination of these harmonics alone is a more rigorous technique than examination of the complete airloads.

It is also interesting to observe in Figure 21 the effect of one spiral instead of the usual three spirals of downwash used in the regular computations. Evidently, very reasonable distributions of higher harmonic airloads can be obtained using fairly simplified rigid wake geometry concepts.

XII. SIMPLIFIED SOLUTIONS

In view of the importance of those portions of the wake in the immediate vicinity of the blade in determining the harmonic airload, a drastic simplification was attempted in computing the airloads. The spiral vortex line was eliminated and replaced by an infinite straight vortex line wherever the blade passed over its own or a wake generated by another blade and only if it passed over such a wake during the first spiral. Following the approach of Reference 4 and Reference 18, this straight vortex was assumed to extend to infinity in both directions below the blade which permitted the following simple solution to be obtained for its downwash (Figure 15)

$$ w = \frac{\Gamma}{2 \pi R} \cdot \frac{(y - \eta) \cos \delta}{z^2 + (y - \eta)^2 \cos^2 \delta} $$

where ηR is the blade station at which the downwash is to be computed; yR is the blade station under which the vortex line passes at any instant; δ is the angle between the vortex line and a line perpendicular to the blade in the plane of the blade and zR is the vertical displacement of the vortex line below the blade. If the blade is at azimuth angle ψ and the vortex line was generated when the blade was at azimuth ϕ then

$$ y = d \cos \psi + \sqrt{\ell^2 - d^2 \sin^2 \psi} $$

and d, the distance travelled by the rotor hub between the time when the blade was at ϕ and its present position at ψ, is given by

$$ d = \mu [S + (\psi - \phi)] $$
$$ z = \lambda [S + (\psi - \phi)] $$

where S is the spacing between blades

79

By setting ($\psi - \phi$) initially equal to zero, the value of d and ϕ may be readily obtained by iteration from these expressions together with the relationship

$$d \sin \psi = \ell \sin(\phi - \psi)$$

The angle δ is obtained from

$$\tan(\phi - \psi - \delta) = \frac{-\mu \cos \phi}{\eta + \mu \sin \phi}$$

The case $\delta = 0$ defines the near wake or $\psi - \phi = 0$, d = z = 0 and y = ℓ . The vortex line is then integrated from 0 to ∞ and, hence, for $\delta = 0$, w has the value

$$w = \frac{\Gamma}{4 \pi R} \cdot \frac{1}{(\ell - \eta) \cos \delta}$$

Since the solution requires no integrations along the wake, computer time is reduced by a factor of the order of 50. Typical results are shown in Figure 23 together with the more complete solution and the experimental data. It is evident that for many engineering applications the simplified method is entirely adequate. Of particular interest is the close agreement between the solution using a constant circulation over the outer 50 per cent of the span and the more complete solution.

One other aspect of the downwash variations predicted by the theory may be briefly reviewed. Large changes in downwash are predicted in the regions of the 90° and 270° azimuth positions and the local blade angle changes associated with this downwash variation will be of the same order as the mean blade angle of attack. The changes occur sufficiently rapidly so that flapping may not provide much relief. Consequently, it may be expected that the stall pattern over the ratio disc will be appreciably different from that predicted by uniform inflow theory. Reference 40 indicates that the result is to provide an appreciable amount of stall alleviation over the retreating side. An examination of Figure 9 indicates that this logically could be expected in view of the increased downwash in this region and on the opposite side of the disc.

CONCLUSIONS

1) The nonuniform downwash induced at the rotor disc by the wake vortex system has a sufficient amount of higher harmonic content to account for the higher harmonic airloads encountered on rotor blades in forward flight. This higher harmonic content does not decrease with forward speed, as does the steady-state component of downwash.

2) The analysis and interpretation of the results are considerably simplified by dividing the wake into a "near" wake extending from the blade to approximately one quarter of the disc aft and a "far" wake containing the rest of the spiral. The higher harmonic content of the downwash is due almost entirely to the far wake and particularly to that portion passing under the blade and generated either by itself or another blade.

3) It follows from the previous conclusion that the harmonic airloads will be sensitive to the vertical spacing of the wake. Consequently, it is necessary to introduce the concept of a nonrigid wake, particularly in low-speed transition flight or under any condition where the wake spacing is reduced such as in a flare. Under these conditions, the wake could be sucked up into the leading edge of the rotor disc. It is believed that this is most probably the source of transition roughness and of the characteristic rotor noise encountered under cetain flight regimes.

4) Unsteady aerodynamic effects are of considerable importance for the rotor because of the proximity of the returning wake to a blade. Analysis of these effects for the three-dimensional rotor is appreciably simplified if the far wake is treated using lifting-line theory, and lifting-surface theory is used only for the near wake. The validity of this approach has been demonstrated by comparing the equivalent treatment of a two-dimensional model of the returning wake system with a treatment using lifting-surface theory for both the far and near wakes.

5) In hovering flight, a simple closed-form solution is obtained for the reduction in lift due to unsteady aerodynamic effects by proceeding to the limiting case of an infinite number of blades. It is shown that for normal rotor or rotor/propeller operating conditions, .he harmonic lift generated by a cyclic change in blade, pitch would be less than half that indicated by simple quasi-static theory and this reduction in lift is substantially independent of frequency.

6) Generalized lift-deficiency functions can be developed for the rotor in forward flight. "From the nature of these results, it is evident that, at advance ratios above about $\mu = 0.2$, these functions approach the classical two-dimensional values. This suggests a simplified treatment of the lift deficiency in which the simple value obtained for the hovering case is faired into the two-dimensional value at $\mu = 0.2$.

7) A simplified approach, using infinite vortex lines to represent the far wake located below the blade at the point at which the blade passes over the vortex, gives results in close agreement with the more accurate treatment. It suggests several possible approximations which would result in a major reduction in required computer time.

NOMENCLATURE

A_n = coefficients of chordwise vorticity distribution.

$A^k_{nc_\ell}$ = coefficient of cosine component of kth harmonic of circulation or downwash at station ℓ due to a cos n ϕ variation of shed wake vortex strength.

$B^k_{ns_\ell}$ = same, except sine component due a sin n ϕ input.

$P^k_{nc_\ell}$ $Q^k_{ns_\ell}$ = same, except due to trailing wake.

C(k,m,h), C(k), C = lift-deficiency function.

$C_n = k \, I_c$

C_T = thrust coefficient = $T / \pi \rho \, \Omega^2 R^4$

$F(\phi)$ = integrand for far shed wake.

I_c , I_s = Integrals defining blade circulation due to near shed wake.

I'_c , I'_s = Integrals defining blade lift due to near shed wake.

L = lift

LN = blade Lock number (inertia parameter).

φ = number of blades

R = rotor radius

$S_n = k \, I_s$

T = rotor thrust.

V = forward velocity

a = distance between center of twist and center of airfoil – positive aft.

a_n = blade-flapping angle (cosine component)

b = blade semichord

b_n = blade-flapping angle (sine component)

d = horizontal distance travelled by rotor hub

$f(\phi)$ = integrand for trailing wake

$g(\phi)$ = integrand for shed wake after integration over ℓ

h = wake spacing

$h^* = bh$

i = angle between rotor disc and relative wind, positive nose up.

$$k = \frac{nb}{\eta R} = \frac{\omega b}{\Omega R \eta} = \text{reduced frequency}$$

ℓ = rotor span parameter

m = number of wake spirals – also used for frequency ratio in two-dimensional solution

n = harmonic of rotor speed – also used for wake identification in two-dimensional solution

u = velocity at airfoil due to airfoil motion.

v = induced velocity due to blade-distributed vorticity

w = induced velocity at blade due to wake

x = distance along blade chord, nondimensionalized with respect to R unless starred

z = vertical distance travelled by rotor hub

Γ = vorticity in wake when unidentified by subscripts or superscripts, otherwise bound circulation on blade -

Ω = rotational speed

α = angle of attack

α_T = blade tip angle of attack

β = blade flapping angle = $a_o - \displaystyle\sum_{n=1}^{\infty} a_n \cos n\psi + b_n \sin n\psi$

γ = element of distributed vorticity

γ_n = nondimensional form of blade circulation = $\dfrac{\Gamma_n}{2\pi b \Omega R}$

γ_r = coefficient of series for blade spanwise circulation

ζ = blade spacing

η = rotor-span parameter

λ = inflow normal to rotor disc

χ = distance from reference point on blade to trailing edge.

μ = advance ratio = $\dfrac{V \cos i}{\Omega R}$

$\bar{\xi}$ = distance to element of vorticity in wake

$\xi^* = b\bar{\xi}$

ρ = density of air

σ = rotor solidity

ϕ = azimuth of wake measured from downwind position; also used for velocity potential in Section VI.

ψ = rotor azimuth measured from blade downwind position

Subscripts

q = quasi-static

N = near

F = far

nc = cosine n input

ns = sine n input

Superscripts

S = shed

T = trailing

REFERENCES

1. Daughaday, H., and Kline, J., "An Approach to the Determination of Higher Harmonic Rotor Blade Stresses, " Proceedings of the 9th Annual Forum, AHS, 1953.

2. Drees, J.M., "A Theory of Airflow Through Rotors and its Application To Some Helicopter Problems," The Journal of the Helicopter Association of Great Britain, Vol. 3, No. 2, July-August-September, 1949.

3. Mangler, K.W., "Calculation of the Induced Velocity Field of a Rotor," RAE Report 2247, February, 1948.

4. Loewy, R.G., "A Two-Dimensional Approach to the Unsteady Aerodyramics of Rotary Wings," JAS, February, 1957, Vol. 24, No. 2.

5. Miller, R.H., and Ellis, C.W., "Blade Vibration and Flutter," Journal of the AHS, July, 1956, Vol. 1, No. 3.

6. Avara, J.,Ham, N.D., and Moser, H.H., "Investigation of Rotor Response to Vibratory Aerodynamic Inputs -- Experimental Results and Correlation with Theory," WADC Report 58-87, Part 1.

7. Von Karman, T., and Sears, W.R., "Airfoil Theory for Nonuniform Motion," JAS, August, 1938, Vol. 5, No. 10.

8. Isaacs, R., "Airfoil Theory for Rotary Wing Aircraft," JAS, April, 1946, Vol. 13, No. 4.

9. Greenberg, J.M., "Airfoil in Sinusoidal Motion in Pulsating Stream," NACA TN 1326, June, 1947.

10. Leone, P., "Theoretical and Experimental Study of the Coupled Flap Bending and Torsion Aeroelastic Vibrations of a Helicopter Rotor Blade," Proceedings of 13th Annual Forum, AHS, 1957.

11. Jones, J., "The Influence of the Wake on the Flutter and Vibration of Rotor Blades," British ARC Report No. 18, 173, January, 1956.

12. Timman, R., and van de Vorren, A. I., "Flutter of a Helicopter Rotor Rotating in its Own Wake," JAS, September 1957, Vol. 24, No. 9.

13. Ashley, H., Moser, H. H., and Dugundji, J., "Three-Dimensional Effects on Unsteady Flow Through a Helicopter Rotor," WADC Report 58-87, Part III.

14. Coleman, R. P., Feingold, A. M., Stempin, C. W., "Evaluation of the Induced Velocity Field of an Idealized Helicopter Rotor," NACA ARR L5E10 (WRL 126), June 1945.

15. Castles, W., and deLeeuw, J. H., "The Normal Component of the Induced Velocity in the Vicinity of a Lifting Rotor and Some Examples of its Application," NACA TR 1184, 1954.

16. Heyson, H. H., and Katzoff, S., "Induced Velocities Near A Lifting Rotor with Nonuniform Disc Loading," NACA TR 1319, 1957.

17. Heyson, H. H., "Tables and Charts of the Normal Component of Induced Velocity in the Lateral Plane of a Rotor with Harmonic Azimuthwise Vorticity Distribution," NASA TN D-809, April, 1961.

18. Willmer, M. A. P., "The Loading of Helicopter Rotor Blades in Forward Flight," RAE Report Naval 2-N-76935 No. 8, April, 1959.

19. Castles, W., and Durham, W. L., "The Computed Instantaneous Velocities Induced at the Blade Axes by the Skewed Helical Vortices in the Wake of a Lifting Rotor in Forward Flight," ASTIA Document No. AD-210613, March, 1959.

20. Tararine, S., and Delest, M., "Experimental and Theoretical Study of Local Induced Velocities over a Rotor Disc for Analytical Evaluation of The Primary Loads Acting on Helicopter Rotor Blades," Giravions Dorand Company, U. S. Army Report DE 2012, October, 1960.

21. Brotherhood, P., and Stewart, W., "An Experimental Investigation of the Flow Through a Helicopter Rotor in Forward Flight," ARC Rand M No. 2734, September, 1949.

22. Falabella, G., and Meyer, J. R., "Determination of Inflow Distributions From Experimental Aerodynamic Loading and Blade Motion Data on a Model Helicopter Rotor in Hovering and Forward Flight," NACA TN 3492, Nov. 1955.

23. Rabbot, J. P., and Churchill, G. B., "Experimental Investigation of the Aerodynamic Loading on a Helicopter Blade in Forward Flight," NACA RM L56I07, October, 1956.

24. Miller, R. H., "Rotor Blade Harmonic Air Loading," IAS Paper No. 62-82, January, 1962.

25. Miller, R. H., "On the Computation of Airloads Acting on Rotor Blades in Forward Flight," Journal of the AHS, Vol. 7, No. 2, April, 1962.

26. Miller, R. H., "Aerodynamics in the next Decade," Canadian Aeronautics and Space Journal, Vol. 9, No. 1, January, 1963.

27. Miller, R. H., "A Discussion of Rotor Blade Harmonic Airloading," Proceedings of CAL/TRECOM Symposium, Buffalo, New York, June 26-28, 1963.

28. Miller, R. H., "Unsteady Airloads on Helicopter Rotor Blades," The 4th Cierva Memorial Lecture, Journal of the RAE, Vol. 68, No. 640, April 1964.

29. Theodorsen, T., "General Theory of Aerodynamic Instability and the Mechanism of Flutter," NACA TR 496, 1935.

30. Scheiman, S., and LeRoy, H. L., "Qualitative Evaluation of Effect of Helicopter Rotor Blade Tip Vortex on Blade Airloads," NASA TN D-1637, May, 1963.

31. Glauert, H., "Airfoil and Airscrew Theory," C. U. Press, 1930.

32. Bisplinghoff, R. L., Ashley, H., and Halfman, R., "Aeroelasticity", Addison and Wesley, 1955.

33. Bierens, DeHaan, D., "Nouvelles Tables d'Integrales Definies," Stechert and Company.

34. Glauert, H., "The Force and Moment on an Oscillating Airfoil," ARC R and M No. 1242, 1929.

35. Peirce, F. , "A Short Table of Integrals," Ginn and Company.

36. Ghareeb, N. , "Programs for Machine Computation of Rotor Blade Downwash," Part 1, MIT ASRL Report No. 107-1.

37. Gessow, A. , and Myers, G. C. , "Aerodynamics of the Helicopter," Macmilland Company, 1952.

38. Duvivier, J. F. , "Study of Helicopter Rotor-Rotor Interference Effects on Hub Vibrations," MIT ASRL TR 95-1, October, 1961.

39. Miller, R. H. , "Some Factors Affecting the Design and Future Operation of Helicopters," Proceedings of the 4th Anglo-American Aeronautical Conference, London, 1953.
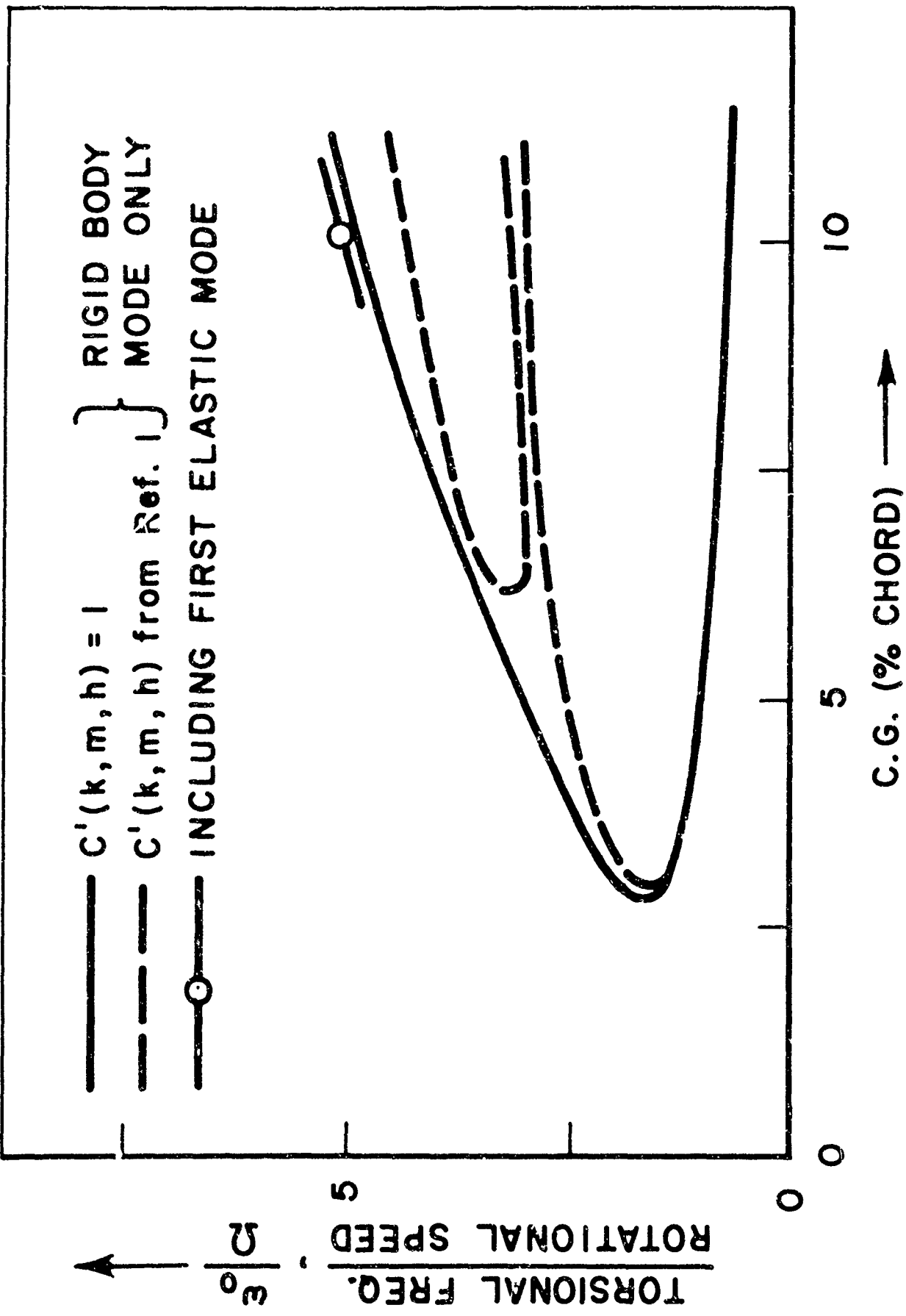
Fig. 1 Flutter Boundaries in Hovering, Showing Comparison Between Unsteady Aerodynamic and Quasi-Static Theory
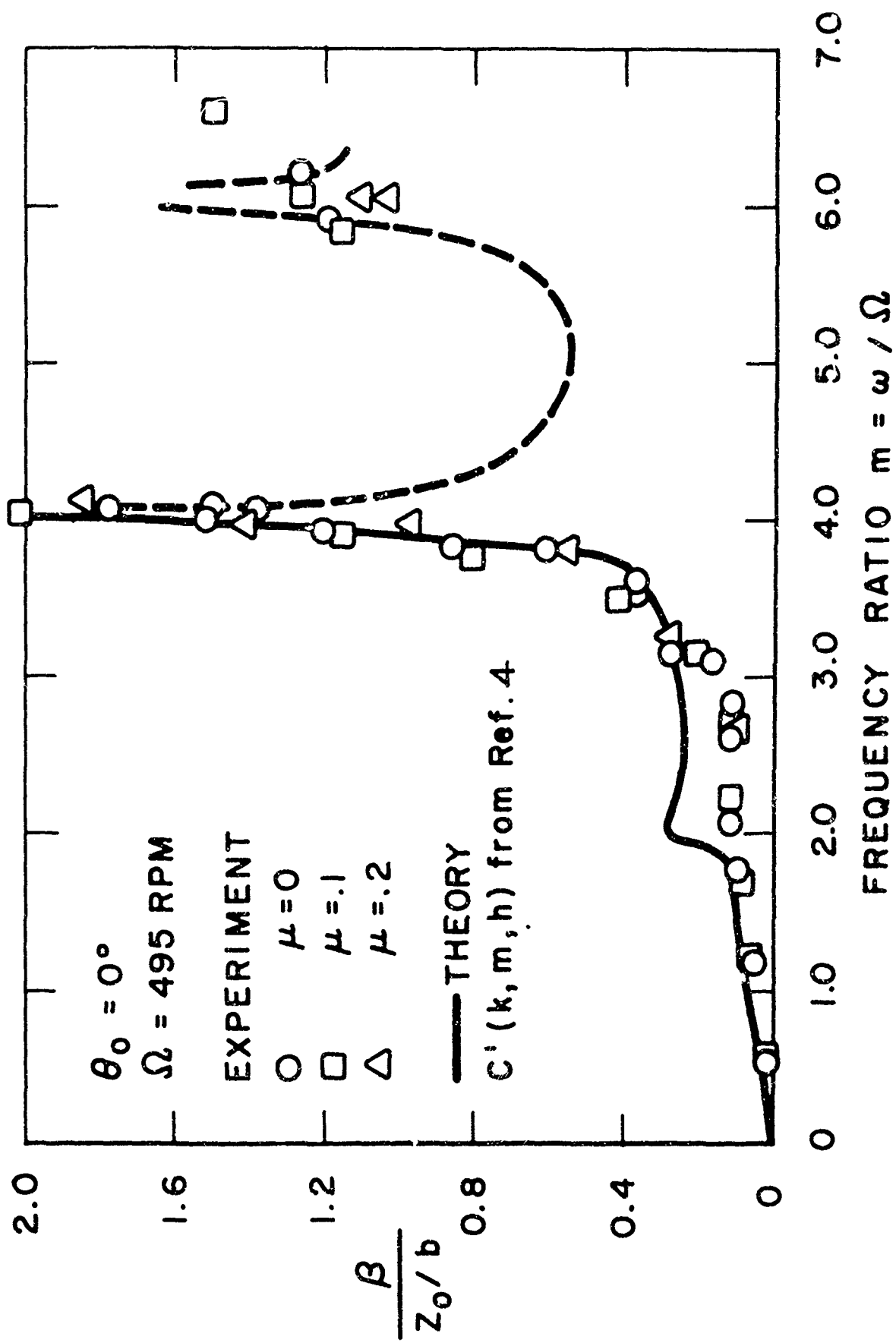
Fig. 2 Flapping Response to Sinusoidal Vertical Hub Displacement as a Function of Frequency Ratio for Different Advance Ratios.
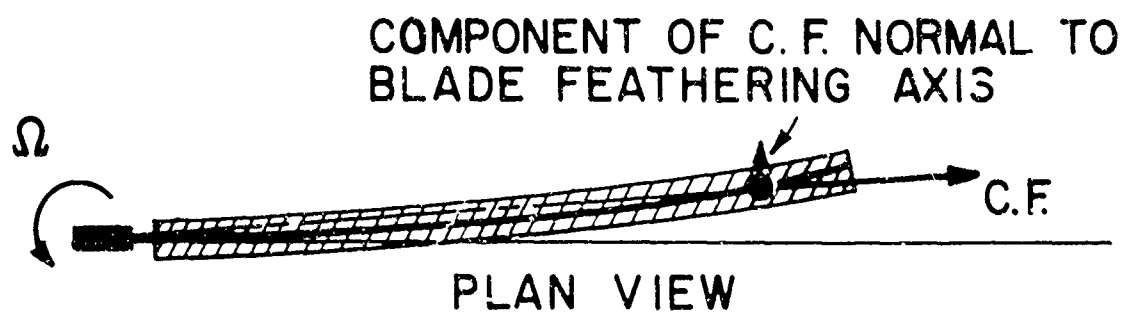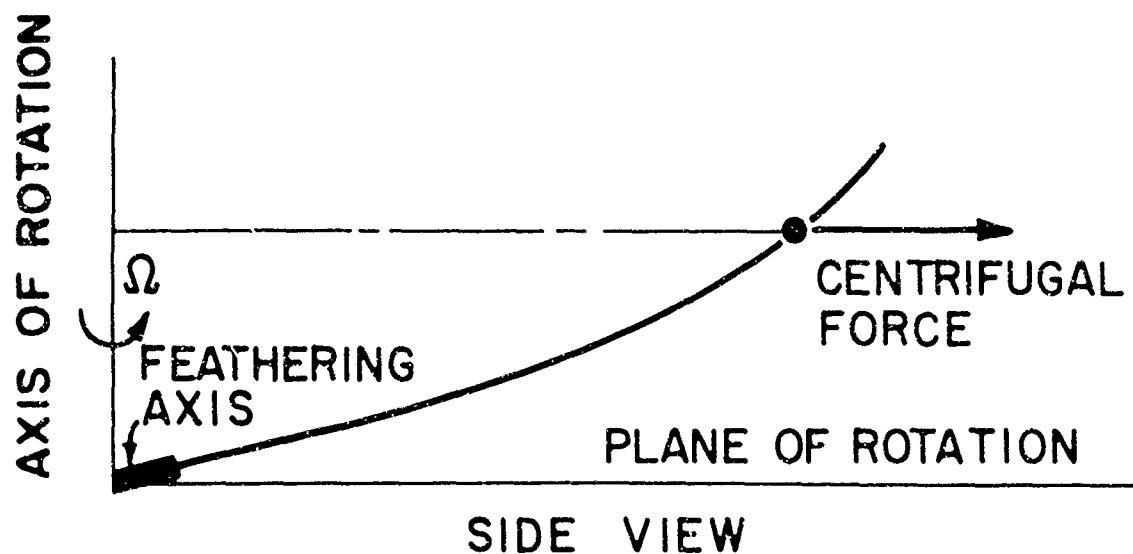
Fig. 3   Side view and plan view of blade bending out of plane of rotation and twisting about a feathering axis located near center of rotation. Component of centrifugal force normal to feathering axis causes additional twisting.
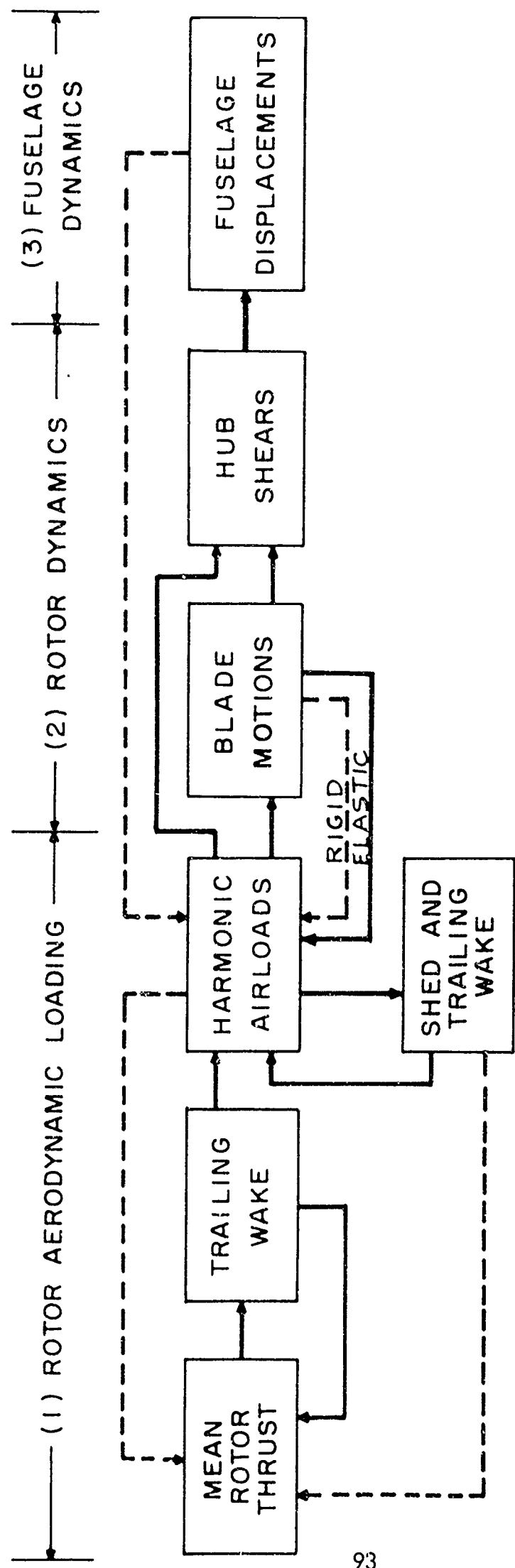
Fig. 4   Block diagram of elements contributing to helicopter vibration showing interactions.

93
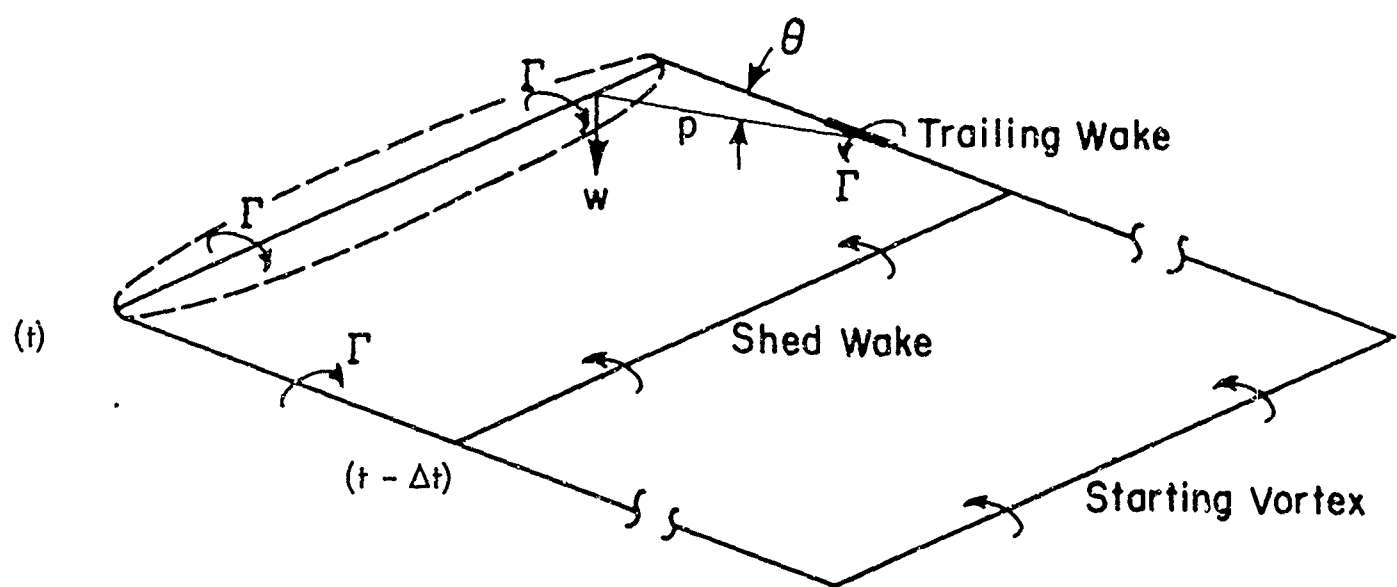
Fig. 5 Simplified Diagram of Fixed Wing Wake Geometry

ELEMENT OF
TRAILING WAKE

ELEMENT
OF
SHED
WAKE

ξ

$\mu = 0.2$
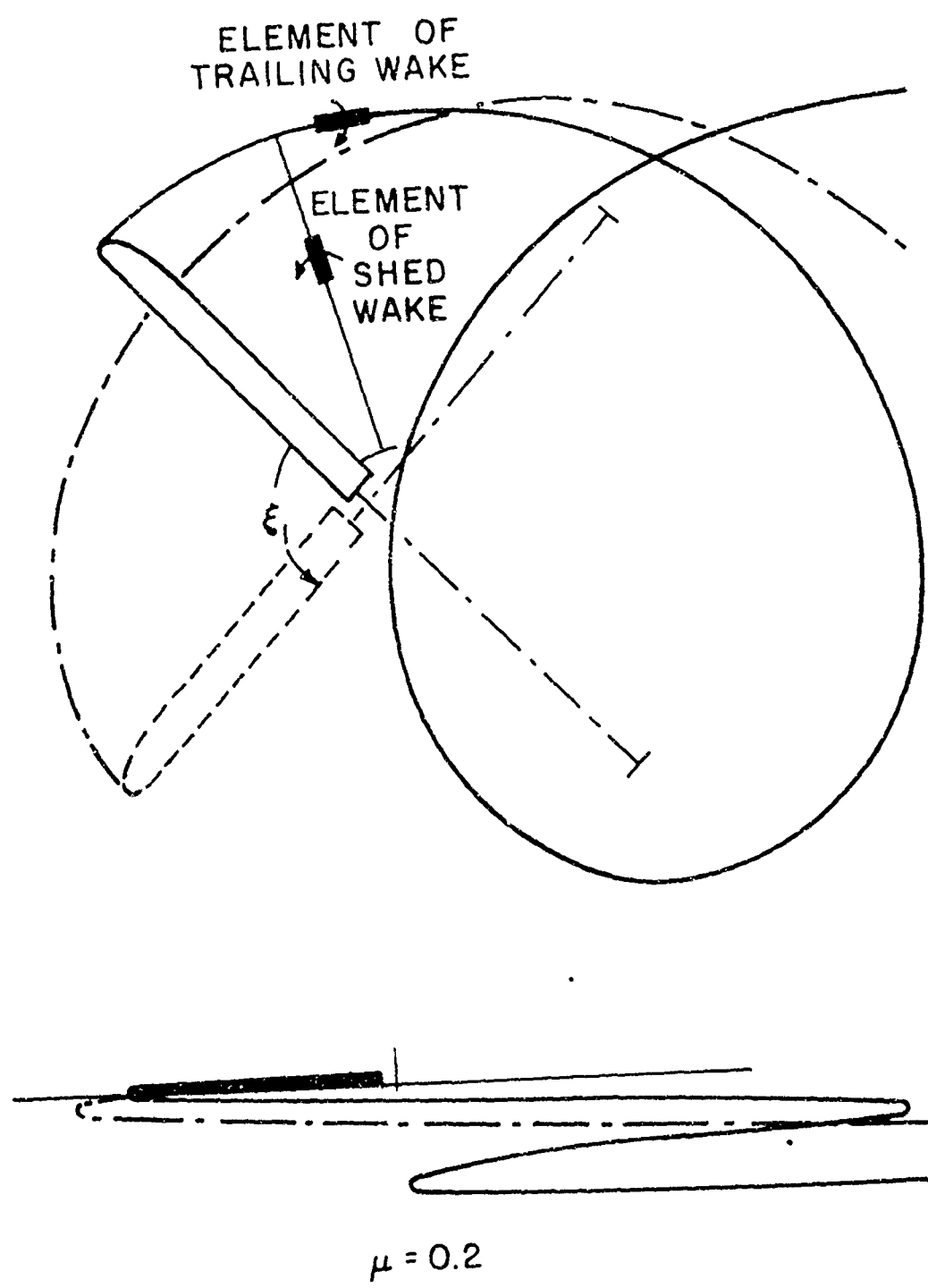
Fig. 6   Wake geometry showing trailing tip vortex and element of shed
wake.
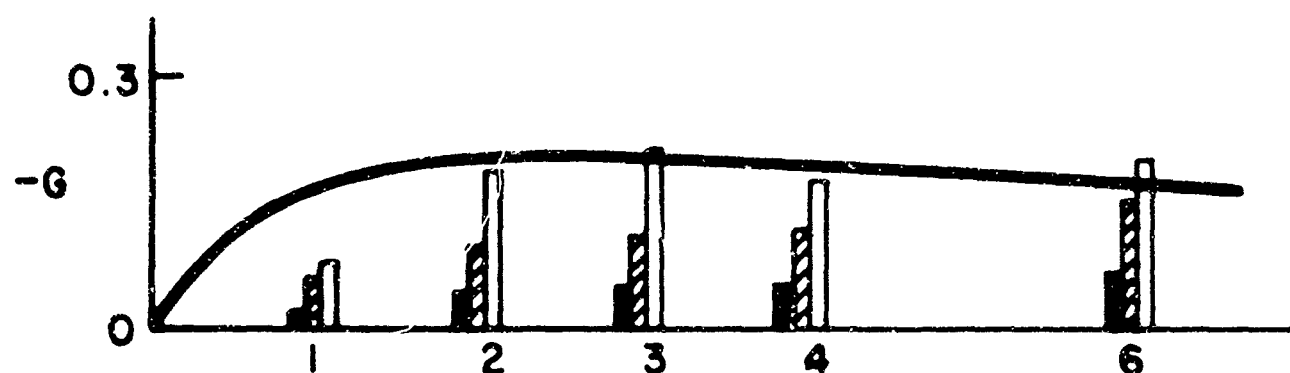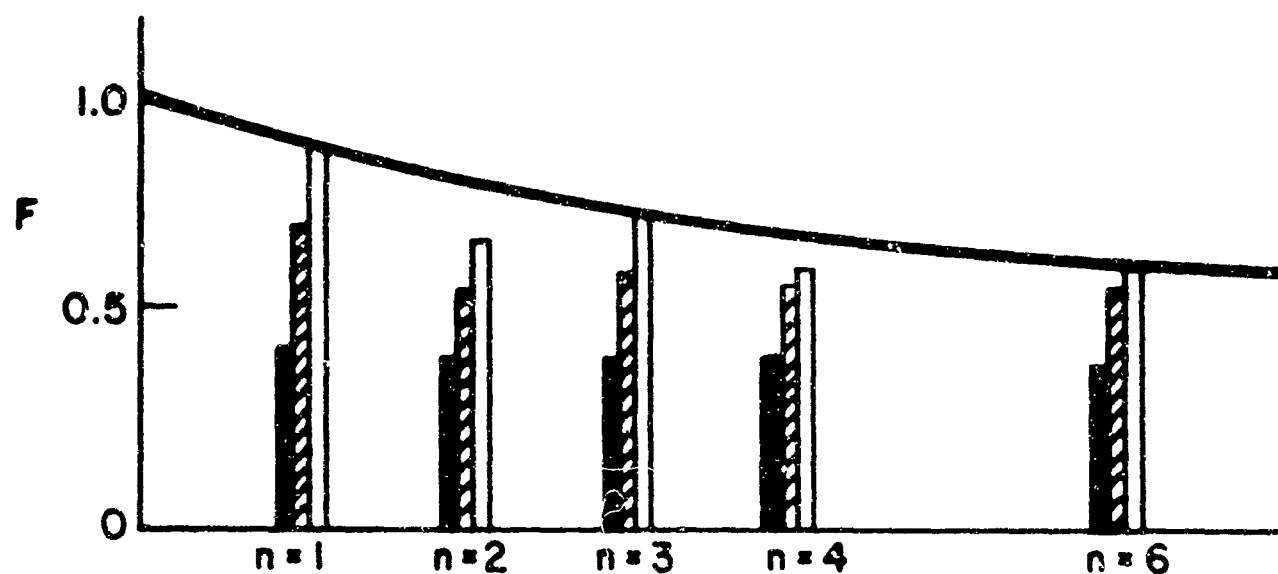
Fig. 7   Three-dimensional lift deficiency F, and phase shift $\tan^{-1} \frac{G}{F}$ as a function of harmonic n.   Conditions same as Fig. 4.

96
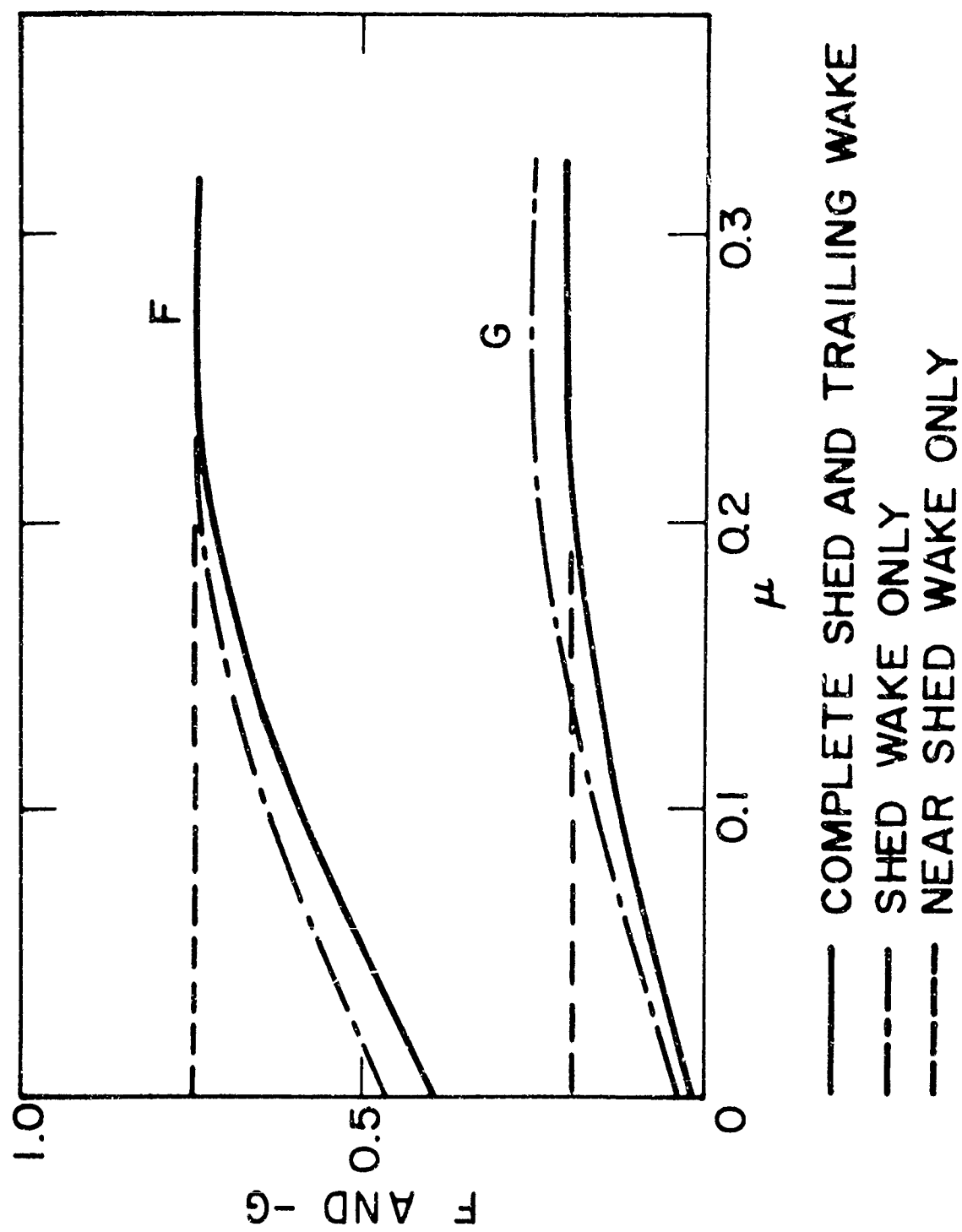
Fig. 8   Effect of advance ratio, μ, on reduction in lift, F, and phase shift $\tan^{-1}\frac{G}{F}$, due to three dimensional unsteady aerodynamic effects. Three blades, $\frac{2b}{R}=0.10$. $\rho=0.8$ $\lambda_0=0.05$ Third harmonic, $n=3.0$.
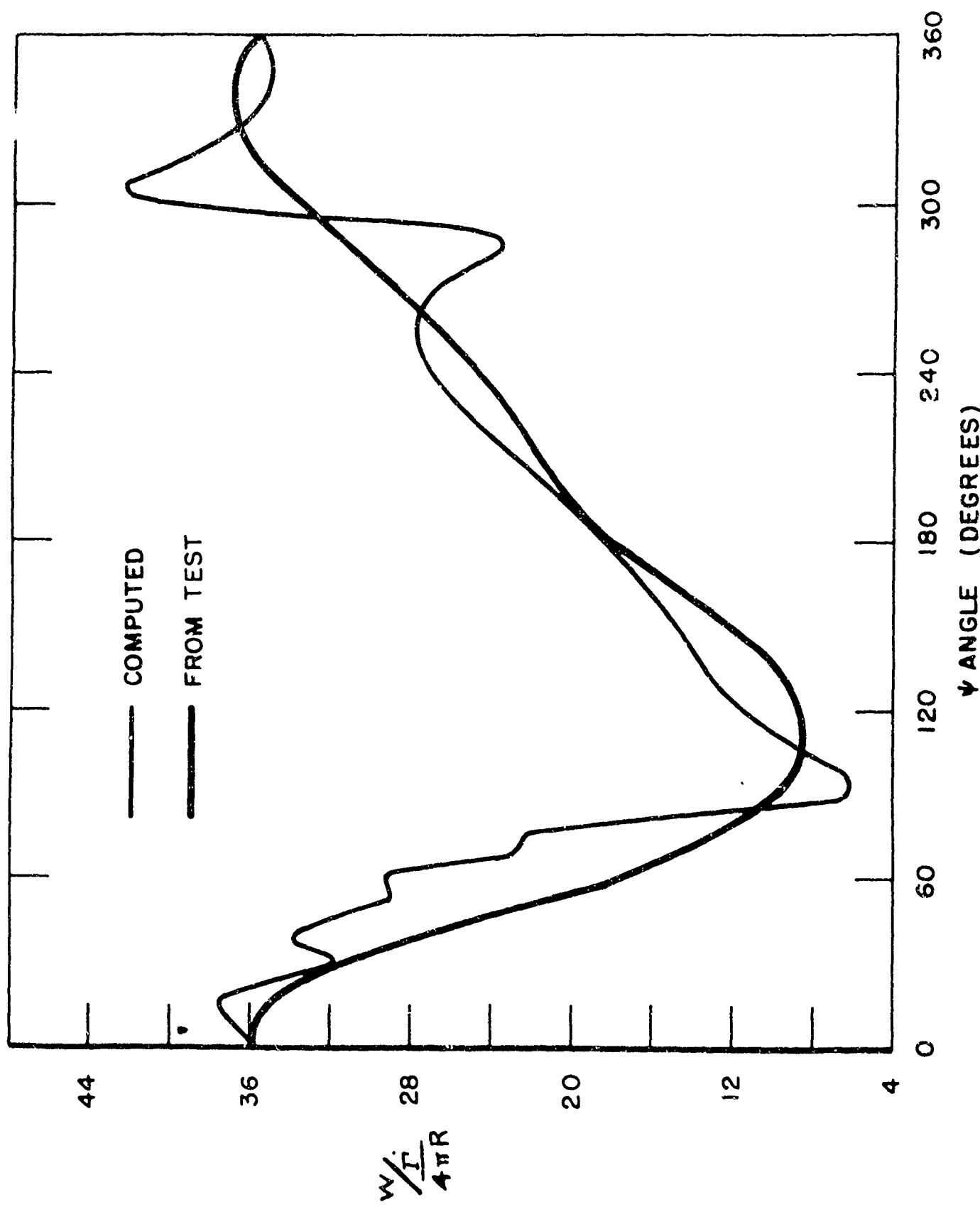
Fig. 9   Comparison of computed and experimental downwash at $\rho = 0.95$
μ = 0.3.
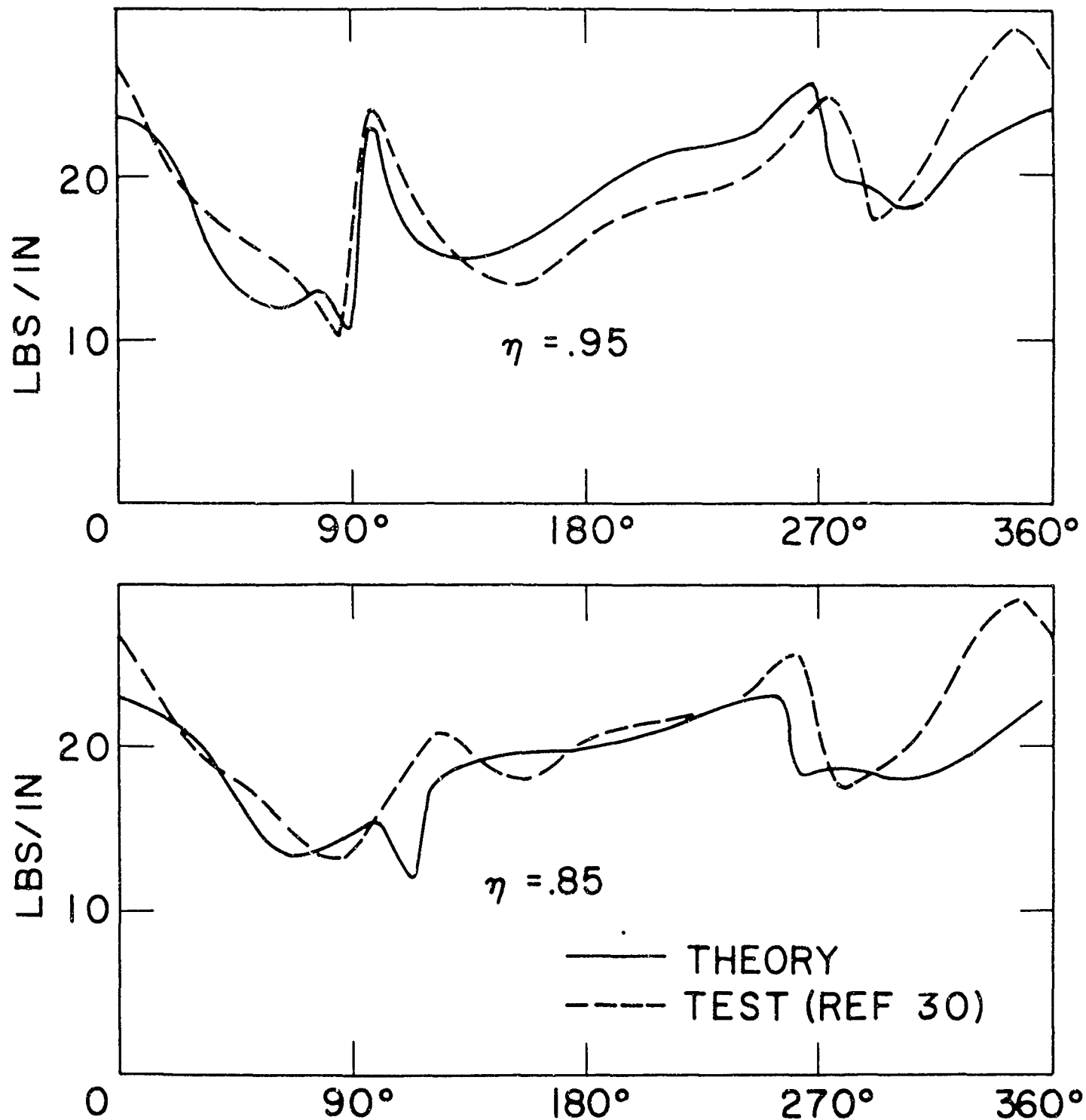
Fig. 10 Comparison of computed and experimental airloads.
Four-bladed rotor $\mu = 0.2$.
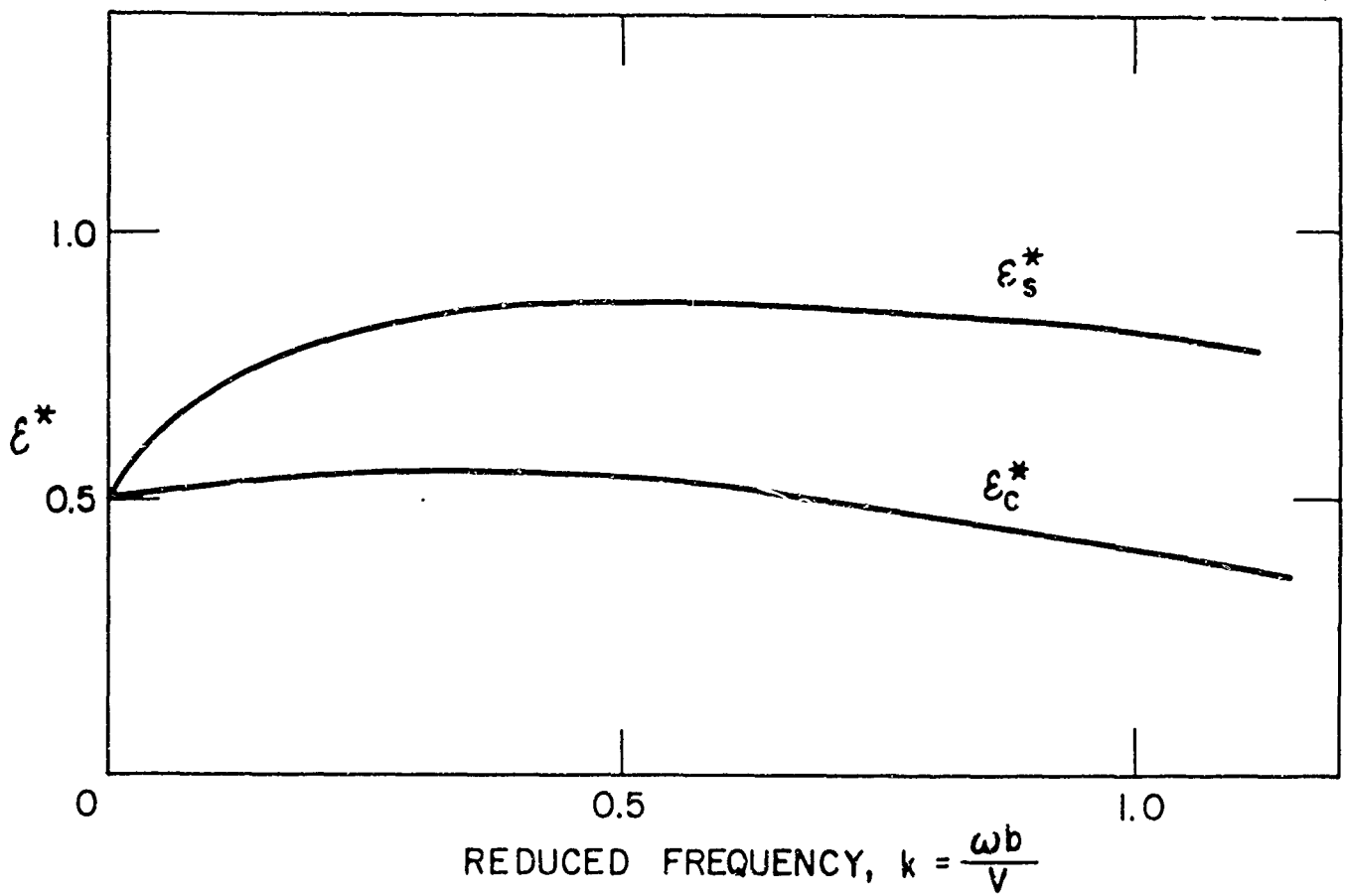
Fig. 11 Limit ε^* for shed-wake integration for use in lifting-line approximation
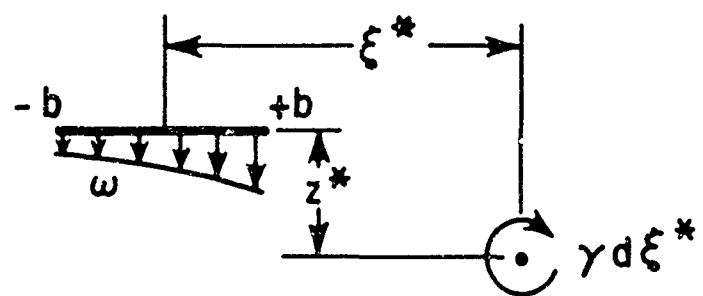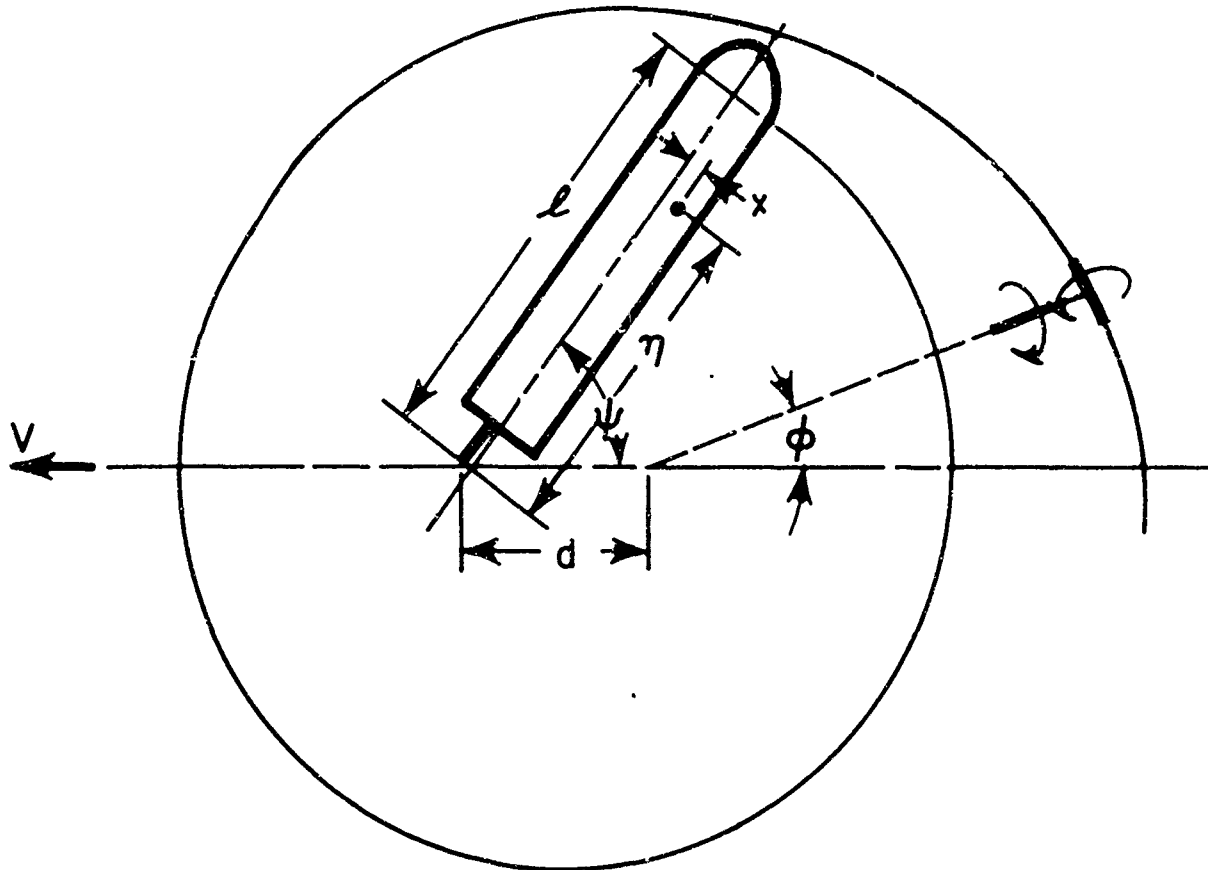
Fig. 12 Geometry of Far Spiral Wake and Near Straight Wake.
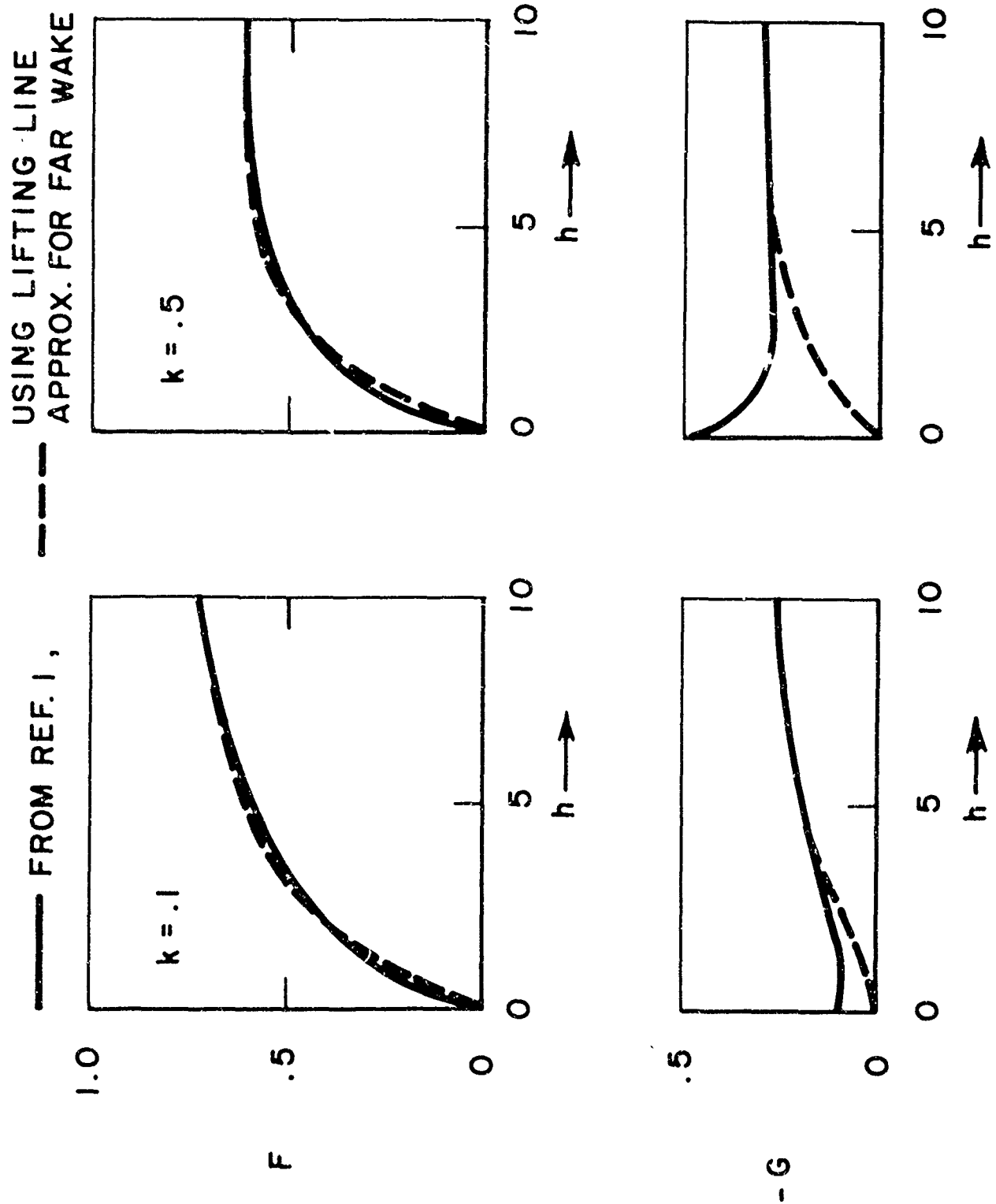
Fig. 13 Comparison Between Exact and Approximate Two-Dimensional Theory.

102
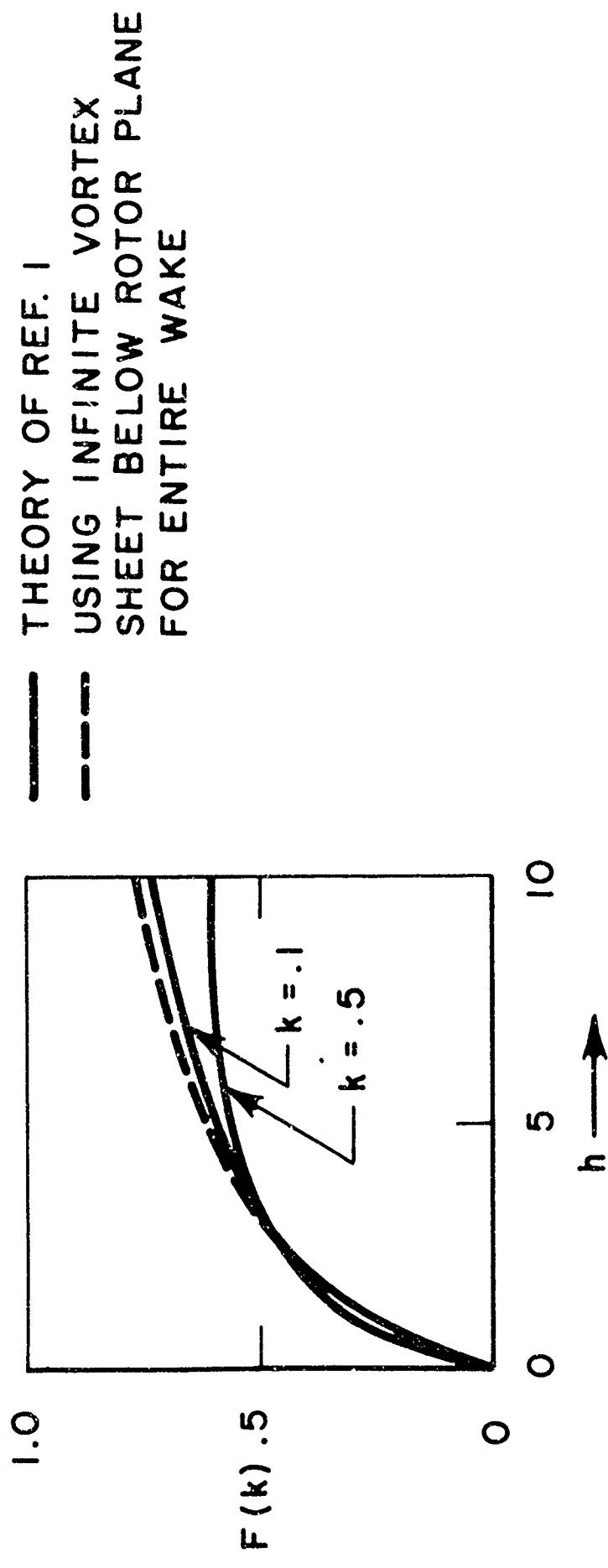
Fig. 14 Effect of Assuming an Infinite Number of Blades in Two-Dimensional Solution.
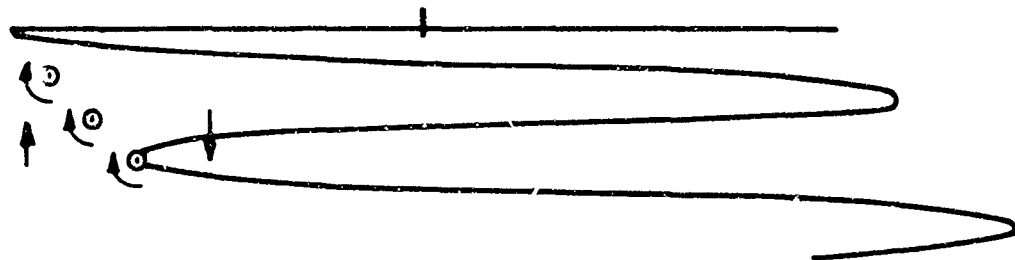
13a   RIGID   WAKE
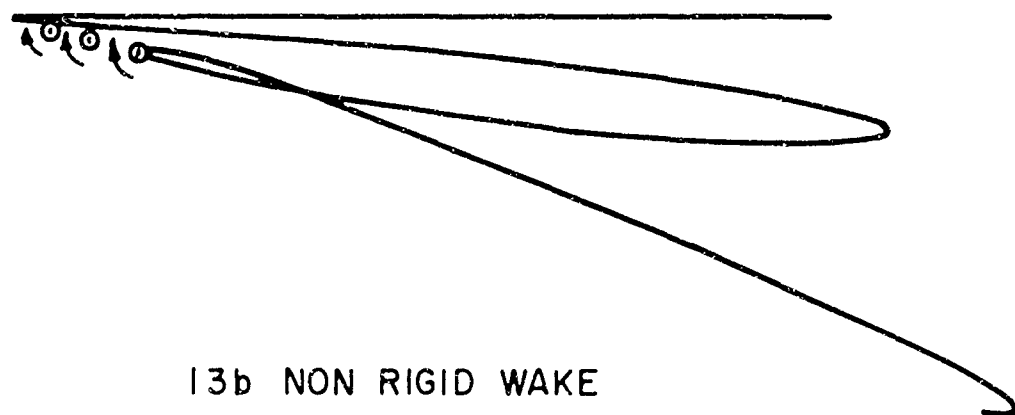
13b   NON RIGID WAKE

THREE BLADES-ONE SPIRAL ONLY SHOWN

Fig. 15   Geometry of wake at μ =.05.

          (a)   Rigid wake showing upwash from vortex lines at lead-
               ing edge of spiral.

          (b)   First approximation to nonrigid wake using downwash
               computed from (a).
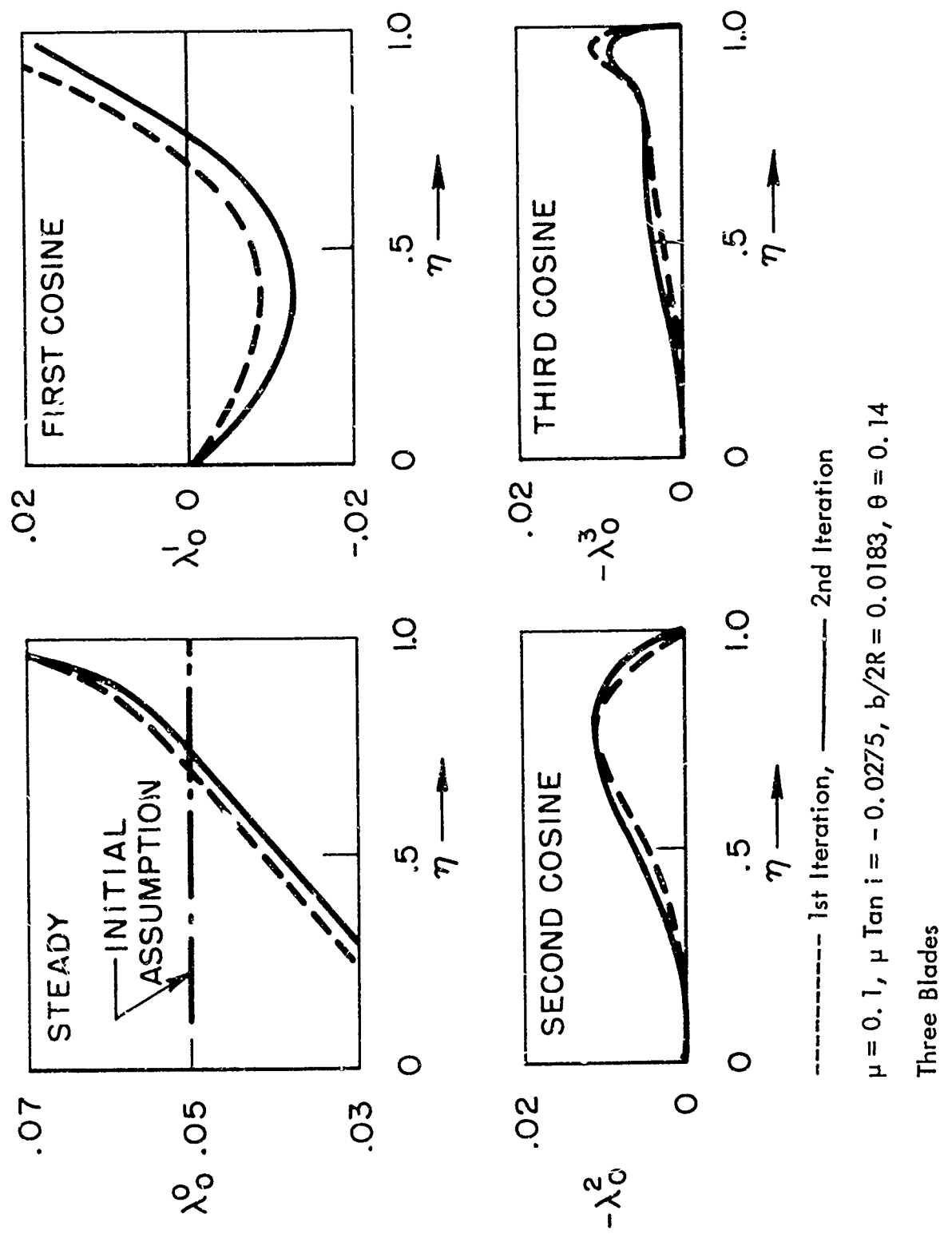
Fig. 16 Selected Harmonics of Downwash for a Straight Untwisted Blade Showing Results From First and Second Iterations

$\mu = 0.1$, $\mu \tan i = -0.0275$, $b/2R = 0.0183$, $\theta = 0.14$

Three Blades

----------- 1st Iteration, ——— 2nd Iteration
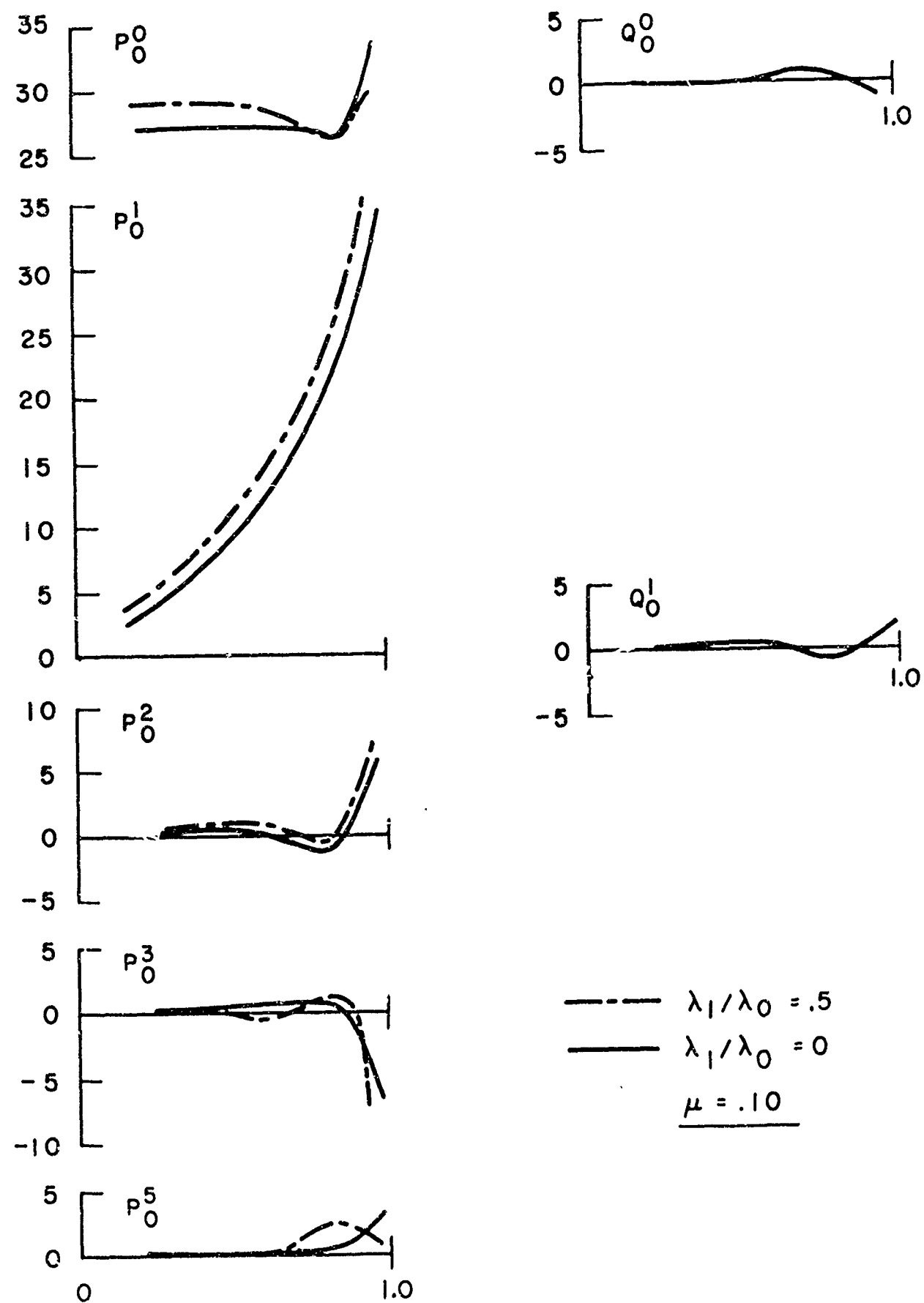
Fig. 17 Spanwise Distribution of Harmonic Downwash Coefficients at Blade Due to
Wake of Constant Strength, n = 0. Transition Flight Regime.
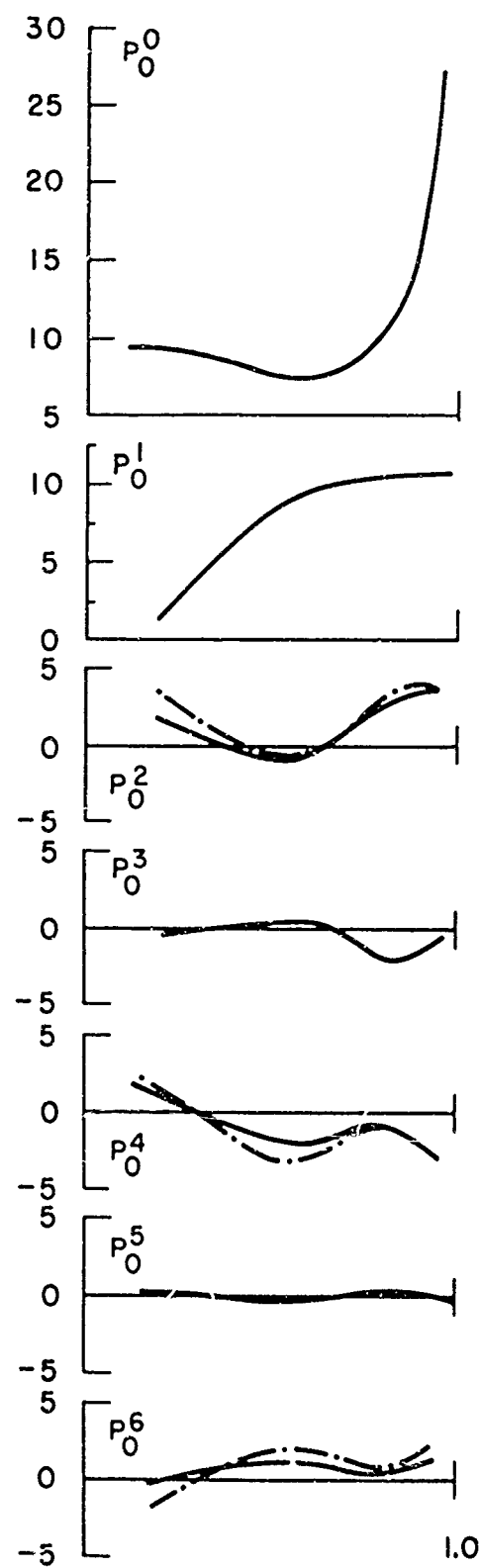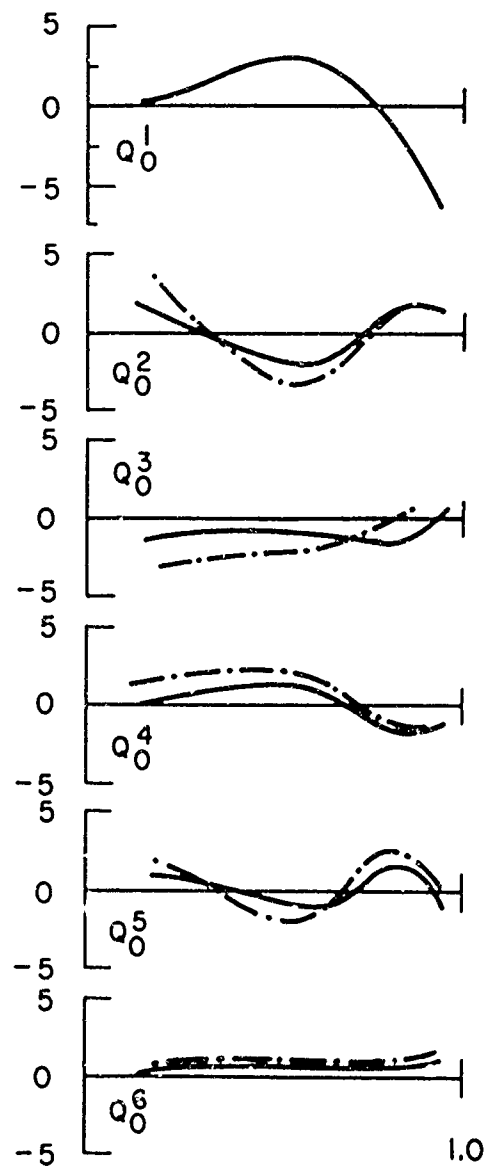
Fig. 18 Spanwise Distribution of Harmonic Downwash Coefficients at Blade Due to Wake of Constant Strength, n = 0. Cruise Flight Regime.
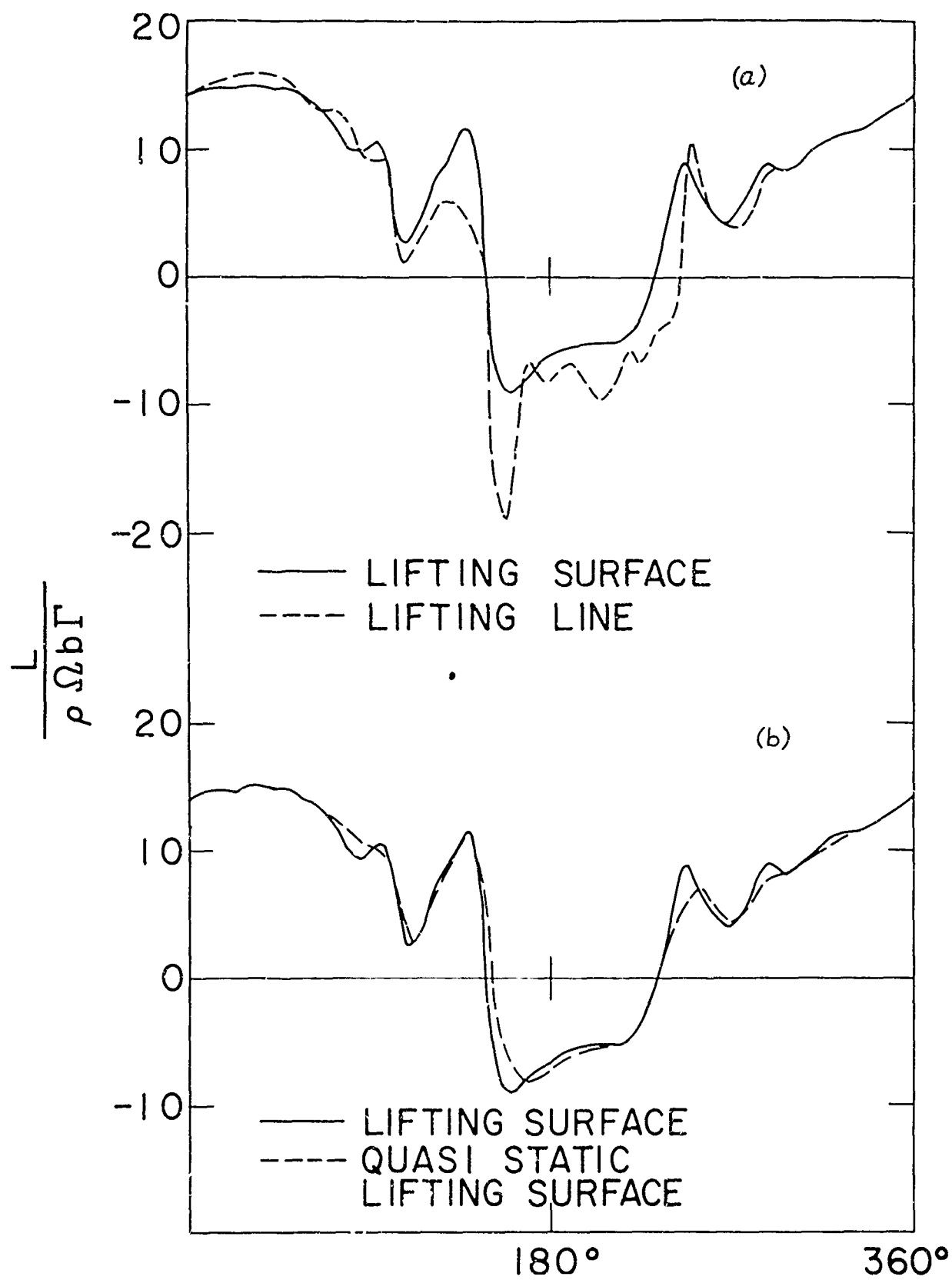
Fig. 19 Comparison between the lift generated by the downwash due to tip vortices of constant strength. Lift deficiency effects due to shed wake; harmonic trailing wake not included. $\mu = 0.2$ $\zeta = 0.75$
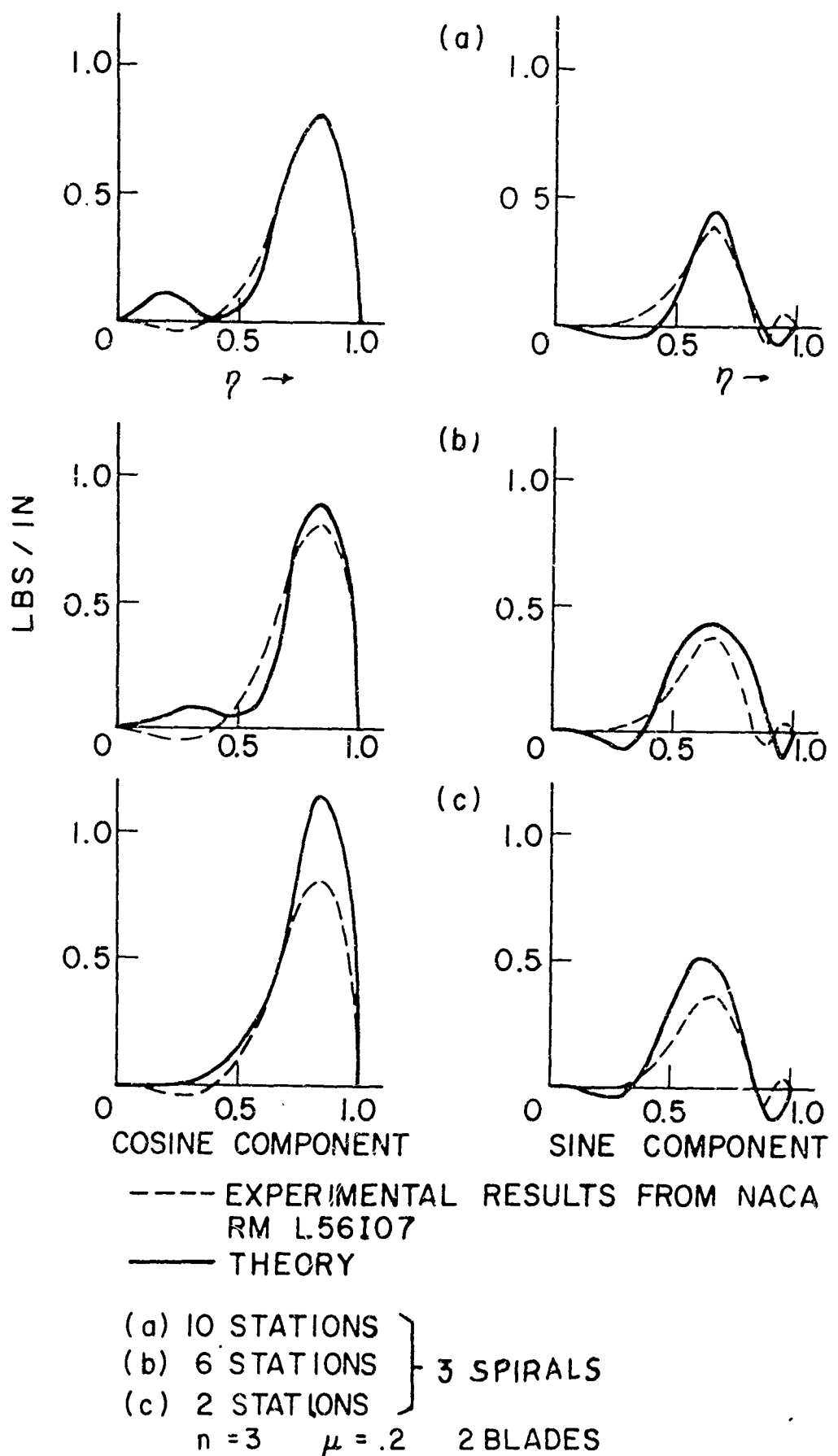
Fig. 20   Correlation between theory and test as a function of number of spanwise stations used in solution. Spanwise distribution of third harmonic airload.
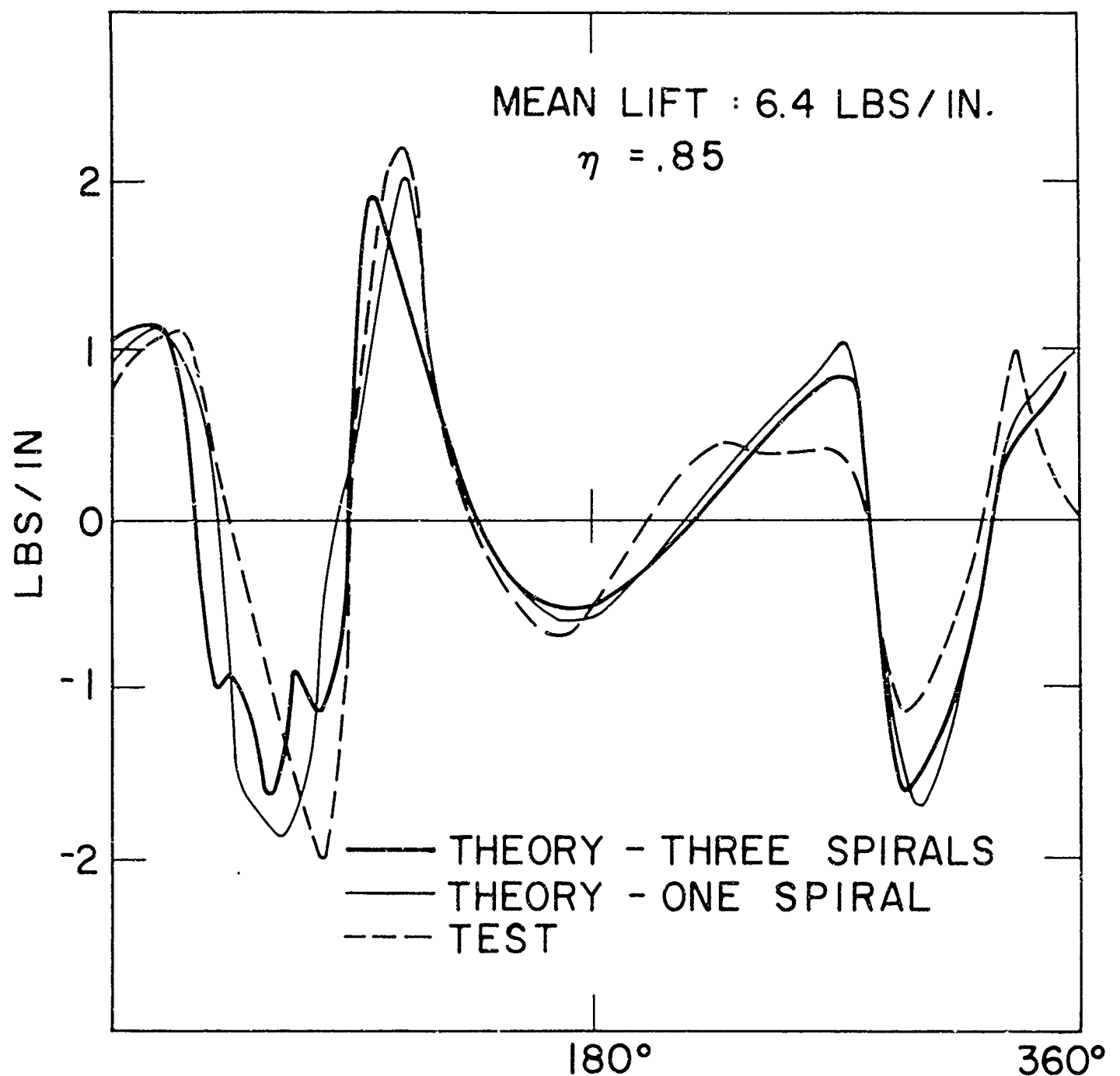
Fig. 21 Two-bladed rotor comparison between theory and test. Harmonics below the third eliminated. $\mu = 0.2$.
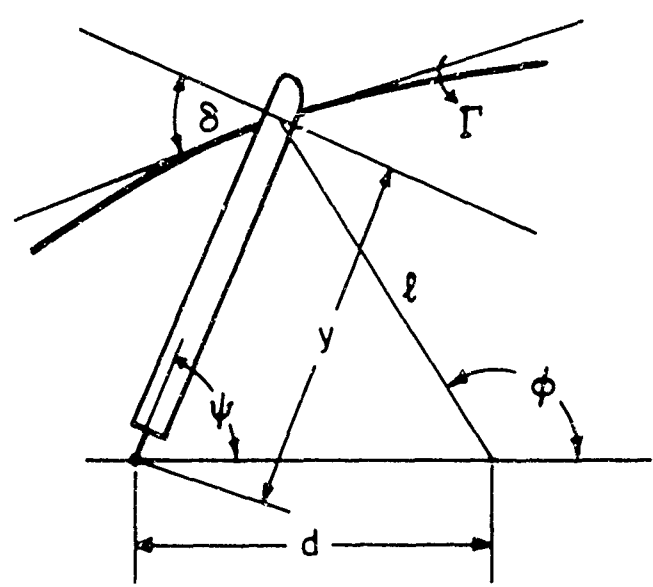
Fig. 22   Geometry of straight-line approximation to spiral vortex line.

Fig. 23 Airloads for four-bladed rotor of Fig. 7 with harmonics below the third eliminated. $\mu = 0.2$ $\eta = 0.95$

112